STUDIES ON MODULUS OF RESILIENCE OF LATERITIC SOIL BLENDS USING CBR, DCP, PFWD, AND CYCLIC TRI-AXIAL TESTS, WITH FEM BASED ANALYSIS ON DYNAMIC LOADING

Thesis

Submitted in partial fulfillment of the requirements for the degree of

DOCTOR OF PHILOSOPHY

by

ANIL KUMAR

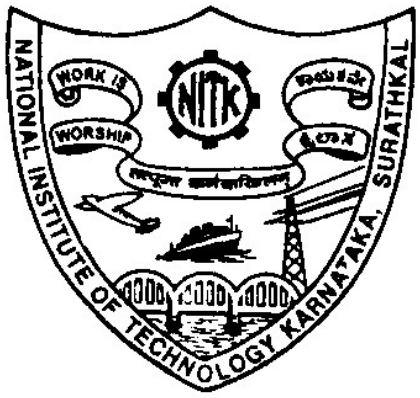

DEPARTMENT OF CIVIL ENGINEERING

NATIONAL INSTITUTE OF TECHNOLOGY KARNATAKA, SURATHKAL

SRINIVASNAGAR, MANGALORE -575025

May, 2018

STUDIES ON MODULUS OF RESILIENCE OF LATERITIC SOIL BLENDS USING CBR, DCP, PFWD, AND CYCLIC TRI-AXIAL TESTS, WITH FEM BASED ANALYSIS ON DYNAMIC LOADING

Thesis

Submitted in partial fulfillment of the requirements for the degree of

DOCTOR OF PHILOSOPHY

by

ANIL KUMAR

(Reg. No. 110647CV11P01)

Under the Guidance of

Dr. Varghese George

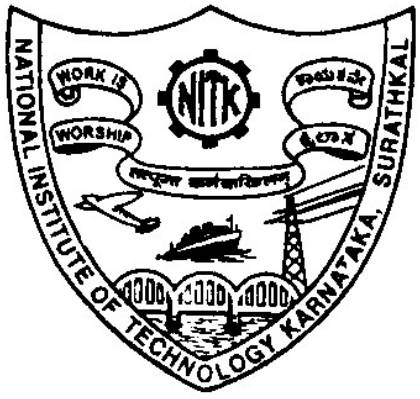

DEPARTMENT OF CIVIL ENGINEERING

NATIONAL INSTITUTE OF TECHNOLOGY KARNATAKA, SURATHKAL

SRINIVASNAGAR, MANGALORE -575025

May, 2018

NATIONAL INSTITUTE OF TECHNOLOGY KARNATAKA, SURATHKAL

D E C L A R A T I O N

I hereby *declare* that the Research Thesis entitled "**STUDIES ON MODULUS OF RESILIENCE OF LATERITIC SOIL BLENDS USING CBR, DCP, PFWD, AND CYCLIC TRI-AXIAL TESTS, WITH FEM BASED ANALYSES ON DYNAMIC LOADING**" which is being submitted to **National Institute of Technology Karnataka Surathkal,** for the award of degree of **Doctor of Philosophy** in the **Department of Civil Engineering,** is a *bonafide report of the work carried out by me*. The material contained in this Report has not been submitted to any University or Institution for the award of any degree.

(Reg. No. 110647CV11P01) ANIL KUMAR

(Register Number, Name and Signature of Student)
Department of Civil Engineering

Place: NITK SURATHKAL

Date:

DEPARTMENT OF CIVIL ENGINEERING
NATIONAL INSTITUTE OF TECHNOLOGY KARNATAKA, SURATHKAL
SRINIVASNAGAR - 575 025(D.K), KARNATAKA, INDIA

C E R T I F I C A T E

This is to *certify* that the Research Thesis entitled **"STUDIES ON MODULUS OF RESILIENCE OF LATERITIC SOIL BLENDS USING CBR, DCP, PFWD, AND CYCLIC TRI-AXIAL TESTS, WITH FEM BASED ANALYSIS ON DYNAMIC LOADING"** submitted by **ANIL KUMAR** (Reg. No. **110647CV11P01**) as the record of the work carried out by him, is accepted as the *Research Thesis/ Synopsis submission* in partial fulfillment of the requirements for the award of degree of **DOCTOR OF PHILOSOPHY** in the **Department of Civil Engineering**, National Institute of Technology Karnataka, Surathkal.

Dr.Varghese George
Thesis Supervisor, Professor
Department of Civil Engineering,
National Institute of Technology Karnataka,
Surathkal-575025, Karnataka, India

Dr.Varghese George
Professor and Head and Chairman- DRPC
Department of Civil Engineering,
National Institute of Technology Karnataka,
Surathkal-575025, Karnataka, India

DEDICATED

TO

MY GUIDE,

MY PARENTS,

AND MY TEACHERS

WHO MOULDED ME;

MY WIFE, MY DAUGHTER, AND MY MOTHER IN-LAW WHO WERE A SOURCE OF ENCOURAGEMENT;

AND

THE ALMIGHTY

WHO BLESSED ME ABUNDANTLY.

Acknowledgements

I am grateful to the Almighty God for having given me the patience and divine guidance to complete this research. I would like to express my deepest and heart-felt gratitude to my supervisor Dr. Varghese George, Professor and Head of the Department of Civil Engineering, for his expert guidance, valuable suggestions, un-tiring effort in reviewing this thesis, continuous encouragement, and reference material provided throughout the course of my research work.

I also take this opportunity to express my gratefulness to, Dr. Katta Venkataramana, Member RPAC, for his help and encouragement provided at various stages of this work. I also wish to thank Dr. P Mohanan, Professor, Department of Mechanical Engineering, Member RPAC, for his valuable inputs that helped in steering this research in the right direction. I would also like to express my sincere thanks and gratitude to Dr. Sitaram Nayak, Professor, Department of Civil Engineering, for his encouragement and valuable suggestions.

I thank the support rendered by Dr. S.V. Dinesh, Professor and Head, Dept. of Civil Engineering, SIT Tumkur, for having extended the laboratory facilities for conducting the experiments using the Cyclic-triaxial Test equipment. I also express my gratitude to Mr. Shriram Marathe & Mr. Naveen B, M.Tech students who helped me in performing part of the experimental work for this research.

I would also like to express my sincere thanks to the laboratory staff, Sri. Chandrashekar Karanth, Sri. Sadanand Kadri, Sri. Narayan Nayak, Sri. Ramanatha Acharya, Sri. Yathish Kumar and the contingent staff Sri. Shashikantha and Sri. Vishwanatha, for their cooperation and assistance in the experimental work.

I also extend my sincere appreciation to the Director NITK for extending all facilities of the Institute for this research.

I owe my deep sense of gratitude to my institution, NMAMIT, Nitte and Dr. Niranjan N. Chiplaunkar, Principal, NMAMIT for having given me an opportunity to do research at NITK as a part-time research scholar. I also thank the Department of Civil Engineering, NMAMIT for the help and support provided during the research work.

I sincerely acknowledge the constant support and encouragement provided by my parents, Sri. K Chitharanjan and Smt. Kaveri, my brothers, Sri. Guruprasad and Sri. Naveen Kumar, my wife, Smt.Sunayana S., my daughter Niharika, and my mother in-law Smt. Mohini S. They were a source of inspiration for me during my work.

I express my thanks to all my young friends and co-research scholars for the memorable days at NITK.

Anil Kumar

Bio-data of the Research Scholar

Anil Kumar

Contact: 8722609983
Email: anil_nitk@yahoo.com

Present Address:
Asst. Professor (Grade-II)
Dept. of Civil Engineering
NMAMIT, Nitte - 574110
Karkala Taluk, Udupi District

Permanent Address:
S/o K. Chitharanjan
Door No 16-82/C, Mitta Parari
Modankaup, BC Road - 574219
Dakshina Kannada, Mangalore

Date of Birth : 16 March 1986
Nationality : Indian
Marital Status : Married

Education:

- S.S.L.C. (Std. X) - Kendriya Vidyalaya, Mangalore No-2 (Central Board of Secondary School of Education), 2002.
- Pre-University Course - St. Sebastian P.U. College Thokottu, Mangalore (Karnataka State Board), 2004
- Bachelor of Engineering (BE-Civil) Nitte Mahalinga Adyanthaya Memorial Institute of Technology (NMAMIT), Karkala (affiliated to Visveshwarya Technological University), 2008.
- Master of Technology (Geotechnical Engg.) – National Institute of Technology Karnataka, Surathkal (Deemed University), 2010.

Employment Details:

From	To	Position	Institute
2010	2011	Asst. Lecturer	National Institute of Technology, Surathkal.
2011	2012	Asst. Professor	Srinivas School of Engineering, Mukka.
2012	2013	Asst. Lecturer	National Institute of Technology, Surathkal.
2013	2014	Asst. Professor	Alvas Institute of Engineering and Technology, Mijar, Moodabidri.
2014	Continuing in Service	Asst. Professor	Nitte Mahalinga Adyanthaya Memorial Institute of Technology, Karkala.

List of Publications:

- Enclosed

Abstract

Design and construction of highway embankments constitute a major component of highway engineering science. Poor sub-grade strength, overloading due to traffic loads, and seismic vibrations can cause distress to pavement sub-grades and embankments. Inadequate compaction and poor sub soil drainage, in addition to low bearing strength of soils cause failure of embankments especially in submersible regions.

The coastal, and peninsular regions of India, and the District of Dakshina Kannada in particular are characterized by the presence of *lateritic* and *lithomargic* or *silty* soils (locally known as Shedi soil). These soils are characterized by the presence of more of silty fines and lesser clay content. In the process of expansion and widening of highways in this region, engineers are often required to design embankments using soils of predominantly *lateritic* and *lithomargic* origin. The effective use of these soils is therefore often hindered by difficulty in handling particularly under moist and wet conditions typical of tropical regions soils that present such problems during construction processes are termed problematic. *Lateritic* and *lithomargic* soils are not expansive in nature. However, it is required to perform a comprehensive study on the type of soil, the strength and stiffness of the soil in order to understand the phenomenon of pavement and embankment failure.

The design of pavements require details on soil stiffness which in turn depends upon the density, soil-moisture content, degree of saturation, the drainage condition, the confining pressure, the homogeneity, and the load applied. Due to this reason, the evaluation of sub-grade strength and stiffness is of immense importance in pavement design.

Vehicular loads applied on pavement surfaces are dynamic in nature. Due to this reason, the study of pavement sub-grades necessitates the analysis of elastic behaviour of underlying soil layers when subjected to repeated loads. Traditional and qualitative methods for subgrade evaluations include visual inspection, proof rolling (passing over subgrade with heavy roller to locate soft spots), time-consuming moisture density tests, and observations of settlements due to heavy construction equipment in addition to other destructive and non-destructive approaches. In the recent years, non-destructive approaches to pavement evaluation using the FWD, PFWD, Geo-Gauge, DCP and test using cyclic tri-axial test have gained popularity. Additionally, present sub-grade evaluation, and pavement design procedures give more importance to the use of *modulus of resilience* as a measure of pavement strength and stiffness that can be easily determined using non-destructive approaches.

Moreover, there has been a change in approach in the design of flexible pavements with the introduction of mechanistic empirical method that necessitates the use of the *modulus of resilience* in place of soil stiffness measured using the CBR and the DCP. Field engineers in developing countries need to at times depend on conventional methods to assess the soil-stiffness due to non availability of the PFWD, or FWD, or the cyclic tri-axial test equipment. Additionally, the cost of purchase and installation of the FWD and the cyclic tri-axial test equipment is quite high. The use of such equipment is also quite difficult considering the need to employ additional skilled personnel.

Recent pavement design procedures such as the Mechanistic-Empirical design approaches incorporate use of *modulus of resilience* or *resilient modulus*. Here, the design of the pavement is modeled based on the structural response measured in terms of stress, strain or deflection and the physical parameters of the pavement material. The *resilient modulus* or *modulus of resilience* (*M*r) is defined as the ratio of cyclic deviator stress to the recoverable strain.

This research work deals with a parametric study on laterite sub-grades using standard soil-testing procedures, and performing investigations on the engineering properties of *lateritic* and *lithomargic* soils for the District of Dakshina Kannada, Karnataka State, India. The study encompasses experimental investigations on static properties of soil such as, the Atterberg's limits, grain-size distribution, specific gravity, maximum dry density (MDD), optimum moisture content (OMC), tests for California Bearing Ratio (CBR), tests for unconfined compressive strength (UCS), and tri-axial tests. This is followed by a study on the soil strength using the dynamic cone penetrometer (DCP) and the portable falling weight deflectometer (PFWD). Further tests were performed for determining the *modulus of resilience* (M_r) using the cyclic tri-axial testing equipment.

Further studies were performed on strength and stiffness characteristics of laterite soil-samples with varying percentages of fines and moisture contents close to optimum moisture conditions (OMC), for standard proctor density conditions. The results obtained using the PFWD, CBR, and DCP tests conducted in the laboratory, and correlations between the results for various tests were analyzed using suitable statistical techniques. Also, the test results for various equipments were correlated to the observations on various soil parameters such as the percentage of fines, percentage of sand, percentage of gravel MDD and OMC. Investigations on this phase of study was conducted on remolded soils at MDD and at three moisture contents (OMC-3%, OMC and OMC + 3%) for soaked and un-soaked conditions using special test-boxes designed for the purpose.

A number of regression models were then developed correlating the important observations made in the experimental studies. Additionally, the results of the experimental studies were further used in developing *FEM*-based models in *PLAXIS-2D* to study the impact of vehicular loads on soil embankments.

It is felt that the findings of this study will provide a strong basis for further research in pavement engineering. The correlations developed as part of this study relating the results obtained using the triaxial, PFWD, CBR, DCP and the modulus of resilience obtained by cyclic tri-axial test can be used effectively by field engineers in assessing the subgrade strength of laterite sub-grades. The results of this study can further provide the basis for future investigations on the effect of intrusion of fines in laterite soils.

CONTENTS

LIST OF FIGURES

LIST OF TABLES

CHAPTER I

INTRODUCTION

1.0 INTRODUCTION TO THE STUDY

Pavement engineering mainly deals with evaluation of subgrade strength and stiffness, and design and construction of embankments and pavement structures. Poor subgrade strength, overloading due to traffic loads, and seismic vibrations can cause distress to pavements and embankments. Inadequate bearing strength of subgrade layers and poor sub-soil drainage conditions result in failure of embankments. Especially in submersible regions, it is required to ensure minimum subgrade strengths for effective distribution of traffic loads.

The southern peninsular and coastal regions of India, including the District of Dakshina Kannada are characterized by the presence of *lateritic* and *lithomargic soils* that constitute 40% of the soil in this region (Rao et al. 2008). Lateritic soils often occur in weathered conditions due to the effect of high temperatures and humidity with alternating wet and dry seasons typical of tropical areas. These soils are characterized by the presence of more of silty fines and lesser clay content. The effective use of these soils as part of subgrades is often hindered by reduction in load-carrying capacity under moist and wet conditions typical of tropical regions.

However, in the process of expansion and widening of existing highways in this region, engineers are often required to design embankments and pavement structures on soil subgrades that are predominantly *lateritic* and *lithomargic* origin. Although these soils possess poor engineering properties such as high plasticity, high permeability, poor workability, and lower strengths when exposed to high moisture conditions, these soils are not expansive in nature, which provides scope for effect improvement of subgrade strength. It is also observed that in a number of pavement-construction sites, the existing soil subgrades comprise soils of *lithomargic* and *lateritic* characteristics intermixed with each other. Lateritic-lithomarges comprise lesser amount of lateritic soil constituents varying from 25–50%, while lithomargic-laterites comprise more amount of lateritic soil constituents varying from 50–75% (Rao et al. 2008). Therefore, the effective use of soil subgrades comprising *lateritic* and *lithomargic* soil fractions can be advocated only based on a complete study of the soil characteristics and the soil strength.

It is commonly found that the while the top 1 to 2 meter of the soil in many parts of the southern peninsular region of India comprises *lateritic* soils, the soil layers below are *lithomargic* in nature. The top layers comprising reddish *lateritic* soils are formed by the leaching of sedimentary, igneous, and metamorphic rocks in addition to mineralized proto-ores that result in the retention of insoluble ions of iron and aluminium (Yves, 1997), while the lower layers comprise finer silty fractions.

The design of pavements require details on soil stiffness which in turn depends upon the density, soil-moisture content, degree of saturation, the drainage condition, the confining pressure, the homogeneity, and the load applied. Due to this reason, the evaluation of subgrade strength and stiffness is of immense importance in pavement design. Since the 1980s, the California Bearing Ratio (CBR) test was considered as the basis for pavement design among other tests (WsDOT website, 2008). However, a number of researchers (US Army Field Manual, 1987, Gudishala, 2004) consider the CBR approach as an empirical method, since vehicular loads on pavements are thought to be dynamic in nature.

Huang (2004) states that in ideal traffic loading conditions, the deformation caused due to the effect of repeated application of smaller loads is proportional to the load, and is fully recoverable. This leads us to the concept of *resilient modulus* or the *modulus of resilience*. The *resilient modulus* or *modulus of resilience* (*Mr*) is defined as the ratio of cyclic deviator stress to the recoverable strain for rapidly applied loads. In studies using the cyclic triaxial test equipment, the resilient modulus is defined as the ratio of the applied axle deviator stress and the axle recoverable strain (Website: Dot-Minesotta). American Association of State Highway and Transportation Officials (AASHTO) formulated the guidelines for the analysis of pavement structures based on the *resilient modulus* for the Mechanistic-Empirical approach for design of pavement structures (AASHTO 1986, Monismith 1989). Investigations on determination of the *modulus of resilience* using the cyclic tri-axial test equipment is one of the *direct laboratory- based* approaches recommended by AASHTO (1993) for characterizing base and subgrade soils.

This can be measured using the falling weight deflectometer (FWD), the portable falling weight deflectometer (PFWD), and the repeated load (cyclic) triaxial test methods. The current pavement evaluation techniques using the FWD, PFWD, Geo-Gauge, and the dynamic cone penetrometer (DCP), are mainly non-destructive test approaches when compared to traditional methods such as the CBR, and the triaxial test approaches. However, it is felt that it is necessary to correlate the observations obtained using the traditional

investigation approaches such as the CBR, and the static triaxial tests to the *modulus of resilience* since these pavement evaluation methods are still being employed by practicing engineers in developing countries.

Interestingly, the AASHTO Supplement-1998 (AASHTO, 1998) to the AASHTO Design Guidelines, suggests a *hierarchical design concept* where for routine pavement designs, either the *California bearing ratio* or the *resilient modulus* of the soil may be used to represent the characteristic property of the subgrade soil for asphalt pavements, whereas the *modulus of subgrade reaction* of the soil obtained from plate bearing tests may be used in the case of concrete pavements. This has resulted in new research initiatives focused on development of relationships between results obtained using alternative methods of subgrade and pavement evaluation using the CBR, the PBT, the DCP and the FWD (Farsakh et al,2004).

Additionally, it may also be observed that the finite element method (*FEM*) can be further employed in the analysis and modelling of soil structures, which will provide an insight into the influence of loads on the underlying subgrade layers. The *FEM*-based technique provides approximate solutions to actual field-problems, and is flexible enough to incorporate the use of various types of materials, geometries, and boundaries of components to be studied.

The present study is focused on performing investigations on the engineering properties of *lateritic* (100%L+0%) and *lithomargic* (0%L+100%) soils for the District of Dakshina Kannada, Karnataka State, India. The study encompasses experimental investigations on static properties of soil such as, the Atterberg's limits, grain-size distribution, specific gravity, maximum dry density (MDD), optimum moisture content (OMC), tests for California Bearing Ratio (CBR), tests for unconfined compressive strength (UCS), and triaxial tests. This is followed by a study on the soil strength using the dynamic cone penetrometer (DCP) and the portable falling weight deflectometer (PFWD). In connection with the tests using the PFWD, studies were performed on the effect of *influence depth* and *influence width* for investigations using the *PFWD* which were supported by FEM-based analyses using *Plaxis-2D*. Additionally, tests were performed for determining the *modulus of resilience* (M_r) using the cyclic triaxial testing equipment. A number of regression models were then developed correlating the important observations made in the experimental studies. In the later stages, the results of the experimental studies were further used in

developing *FEM*-based models in *PLAXIS-2D* to study the impact of vehicular loads on soil embankments.

Lithomargic or *silty* soils are also locally known as Shedi soils. These soils are characterized by the presence of more of silty fines and lesser clay content. In the process of expansion and widening of highways in this region, engineers are often required to design embankments using soils of predominantly *lateritic* and *lithomargic* origin. The effective use of these soils is therefore often hindered by difficulty in handling particularly under moist and wet conditions typical of tropical regions soils that present such problems during construction processes are termed problematic.

It is felt that the findings of this study will provide a strong basis for further research in pavement engineering. The regressions developed for estimating the *modulus of resilience* based on simpler experimental approaches such as the CBR, the DCP, and the PFWD, will be of special advantage to pavement engineers in developing nations.

1.1 PROBLEM SCENARIO AND PROBLEM DEFINITION

Mangalore is one of the fastest growing cities in India with a major thrust on development of infrastructure, and investment in the industrial sector, aimed at a growth rate that surpasses the projected growth rate of India. It is the administrative headquarter of the District of Dakshina Kannada in the State of Karnataka, in southern India. The existing road infrastructure is in the process of being improved with the widening of existing highways.

Soil in the region of Dakshina Kannada, and the most parts of Southern peninsular region of India is mainly interspaced with *lateritic* and *lithomargic soils* that constitute about 40% of the soil in this region (Rao et al. 2008). *Lithomargic* or *silty* soils, also locally known as Shedi soils, are typically weak soils with high silt content and lesser amounts of clay. Engineers engaged in road construction activities often encounter the need to use lateritic and lithomargic soils as part of construction of embankments and road subgrades. It is known that though *lateritic* soils are strong in dry conditions, these soils tend to lose about 40-50% of the strength when exposed to moist climatic conditions. However, *lithomargic* soils tend to lose about 90% of the strength when exposed to moist conditions.

It must be known that in the process of expansion and widening of highways in this region, engineers are often required to design embankments using soils of predominantly *lateritic* and *lithomargic* origin. The effective use of these soils is therefore often hindered by difficulty in handling particularly under moist and wet conditions typical of tropical region

soils. One of the advantages of *lateritic* and *lithomargic* soils that enable these to be used as road subgrades is that these soils do not swell when exposed to moisture. However, the properties of these soils need to be studied in detail to understand the influence of traffic loads on underlying subgrade layers.

Moreover, there has been a change in approach in the design of flexible pavements with the introduction of mechanistic empirical method that necessitates the use of the modulus of resilience in place of soil stiffness measured using the CBR and the DCP. Field engineers in developing countries need to at times depend on conventional methods to assess the soil-stiffness due to non availability of the PFWD, or FWD, or the cyclic triaxial test equipment. Additionally, the cost of purchase and installation of the FWD and the cyclic triaxial test equipment is quite high. The use of such equipment is also quite difficult considering the need to employ additional skilled personnel.

One of the objectives if this study related to the development of correlations among the results of the CBR, the DCP, the PFWD, and the cyclic triaxial test is aimed at providing field-engineers with simpler methods to determine the *modulus of resilience* using conventional testing equipment. It is also felt that the effect of fines on the strength and stiffness of lateritic soils also need to be investigated.

The expansion and widening of road network system, necessitate the design of bridge abutments, and embankments. Engineers in the region of Dakshina Kannada often face situations that require the construction of embankments with *lateritic,* and *lithomargic* soils. The study of failure of embankments constructed on lateritic soils need to be analysed using suitable analytical methods with regard to the influence of traffic loads on the underlying subgrade layers, and the functioning of the embankments with various heights and toe angles.

1.2 SCOPE AND OBJECTIVES OF THE STUDY

The type of soil available in Udupi and Dakshina Kannada districts in Karnataka State can be classified as *lateritic* soil and *lithomargic* soil (locally known as Shedi soil). These soils are characterized by the presence of more of silty fines and lesser clay content. It was thus found necessary to perform tests on various blends of *lateritic* and *lithomargic* soils in order to study the stiffness characteristics and their influence on embankments made of such soils.

The scope of the present study was on performing investigations on the strength and stiffness characteristics of *lateritic* and *lithomargic* soils using various subgrade evaluation

techniques, and correlation of results obtained using such approaches, to the *modulus of resilience* of lateritic soils measured using the PFWD and the cyclic triaxial test equipment. This study will further facilitate the design and construction of pavements based on the mechanistic empirical method where the *modulus of resilience* plays a major role. The present work also includes details on an FEM-based analysis of embankment models on lateritic soil subgrades.

The objectives of the research work can be explained based on the description of various phases of work planned to be performed as illustrated in Fig.1.1, and based on the description given below:

- In the *first phase* of the investigation, studies were performed on the engineering properties of various blends of *lateritic* and *lithomargic soils*.

  As part of the above phase of study, investigations were performed on determination of the influence depths based on Boussinesq's equation and further modelling was performed using the FEM approach for the analysis of stress contours and deformations of cylindrical models of *lateritic* and *lithomargic* soils. The findings of the above study were then used in determining the influence depth for studies using the *portable falling weight deflectometer* (PFWD), and in the determination of modulus of resilience for soaked and un-soaked blended soil for various moisture contents using the PFWD.

- In the *second phase*, investigations were conducted using the cyclic triaxial test equipment in order to assess the *modulus of resilience* (M_r) for various blends of *lateritic* and *lithomargic* soils.

- In the *third phase* of the study, regression models were developed correlating the important observations made in the tests for soil stiffness using the CBR, DCP, and the PFWD, in addition to tests performed using the cyclic triaxial test equipment.

- In the *fourth phase* of the study, *FEM*-based analyses were performed using *Plaxis-2D* on embankments models for various blends of *lateritic* and *lithomargic* soils. The models were subjected to loads that simulated the movement of vehicular traffic on roads. The stresses and strains induced, and the displacements were then analysed. In order to perform the *FEM*-based studies on embankment models for traffic loads, it was necessary to derive the values of stresses induced due to a standard wheel load on the top of the pavement subgrade. The *KENLAYER* sub-module of *KENPAVE* software for pavement

analysis was used for this purpose. Analyses were performed on embankments of heights varying between 2-5m with toe angles varying between 30-60 degrees. The relevant results obtained in the previous phases of studies were then compared with the results obtained using the *Finite element method* (*FEM)*.

1.3 ORGANIZATION OF THE THESIS

Chapter I provide details on introduction to present work with details on the problem scenario, scope and objectives of study and sequence of activities related to present work on *lateritic* and *lithomargic* soils.

Chapter II provides an overview of literature studies on topics related to the evaluation of soil strength for subgrade and embankments. It also provides information on studies on soil strength in slopes and embankment. The literature survey also incorporates investigations on previous studies on correlation between the results of various methods of testing soil strength. This chapter also includes an overview of studies performed in *FEM* based analyses of slopes for dynamic loads.

Chapter III provides details on some of the theoretical aspects of conventional approaches to subgrade evaluation, and non destructive testing approaches including details on the DCP and PFWD tests.

Chapter IV provides an overview of the methodology adopted in the present study, details on the study area, and materials used and basic properties of soil blends. This chapter also provides details on the *first phase* of investigations on subgrade strength focusing on determination of the index properties of *lateritic* and *lithomargic* soil blends, with details on determination of OMC, and permeability of various lateritic soil blends. This chapter also deals with the determination of soil stiffness characteristics using the CBR, PFWD, and the DCP, with test results on UCS and the static triaxial tests.

Chapter V provides details on the *second phase* of the study with details on determination of the *modulus of resilience* using the cyclic triaxial equipment for various blends of lateritic soils tested at OMC, dry-side of OMC (OMC-3%), and wet-side of OMC (OMC+3%).

Chapter VI gives details on the *third phase* of the study with discussions pertaining to the correlations developed based on the test results of investigations performed in the previous phases. Correlations where developed considering the *percentage of fines* as an important dependent variable. Regression equation where also developed considering the

values of *UCS*, cohesion and angle of internal friction determined using *static triaxial test*, the values of *CBR*, *DCPI*, Modulus of resilience determined using *PFWD* and the *Cyclic triaxial test*. The test for validation was also performed.

Chapter VII provides details on the *fourth phase* of the study with details on *FEM* based analyses using *Plaxis-2D* for various configurations of embankment models for tests performed on various lateritic soil blends, along with discussions on the results.

Chapter VIII provides a summary of the major research findings along with conclusions of the study.

Chapter IX provides an overview of the major contributions of the present study, the limitations of the study, and the future scope research in this area.

CHAPTER II

LITRATURE REVIEW

2.0 INTRODUCTION

Subgrades need to be investigated for soil stiffness and strength. It is necessary to study the influence of soil properties of subgrades in order to access the performance of pavements. Soil subgrades transmit the vehicular loads safely to the soil strata below. Thus, subgrades need to be designed to resist the wheel loads during the design life of the pavements.

Lateritic subgrades that occur in the region of Dakshina Kannada in Southern India, poise great challenges to pavement engineers since these soils are easily affected by changes in temperature and humidity. *Lithomargic laterite* soils that comprise more of silt content, and *lateritic lithomarge* soils with higher contents of granular material with oxides of iron often co-exist in various proportions in nature. Although these soils do not swell with increase in moisture content, the soil strength and stiffness vary for different lateritic and lithomargic soil contents. This poses challenges in the design and construction of pavements, and embankments.

Pavements need to be designed to resist wheel load stresses during the life without failure. Additionally, pavement engineers encounter situations where subgrades of *lateritic* and *lithomargic* origin need to be strengthened in order to construct roads and embankments. In this connection, it is required to assess the strength, stiffness and stability of pavement subgrades in a reliable manner.

Traditionally the CBR approach was adopted for the design of flexible pavement especially from the 1980s. A number of researchers are of the opinion that the conventional approach to the design of flexible pavements using the CBR method is not reliable since it is not capable of explaining the effect due to repeated traffic wheel-loads on pavement subgrades (Gudishala, 2004). Considering the role of *modulus of resilience* as a measure of soil stiffness, the American Association of State Highway and Transportation Officials formulated the guidelines for the analysis of pavement structures in 1986 based on mechanistic analysis and design of pavements (AASHTO, 1986; Monismith, 1989). Also, AASHTO (1993) guidelines strongly recommend the use of the *modulus of resilience* for characterising the base and subgrade soils in the design of flexible pavements.

The *modulus of resilience* can be determined based on studies using the repeated load (cyclic) triaxial test, the FWD (falling weight deflectometer), and the PFWD (portable falling weight deflectometer). But considering the needs of practicing engineers of developing countries with limited access to sophisticated equipment, it was felt necessary to develop simpler procedures to estimate the *modulus of resilience* by co-relating the results of the studies using the PFWD (portable falling weight deflectometer), to the observations made using the DCP (dynamic cone penetrometer), static triaxial tests, tests on UCS (unconfined compressive Strength), and the tests for CBR (California bearing ratio). The following sections of this chapter provide an overview of literature survey performed on various aspects mentioned above.

2.1 HISTORICAL PERSEPCTIVE OF SOIL STRENGTH EVALUATION AND DEVELOPMENT OF CORRELATIONS FOR SUBGRADE

Boussinesq (1885) provided the theoretical background and derivation for stress distribution on soil due to a point load, based on the mathematical theory of elasticity, where the soil subgrade is assumed to be a semi-infinite, elastic, homogeneous, and isotropic medium. Here, it is assumed that the soil obeys Hooke's law, and that the stresses are distributed symmetrically about the Z axis, while the self weight of the soil is ignored (Venkatramaiah, 2006).

Mehta and Veletsos (1959) developed the theory and computer program for analyzing up to five layers. Michelow (1963) performed further investigations on similar lines which later led to the development of CHEVRON in 1960s, a program for computing vertical, tangential, and radial stresses and strains. Das (1983) observed that theoretical computations of vertical stresses compare reasonably well with actual field stresses within an error of 20-30%.

In the aftermath of the II World War, it was necessary to rehabilitate the airfields and pavements that were damaged due to the deployment of heavy bombers. The US Army Corps of Engineers was then entrusted with the responsibility of conducting detailed investigations on the application of the California Bearing Ratio (CBR) method for flexible pavement design for heavier wheel loads. The CBR method was thus modified to cater to various categories of wheel loads in the 1950s. In this method, the thicknesses of flexible pavements are computed using empirical design charts (US Army Corps of Engineers, 1950; Porter, 1950). The relative stability of subgrades with respect to that of crushed rock-based material is determined (Mak-wai-kin, 2006), based on the load-deformation tests. The CBR method

for the measurement of pavement strength, is an empirical approach to pavement design developed by O. James Porter for the California highway Department in 1929 (Priddy et al., 2012) for the design of pavements in view of the increasing road traffics (Porter, 1938).

The AASHTO guidelines of 1993 (AASHTO, 1993) recommended the need to employ the *modulus of resilience* for characterizing the base and subgrade soils and for the design of flexible pavements. The Indian Roads Congress (IRC, 2012; IRC, 2014) also laid guidelines for road construction and evaluation based on mechanistic-empirical methods. Thus, considering the importance of the mechanistic-empirical procedure in flexible pavement design, it is required to determine the *modulus of resilience* using the falling weight deflectometer (FWD) or the cyclic triaxial test equipment, or the PFWD (Portable falling weight deflectometer).

The traditional methods of evaluation of subgrade strength using the CBR test, the UCS test, the static triaxial test, and the tests using SPT (standard penetration tests) provide a basis for comparing soil strength characteristics. But these approaches are not capable of accurately explaining the load carrying properties of soil subgrades. Although the CBR approach had gained wide popularity in pavement design, it is felt that the measurement of the in-situ CBR is time consuming, and requires accessibility of the site to vehicles (Habib-ur-Rehman, 1995). In spite of the limitations attributed to the use of the above mentioned traditional approaches, these methods are still adopted in subgrade strength evaluation in many developing countries.

George et al. (2009a); Rao et al. (2008), Huang and Yumin (2010); Guzzarlapudi et al. (2016) formulated a number of correlations to link the observations made using the PFWD to the observations made using the DCP, CBR, and PBT (Plate Bearing Test). The *modulus of resilience* can also be determined using the cyclic triaxial test equipment for various soil subgrades.

2.1.1 STUDIES ON CORRELATIONS BETWEEN *CBR* AND *DCPI*

The DCP is a simple equipment that can be used to measure the strength of subgrades. It measures the resistance offered to penetration of a standard cone driven into the pavement structure or subgrade by a falling weight of 8 kg. The penetration measured in mm per blow is called as the dynamic cone penetration index or *DCPI*. This section provides a brief

overview of investigations on correlation studies carried by various researchers relating the *CBR* values of subgrades to the values of the dynamic cone penetrometer indices (*DCPI*) expressed in mm/blow.

As early as the 1960s, the US Army Corps of Engineers (Webster et al. 1992) attempted to correlate the *CBR* values to the *DCPI* for various types of soils in the U.S. using the following expression:

$$CBR = 292\ (DCPI)^{-1.12} \qquad \text{Eq. 2.1}$$

Riley et al. (1987) developed similar correlations between the *CBR* values and the *DCPI* values based on tests performed on various types of soils in a number of countries, one of which is given below:

$$CBR = 240\ (DCPI)^{-1.18} \qquad \text{Eq. 2.2}$$

Livneh et al. (1992) developed regressions correlating the CBR values to the DCPI values for granular and cohesive material as given below:

$$\log (CBR) = 2.45 - 1.12 \log (DCPI) \qquad \text{Eq. 2.3}$$

Webster et al. (1992) reported a correlation between the *CBR* values and the penetration rate (*DCPI*) expressed in mm per blow by the U.S. Army Corps of Engineers for a wide range of granular and cohesive materials as shown below. This correlation was widely adopted by a number of researchers (Webster et al., 1992; Seikmeir et al., 1999).

$$\log CBR = 2.465 - 1.12 \log (DCPI) \qquad \text{Eq. 2.4}$$

NCDOT (1998) developed a correlation for *CBR* and *DCPI* values for subgrades overlaid with base courses of cohesive soils and aggregates as follows:

$$\log(CBR) = 2.60 - 1.07 \log(DCPI) \qquad \text{Eq. 2.5}$$

Chen et al. (1999) derived a correlation between CBR and DCP values as given below:

$$\log CBR = 2.20 - 0.71\ (\log DCPI)^{1.5} \qquad \text{Eq. 2.6}$$

Gabr *et al.*(2000) investigated the use of DCP for the evaluation of pavement distress and performed experiments on subgrades overlaid with aggregate base courses of granite of Los Angeles value of 20%, and developed a correlation as shown below:

$$\log(CBR) = 1.4 - 0.55 \log(DCPI) \qquad \text{Eq. 2.7}$$

Abu-Farsakh *et al*. (2004) developed a correlation between *CBR* and *DCPI* values as given below, based on laboratory investigations:

$$\log(CBR) = 2.256 - 0.954 \log(DCPI) \qquad \text{Eq. 2.8}$$

Abu-Farsakh *et al*. (2004) also developed correlations between *CBR* and *DCPI* values with an R^2 value of 0.93 as follows:

$$CBR = 5.1/ (DCPI^{0.2} - 1.41) \quad \text{Eq. 2.9}$$

Rao et al. (2008) also provided details on a correlation developed between the CBR for unsoaked remoulded soils (CBR_u) and the DCP measured penetration indices (*DCPI*) with an R^2 value of 0.94 for blended lateritic soils as given below. The soil samples were remoulded at water contents of OMC, OMC+3%, and OMC-3%.

$$CBR_u = 75.18\ DCPI^{-1.09} \quad \text{Eq. 2.10}$$

2.1.2 STUDIES ON CORRELATIONS BETWEEN *MODULUS OF RESILIENCE* AND *CBR*

The section provides a review of investigations on correlation studies relating the values of the *modulus of resilience* (E_R) to the *CBR* values of subgrades.

Huekelom and Klomp (1962) developed a correlation to estimate the subgrade *resilient modulus*, based on the values of the Young's modulus (*Es*) of the subgrade determined based on the *CBR* values or the *DCPI* values. The U.S. Army Corps of Engineers (Green and Hall, 1975) also developed a correlation to estimate the *resilient modulus* (E_R) based on the *CBR* values as follows:

$$E_R \text{ (psi)} = 5409\ CBR^{0.71} \quad \text{Eq. 2.11}$$

The AASHTO Guide for Design of Pavement Structures (AASHTO, 1993) adapted the expression developed by Huekelom and Klomp (1962) for calculating the *resilient modulus* (E_R) of the subgrade as shown below. The expression developed by AASHTO in 1993 given below was also reported by Chen et al. (2005)

$$E_R \text{ (psi)} = 1500\ CBR \quad \text{or,} \quad E_R \text{ (MPa)} = 10.34\ CBR \quad \text{Eq. 2.12}$$

Powell et al. (1984) developed a correlation to estimate the *resilient modulus* (E_R) estimated based on the *CBR* values for soil samples with *CBR* values lesser than 5% as follows:

$$E_R \text{ (MPa)} = 10\ CBR \quad \text{Eq. 2.13}$$

Brown el al. (1990) developed a correlation to estimate the *resilient modulus* (E_R) based on the *CBR* values based on experiments on soil samples with CBR values greater than 5% as follows:

$$E_R \text{ (MPa)} = 17.6\ CBR^{0.64} \quad \text{Eq. 2.14}$$

The National Council of Highway Research Program (NCHRP, 2001) proposed an expression for the modulus of resilience based on CBR values as given below based on studies performed at Transportation research laboratory (TRL):

$$E_R \text{ (psi)} = 2555\ CBR^{0.64} \quad \text{Eq. 2.15}$$

Nazzal (2003) reported details of studies on correlating the *CBR* values to the *modulus of resilience* measured using Prima 100 LFWD (E_{pfwd}), and developed an expression as given below. This relationship was developed for E_{pfwd} values ranging between 2.5 and 174.5 MPa, and had an R-square value of 0.83.

$$CBR = -14.0 + 0.66\ E_{pfwd} \quad \text{Eq. 2.16}$$

Abu-Farsakh *et al.* (2004) developed a correlation between the stiffness modulus values determined using the Geo-gauge (E_G) and the *CBR* values based on field investigation as given below:

$$CBR = 0.00392(E_G)^2 - 5.75 \quad \text{Eq. 2.17}$$

Wu and Sargand (2007) reported the use of a correlation developed by the U.S. Army Corps of Engineers Research, and Development Centre Waterways Experimental Station, between the values of the *modulus of resilience* (MPa) determined using the PFWD (E_{pfwd}) and the *CBR* values as given below:

$$E_{pfwd} = 37.3\ CBR^{0.711} \quad \text{Eq. 2.18}$$

Rao et al. (2008) developed correlations between CBR values for unsoaked soil samples (CBR_u) and the modulus of resilience (E_{pfwd}) measured using PFWD with an R^2 value of 0.92 as given below. Similar relationships were developed by Nazzal (2003).

$$CBR_u = 0.2376\ (E_{pfwd}) - 3.6089 \quad \text{Eq. 2.19}$$

2.1.3 STUDIES ON CORRELATIONS BETWEEN *MODULUS OF RESILIENCE* AND *DCPI*

This section provides details on investigations on correlation studies relating the values of the *modulus of resilience* (E_R) to the *DCPI* values of subgrades expressed in mm/blow.

Powell et al (1984) developed a correlation between the *resilient modulus* and the DCPI values for subgrade soils as given below:

$$E_R = 338\ DCPI^{-0.39} \quad \text{Eq. 2.20}$$

Rao et al. (2008) also provide a correlation between DCP measured penetration indices (*DCPI*) and the *modulus of resilience* measured using PFWD (E_{pfwd}) for field observations as given below:

$$E_{pfwd} = 207.58 \text{ (DCPI)}^{-0.6659} \quad \text{Eq. 2.27}$$

2.1.4 STUDIES ON CORRELATIONS BETWEEN *MODULUS OF RESILIENCE* MEASURED USING THE FWD TO THAT MEASURED USING THE PFWD

This section provides details on investigations on correlation studies relating the values of the *modulus of resilience* (E_R) measured using the falling weight deflectometer (E_{fwd}) and the portable falling weight deflectometer (E_{fwd}) to other independent variables for subgrades.

Wu et al. (1998) developed the relationship between the *modulus of resilience* back-calculated from experiments using the FWD (E_{fwd}) expressed in MPa, and the *modulus of resilience* measured using the soil stiffness gauge (K_{ssg}) expressed in MN/m with an R square value of 0.66 as follows:

$$E_{fwd} \text{ (MPa)} = 22.96 \text{ e}^{0.12\,K_{ssg}} \quad \text{Eq. 2.28}$$

Chen et al. (1999) suggested that a general linear relationship between E_{fwd} and the *modulus of resilience* measured using the soil stiffness gauge (K_{ssg}) could be developed as shown below:

$$E_{fwd} \text{ (MPa)} = 37.65\, K_{ssg} - 261.96 \quad \text{Eq. 2.29}$$

2.2 HISTORICAL PERSPECTIVE OF SOIL STRENGTH IN SLOPES AND EMBANKMENTS WITH STUDIES ON CYCLIC TRIAXIAL EQUIPMENT

Embankments play a major role in providing the required grading to highways. Engineers encounter different types of soil in activities related to construction of embankments. In regions with lateritic and lithomargic soils, various blends of the soil are found to exist at the highway construction sites. It is required to have a proper understanding of the strength of such soils in pavement construction. The following sections provide details on studies on soil strength on slopes and embankments.

Diaz-Rodríguez (1989) performed investigations using the cyclic triaxial test equipment on undisturbed soft silty clay wet soil samples of Mexico. The effect of seismic forces on soil was simulated by analyzing the soil properties after application of 100 cycles of loadings. The soil exhibited elastic behavior under seismic loadings in spite of a high water-

content. Further application of seismic loading was not have any significant impact on the soil properties.

Lefebvre, Le.Boeuf and Demers (1989) performed experimental investigations using the cyclic triaxial tests on clay soil samples obtained from Hudson Bay region. The authors defined a stability threshold that referred to the stress level below which the soil did not undergo failure even after repeated application of cyclic loads.

Ansal and Erken (1989) conducted a series of cyclic triaxial tests on kaolinite samples under controlled stress conditions. The scatter plot of load vs. deformation followed a linear trend on a semi-log scale. The slope of the trend line was taken as the cyclic yield stress ratio. The authors also defined a critical yield stress ratio below which no pore water pressure would develop.

A number of studies have been performed on determination of the modulus of resilience using the cyclic triaxial test equipment (Fortunato et al. 2010; Dash et al. 2010; Youngji et al. 2010; Trinh et al. 2012; Inam et al. 2012, Zhong and Vanapalli 2016).The modulus of resilience measured using the cyclic triaxial equipment was found to be affected by a number of factors such as,

- effect of confining stress
- effect of deviator stress
- temperature effects
- effects of end conditions
- effect of other related factors on resilient modulus of subgrade soils

Additionally, Tripathy et al. (2014) indicate that measurement of soil suction is essential in the study of properties of unsaturated soils.

2.2.1 Effect of Confining Stress on Resilient Modulus of Subgrade Soils for Cyclic Triaxial Tests

Resilient modulus is derived from elastic stress-strain relationships. Subgrade materials derive their resistance to stress-caused deformation from inter-particle friction. Therefore, their stiffness depends very substantially on the inter-granular (effective) confining stress existing at the location being considered as well as on the applied deviatoric stress (Hardcastle, 1992; Cai et al. 2012; Han and Vanapalli, 2016). The effect of confining

stress is more pronounced on granular non-cohesive soils than on cohesive fine-grained soils. Granular soils develop inter-particle friction from effective confining stress.

Cohesive soils generate resistance from cohesion as well as confining stress. Fig.2.1 shows the effect of confining stress on resilient modulus. The degree to which the confining stress affects resilient modulus depends on the material properties for a given soil. Resilient modulus of fine-grained increase slightly with increasing confining stress. This behavior is typical for fine-grained soils as noted by Seed et al., (1962), Thomson and Robnett (1976), Pezo and Hudson (1994).

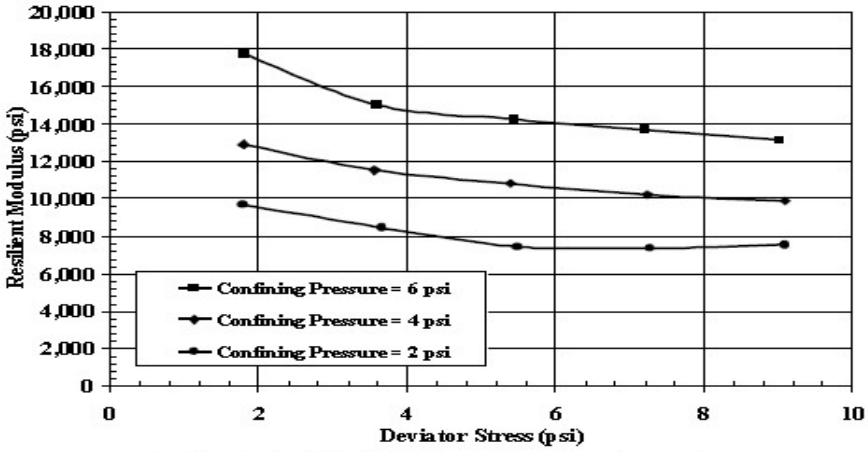

Fig.2.1 Relationship between Resilient Modulus and Deviator/ Confining Stress (Maher et al., 2000)

In the case of coarse-grained soils, the resilient modulus is usually described as a function of the confining pressure (Rada and Witzack, 1981) or the bulk stress AASHTO T-274-82 (AASHTO, 1986). Thus the *resilient modulus* increases with the confining pressure. Also, the *resilient modulus* increases with increasing deviator stress. This is referred to as *strain hardening behavior* due to the reorientation of the grains into a denser state.

2.2.2 Effect of Deviator Stress

The *resilient modulus* of fine-grained cohesive soils generally decreases with increasing *deviator stress* referred to as *stress softening behavior* (Boateng-Poku and Drumm, 1989). As the deviator stress increases, the resilient modulus rapidly decreases as shown in Fig.2.2. This is referred to as *strain softening*. For coarse grained soils, the *resilient modulus* increases with increasing deviator stress as shown in Fig.2.3 which indicates a *strain hardening effect* due to the reorientation of the grains into a denser state.

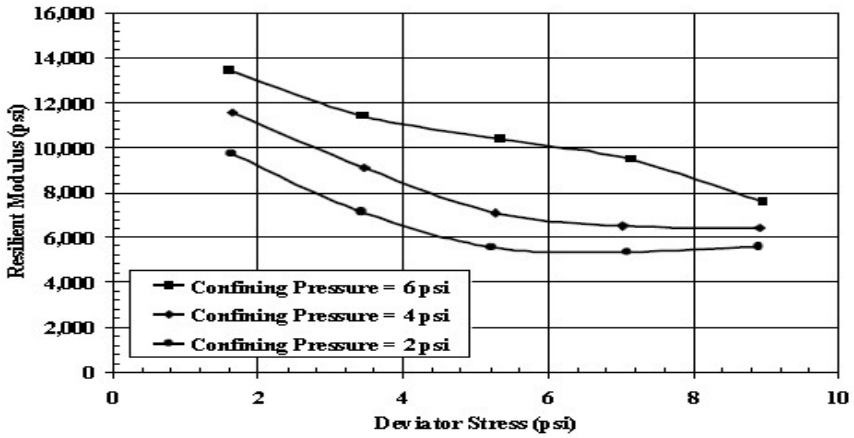

Fig.2.2 Effect of Deviator Stress on Fine-Grained Cohesive Material (Maher et al., 2000)

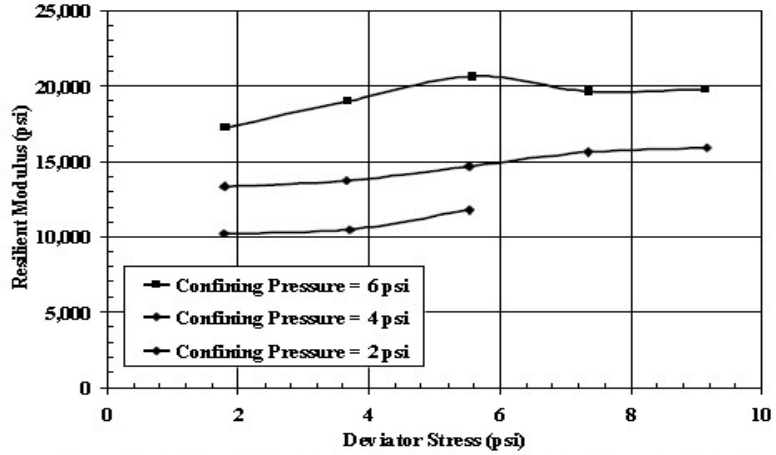

Fig.2.3 Effect of Deviator Stress on Coarse-Grained Non-Cohesive Material (Maher et al., 2000)

Fine- grained subgrade soils are especially problematic due to the generation of pore pressure during cyclic loading and their inability to rapidly dissipate the excess pore pressure due to low hydraulic conductivity. As a result the effective stress will decrease resulting in excess permanent deformation of the pavement system and reduction of resilient modulus.

2.2.3 Temperature Effects

Temperature effects may have a great influence on the resilient modulus of the pavement system. In general, the significant effect of the system can be classified in three different categories: frozen, unfrozen or recently thawed condition. Freezing of fine and coarse-grained soils (Fig.2.5) have shown significant increase in the resilient modulus compared to the unfrozen conditions as shown by (Chamberlain et al., (1989), Vinson (1978) and Cole et al., (1981). The resilient modulus of frozen soil is practically independent of

confining stress. However it varies slightly with higher deviator stress levels and temperatures (Cole et al., 1981).

2.2.4 Effects of End Conditions

Before conducting a resilient modulus test, AASHTO requires the specimen to undergo 500-1000 conditioning cycles to provide a uniform contact between the top and bottom platens and the soil specimen. The main purpose of the conditioning sequence is to minimize an uneven contact between the specimen and platens. Pezo et al., (1992) concluded that the conditioning sequence is an unnecessary step if the ends of this specimen are grouted to the platens. They felt that specimen conditioning did not provide an intimate contact between the specimen and platens. In their opinion, specimen conditioning effected the resilient modulus of the material by subjecting it to high stresses before running the resilient modulus test. Nazarian and Feliberti (1993) corroborated with Pezo et al., (1992) and indicated that stress history plays an important role in the modulus of soils. Therefore, they concluded grouting the specimen to the top and bottom platens should be implemented and the conditioning sequence should be eliminated. Grouting the specimen to the top and bottom platens imposes additional problems. To accurately measure the resilient modulus of specimen, the axial deformations must be measured. In the case of the grouted specimen, the axial deformations could not be measured using the full length of the specimen due to large shear stress generated in the grout zone. Therefore, if the specimens were grouted to the top and bottom loading platens, deformations must be made on the middle third of the specimen. Deformation measurements within the middle third of the sample proved to be a better method (Maher et.al., 1996). An additional problem with grouting the specimen ends isthe effect of pore pressure generation. If a sample is tested under saturated conditions pore pressures might develop since the grout would not allow the excess pore pressure to dissipate. These methods were implemented for research purposes and do not comply with the current AASHTO TP46-94 (AASHTO, 1994) specification for determining the resilient modulus of soils.

2.2.5. Effect of Other Related Factors on Resilient Modulus of Subgrade Soils

There are other factors that affect the resilient modulus of subgrade soils. These factors include soil type and properties such as amount of fines and plasticity characteristics. Material stiffness is affected by particle size distribution. Thompson and Robnett (1976) reported that low clay content and high silt content results in lower resilient modulus values.

They also showed that low plasticity index and liquid limit, low specific gravity and high organic content result in lower resilient modulus. Other research results indicated that the amount of fines has no general trend on the resilient modulus of granular materials (Chou, 1976). The resilient modulus generally decreases when the amount of fines increases (Lekarp et al., 2000). There is an increase in the resilient modulus with the increase in maximum particle size (Janoo and Bayer II, 2001). The resilient modulus to the soil specimen correlates well with age and plasticity index (Pezo and Hudson, 1994). Older is the specimen at the time of testing, lesser the resilient strain which indicates higher resilient modulus.

2.3 EFFECT OF FINES ON BEHAVIOUR OF SOIL

The *resilient modulus* of fine-grained soils investigated using the cyclic triaxial tests are influenced by a number of factors including the stress applied on loading the test specimens, the soil category, and soil-grain structure, compaction, and the soil-moisture content (Hicks and Monismith, 1971; Burczyk et al, 1994; Li and Selig, 1994; Al-Refeai and Al-Suhaibani, 2002, George et al., 2009, Taheri and Tatsuoka, 2012, Nguyen and Abbas, 2014).

Georgiannou (1988) made an investigation on the behavior of clayey sands under monotonic and cyclic loading. The studies concluded that the fines content had a remarkable influence on the stress-strain response of the soil masses. As the fines content increased, the dilatant behaviour of the soils was found to be suppressed, and the response came to be fully dependent on the fines at percentages beyond 40% fines content.

In subgrade materials, the inter-particle friction provides resistance to stresses and deformation. In tests using the cyclic triaxial equipment, Hardcastle (1992) observed that the soil stiffness depended to a large extent on the inter-granular (effective) confining stress and the applied deviator stress. Moreover, it was also seen that the effect of confining stress was more pronounced on granular non-cohesive soils than on cohesive fine-grained soils.

The effect of increasing fines content generally increases the magnitude of deformation (Barksdale 1972, 1991; Thom and Brown 1988); Dodds et al.(1999) confirm this result as the material with 10% fines added showed the highest deformations. Dodds et al.(1999) observed that the pore water pressure reduced the effective stress and thus reduced the level of confinement. Theyse (2002) observed that non-plastic fines up to 9% increased the shear strength while plastic fines decreased the same.

2.4 STUDIES ON *FEM*-BASED ANALYSIS OF EMBANKMENTS FOR DYNAMIC LOADS

The finite element analysis is one of the well known numerical methods in engineering practice and is widely adopted numerical technique for analyzing computer-based models in geotechnical engineering. The basic technique adopted in this approach is to represent a continuous media such as the soil (which possesses a number of known and non-quantified variables) by a mathematical model with a limited number of variables that influence discrete points or nodes in the continuous media (Newmark, 1965).

Carothers (1920) considers the study of analysis of stresses within homogeneous, isotropic elastic half-spaces as similar to that for "long embankments". FEM-based software can be used to study "long embankments" using the *plain strain analysis* approach. Janbu (1957) observes that *FEM* can be effectively used in simulating soil behavior especially in the analysis study of soil structure interaction at various stages of construction of foundations. The FEM approach is capable of modeling deformations and in the prediction of collapse of soil structures (Pockoski and Duncan, 2000).

Plaxis is a finite element software for analysing stresses and deformations in soil and rock, and is popularly used by geotechnical engineers and researchers for more than two decades. It is specially used in the analysis of deformation and the study of stability of soil-structure models. The software was first developed by the Technical University of Delft in 1987 to analyze soft soils of the low lands of Holland (Brinkgreve and Vermeer, 2001). *Plaxis* software can also be used in the investigation of soil-settlement and its effect on existing structure due to drilling activities in underground tunnel constructions (Jafarpisheh and Vafaeian, 2003). Choudhury et al. (2013) performed a number of similar FEM based analytical studies on settlement of embankment slopes.

The stress analysis for pavements can be carried out using *KENLAYER* sub module in KENPAVE. IRC: 37-2012 (IRC, 2012) provides guidelines for the design of flexible pavements. *KENPAVE* assists in the study the vertical displacement, vertical stress and radial stress at different interface layers.

In addition to analyses using FEM based approaches, a number of studies were made incorporating the use of ANN in developing models for estimating the compaction parameters of sandy soil.

2.5 SUMMARY OF LITERATURE SURVEY

The above literature survey provides an overview on studies on estimating soil strength, and development of correlations between the observations of the *modulus of resilience* obtained using the FWD, and PFWD, and the observations made using the DCP, and the CBR.

The later sections deal with studies on soil strength in slopes and embankments with studies using the cyclic triaxial test equipment. The effect of various factors on the measurement of *resilience modulus* using the cyclic triaxial test equipment was also studied in detail.

The literature review also included studies on the influence of fines on soil strength and its behaviour. The above sections also include a brief study on the application of FEM analysis on behaviour of embankments when subjected to dynamic loads.

In the above studies, it was found that literature of relationships between the resilient modulus measured using the triaxial test equipment and the results of the PFWD, DCP, and the CBR were limited especially in the case of studies related to lateritic and lithomargic soils. Moreover, studies on the influence of fines on soil-stiffness and the *modulus of resilience*, and the analysis of embankment models for dynamic loads such as on pavements, for lateritic soils were found to be scarce.

CHAPTER III

THEORETICAL BACKGROUND ON APPROACHES TO SUBGRADE EVALUATION

3.1 INTRODUCTION

Road transportation plays an important role in everyday life. The road network in India is characterized by the presence of a heterogeneous mix of traffic with various types of vehicles including motorcycles, cars, trucks, light commercial vehicles, buses, and auto-rickshaws. Most of the important road links are increasingly overburdened due to heavy traffic, and require strengthening and widening.

The subgrade plays a major role in imparting the required strength to the pavement structure as it receives traffic-loads imposed upon it by the pavement layers above, and transmits the same to the ground below. Subgrades need to be designed to ensure that the stresses transferred are well within the limits of elastic-deformation, and must ensure that the layers below do not undergo shear failure under adverse climatic and loading conditions. Hence, it is necessary to understand the engineering properties of soil structure, and the stress-strain behavior of soil subgrades when subjected to dynamic loading such as due to traffic loads.

A pavement is a structure that consists of the subgrade superimposed by layers of processed material including road aggregates laid with a binder such as asphalt or cement. The strength of the subgrade influences the thickness of the superimposed layers in the construction of roads, and airfield pavements. The assessment of the properties of soil subgrades, sub-base courses, and base courses in terms of density, strength, and other in-situ parameters to measure strength and stiffness is vital in the design of roads, and their performance. It is also seen that the grading of material used in the base course (WBM), and the sub-base course influence the performance of roadways (Ramulu et al., 2012). The strength and stiffness of pavement subgrades can be assessed by various methods including dynamic or static penetration tests, the use of penetrometers, static and dynamic triaxial tests, and other equipment.

In this context, the use of non-destructive testing techniques that could assist in the determination of the modulus of resilience of pavements gained wide acceptance. Currently the falling weight deflectometer (FWD), geo-gauge, dirt-seismic pavement analysers (DSPA), and laboratory-based repetitive cyclic triaxial tests are used to estimate the *modulus*

of resilience of pavement layers (Nazarian et al. 2002; Livneh and Goldberg, 2001; Rahim and George, 2002; Sawangsuriya et al. 2002, Elsa et al. 2012).These equipment can be also used to test the degree of compaction of clay subgrades (Hoffmann et al., 2004; Chai et al., 2014). The FWD and the portable falling weight deflectometer (PFWD) are regarded as nondestructive testing devices that can be used to estimate the *resilient modulus* or *modulus of resilience* of pavement subgrades (Alishibli et al. 2005).

In 1993, the AASHTO guidelines for the design of pavement structures strongly recommended the use of resilient modulus for characterizing base and sub-base materials for the design of flexible pavements (AASHTO, 1993) as part of the *Mechanistic-Empirical* design approach. Here, the design of the pavement is modeled based on the structural response measured in terms of stress applied, recoverable strain, rebound deflection, and the physical parameters of the pavement material.

Since traffic load is dynamic in nature, it is necessary to give more importance to the elastic behavior of pavements when subjected to repeated loading. Fig.3.1 provides a conceptual vie explaining total strain and rebound strain as explained by Huang (2004) based on cyclic load triaxial tests performed. Huang (2004) states that in ideal traffic loading conditions, the deformation caused due to the effect of repeated application of smaller loads is proportional to the loads and is fully recoverable. This observation further confirms the importance of the use of resilient modulus in the design of pavement subgrades.

3.2 CONVENTIONAL APPROACHES TO SUBGRADE EVALUATION

Conventional approaches to determine the strength and stiffness of subgrades include the California bearing Ratio (CBR) test, the plate bearing test (PBT), and the cyclic triaxial test in addition to non-destructive testing approaches.

The California bearing Ratio (CBR) test was regarded as one of the most dependable approaches in pavement design since World War II. The CBR value is determined by an arbitrary penetration procedure to obtain a *modulus* representing the *shearing resistance* of a subgrade. It is defined as the ratio of the force per unit area required to penetrate a soil mass using a circular plunger of 50 mm diameter at a penetration rate of 1.25 mm/min, to that required for a corresponding penetration for a standard material, expressed in percentage. This value is used to determine the required thicknesses of the various base courses through its application to empirically derived design curves' (US Army Field Manual, 1987).

However, the CBR approach is considered to be an empirical design method despite its popularity among practicing engineers.

In a cyclic triaxial test, the soil specimens of specified diameter with a diameter to length ratio of 1:2 are housed in a triaxial cell where confining pressure is applied. A load cell attaches to an actuator applies loads instantaneously every second for a duration of 0.1 seconds, followed by a resting period of 0.9 seconds. The loading cycle is repeated for 100 cycles, and the last 5 cycles are analyzed for determination of the modulus of resilience. A detailed explanation of the theory and working of the cyclic triaxial test equipment will be provided in the later chapters.

3.3 NON-DESTRUCTIVE TESTING APPROACHES TO SUBGRADE EVALUATION

Nondestructive methods for determining the strength and stiffness of subgrades include approaches to measure the *modulus of resilience* in addition to traditional methods that involve the measurement of *resistance to penetration*.

The approaches to measure the *modulus of resilience* include tests using the falling weight deflectometer (FWD), and the portable falling weight deflectometer (PFWD), while the methods of measurement of *resistance to penetration* include the standard penetration test (SPT), and the dynamic cone penetrometer (DCP) test.

However, the methods for measurement of resistance to penetration do not provide an estimate of the *modulus of resilience* although it provides a measure of resistance of the soil to dynamic penetration loads. Thus, in the 1980s, the use of the DCP and the SPT for subgrade evaluation was not popular. This was partly due to the lack of a solid correlation between DCP results and the values of the *modulus* of resilience (Ayers, 1990).

However, in the later years, the US Departments of Transport (DOT) as well as other organizations had shown considerable interest in the use of the DCP (Meier and Baladi, 1988; De Beer and Van der Merwe, 1991). Further research by a number of investigators generated sufficient data to develop correlations to estimate the CBR values based on the measurements made using the DCP (Jahren et al. 1999; Gabr et al. 2000; Al-Amoudi et al. 2002; Gregory 2007; George et al. 2009a; Gill et al. 2010, Nguyen & Abbas 2015). Khasnabis et al. (2010) provide details on the importance of CBR in evaluation of pavements and economic analysis of transportation infrastructure in developing countries.

The development of the falling weight deflectometer (FWD) and the portable falling weight deflectometer (PFWD) signaled as faster and simple method to assess pavement stiffness with computations leading to the measurement of the *modulus of resilience* in a more reliable manner based on rebound deflections (Amir et al., 2010).

3.3.1 Theoretical Foundations for Pavement Evaluation Using the FWD

The deflection caused to the surface of the pavement or subgrade being analyzed is measured using a geophone or an accelerometer located at the center of the loading plate of the FWD. The *modulus of resilience* is determined based on the concept of Boussinesq *elastic half-space*, where the soil subgrade is assumed to extend for an infinite length along the horizontal direction, while the depth over which the load acts vertically is finite. The subgrade material is assumed to have a uniform Poisson's ratio.

The expression for determining the total surface deflection (δ) of the circular plate of radius R under stress (p) applied on it for a two layer system with a *subgrade modulus* of E_2 is given as,

$$\delta = 1.18\, p.R.F/\, E_2 \qquad \text{Eq. 3.3}$$

where, F = a dimensionless factor (F) that depends upon the ratio of the *modulus of the subgrade* (E_2) to the *modulus* of the first (tested) layer (E_1), and the thickness of the tested layer (Yoder and Witczak, 1975).

The F-factor can be obtained using a design chart for vertical surface deflection. Knowing the total deflection and the corresponding stress, and assuming that the E_1/E_2 ratio for the plate load test is the same as that for the FWD test, E_1 can be back-calculated from the calculated E_2.

However, the use of trailer mounted devices such as FWDs set limitations on their use due to restrictions imposed by poor accessibility to subgrades at construction sites (Fleming, 2000). Moreover, evaluation of surfaces with unbound aggregates may result in erroneous readings due to the slipping of sensors in the deflection basins (Gurp et al. 2000).

3.3.2 Theoretical Foundations for Pavement Evaluation Using the PFWD

The *modulus of resilience* of the soil is computed using embedded software in Inspector–2 PFWD, with an LCD screen that displays the deflection, the rebound-deflection, and the impulse duration.

The influence depth of PFWDs in the measurement of *modulus of resilience* values ranges between 280 mm and 380 mm depending upon the soil-stiffness (Nazzal, 2003).
Most portable falling weight deflectometer (PFWDs) are equipped with falling weights of approximately 10 kg for a drop height of around 800 mm falling on circular loading plates of approximately 140 mm diameter for tests on soils that possess modulus of resilience varying from 0 to 1200 MPa. Also, loading plates of 200 mm are used for tests on weaker soils of modulus of resilience lesser than 10 MPa.

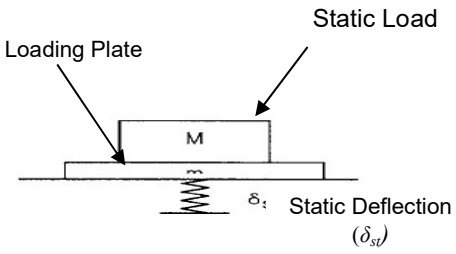

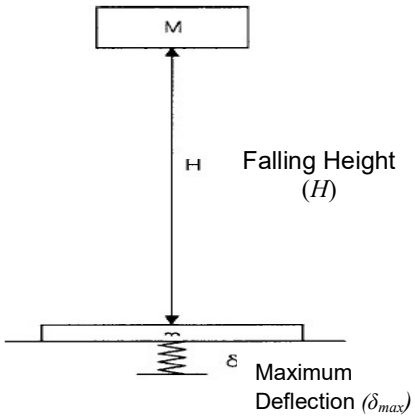

Fig.3.2a Modeling of static load **Fig.3.2b Modeling of Dynamic load**

In a portable falling weight deflectometer (PFWD), it is assumed that the force generated due to the impact of a falling weight is synonymous with a static load which is allowed to fall over a predetermined height, while the subgrade is considered to possess uniform elastic property. The fall of the static load over a given height results in the dynamic loading of the soil subgrade. The accelerometer or a sensor fixed either to the center of the loading plate, or to the center of the intermediate plate measures the *dynamic deflection modulus* or the *modulus of resilience* due to the rebound. The contact pressure (q) applied by a portable FWD can then be calculated by dividing the impact load of the falling-weight to the area of the plate.

For a falling weight of mass 10kg, falling with a velocity of 3.9618 m/s, the impulse load generated below the loading plate for an impact duration of 10ms (0.01 s) can be computed as P = 10 x 3.9618/ 0.01= 3961.8. The soil stiffness for unit deflection can then be computed as, $k = P/\ \delta$ = 3961.8/ 1 = 3961.8. The force below the loading plate due to the impact of the falling weight on a subgrade of stiffness k and $E_k = ½\ mv^2$ = 78.48 kg m. m/s^2 computed above can be given as,

$F_{max} = [2.k.\ E_k\ ]^{\ 0.5}$

= 2 x 3961.8 x 78.48

= 788.57kg or 7.735 kN

Also, the uniformly distributed load (q) applied on the plate of 140mm diameter of the PFWD can be obtained as,

$q = F_{max} / A$ = 7.735N/ (π x 0.07^2) = 502.47 kPa = 0.5025 Mpa.

Thus, the impact force (F) generated by a falling weight in a PFWD creates a uniformly applied load of 0.5025 MPa under a bearing plate of 140mm diameter for a peak impact loading at an impact duration of 10ms.

SUMMARY

This chapter provides details on the conventional approaches used in the determination of the strength and stiffness of subgrades based on the California bearing Ratio (CBR) test, Dynamic cone penetration test (DCP) and the cyclic triaxial test in addition to non-destructive testing approaches. This chapter also provides details on the design and fabrication of the cylindrical mild steel test box based on the working principle and theoretical foundations for performing the tests using PFWD and DCP equipments.

CHAPTER IV

METHODOLOGY, STUDY AREA, MATERIALS USED AND RESULTS FOR THE FIRST PHASE OF STUDY

4.0 INTRODUCTION

The present study focuses on performing investigations on the strength and stiffness of *lateritic* and *lithomargic* soils in the region of Dakshina Kannada, Karnataka state, India. Depending on the proportion of lateritic soils in this region, the soils can be classified as *lateritic lithomarges* and *lithomargic laterites.* In view of the need to improve the economy of the region, there has been an intense interest in road construction activities related to widening of existing two-lane roads to four-lanes and six-lanes. Practicing engineers in the file of pavement construction often face difficulties in providing subgrades of adequate strength as the soil types vary from *lateritic lithomarges* to *lithomargic laterites* in the region of Dakshina Kannada.

The studies on engineering properties of lateritic soils of the region were performed in various phases. The details of the methodology adopted in each phase of the investigation are illustrated in the following sections.

4.1 METHODOLOGY

The following steps indicate the methodology adopted in the investigations performed in this study:

First Phase of Investigations:

- Preparation of blended soils samples with various percentages of *lateritic* and *lithomargic* soils.
- Performing investigations on the index properties of various blends of *lateritic* and *lithomargic soils* including tests for determination of Atterberg's limits, grain-size distribution, and specific gravity for various soil blends.
- Determination of the optimum moisture content (OMC) using the Modified proctor compaction tests for various soil blends.
- Performing tests for permeability of various soil blends, and determination of permeability constants.
- Preparation of soaked and unsoaked soil blends compacted to OMC, *dry-side of optimum* (OMC–3%), and *wet-side of optimum* (OMC+3%), for various *lateritic* and *lithomargic* soil blends.

- Determination of the *California Bearing Ratio* (CBR).
- Determination of the *unconfined compressive strength* (UCS) for various soil blends and for various moisture contents for soaked and unsoaked soils.
- Performing tests for static *triaxial strength* for various soil blends and for various moisture contents for un-consolidated un-drained conditions (designated as UU-tests).
- Determination of dynamic properties of soil including the *modulus of resilience* using the *dynamic cone penetrometer* (DCP).
- Performing studies on the influence depths based on Boussinesq's equation, conducting analyses using the FEM approach for stress contours and deformations of cylindrical models for various blends of *lateritic* and *lithomargic* soils at OMC conditions and determination of the *influence depth* for studies using the *portable falling weight deflectometer* (PFWD).
- Conducting experiments using the PFWD for various blends of soils on soaked and unsoaked specimens.

Second Phase of Investigations:

- In this phase, investigations were conducted using the *cyclic triaxial* test equipment in order to determine the *modulus of resilience* (M_r) for various blends of *lateritic* and *lithomargic* soils compacted to OMC for unsoaked soil conditions.

Third Phase of Investigations:

- In this phase, regression models were developed correlating the important observations made in the tests for soil stiffness using the CBR, DCP, and the PFWD, in addition to tests performed using the cyclic triaxial test equipment.

Fourth Phase of Investigations:

- In the *fourth phase* of the study, *FEM*-based investigations were performed using *Plaxis-2D* on embankments models for various blends of *lateritic* and *lithomargic* soils. The models were subjected to loads that simulated the movement of vehicular traffic on roads. The stresses and strains induced, and the displacements were then analysed. In order to perform the *FEM-based* studies on embankment models for traffic loads, it was necessary to derive the values of stresses induced due to a standard wheel load on the top of the pavement subgrade.
- The *KENLAYER* sub-module of *KENPAVE* software for pavement analysis was used for this purpose. Analyses were performed on embankments of heights varying between 2-5m with toe angles varying between 30-60 degrees. The relevant results

obtained in the previous phases of studies were then compared with the results obtained using the *Finite element method* (*FEM)*. In this study, the stresses on the subgrade due to a design static wheel load of 5100kg (50kN) assuming a contact pressure of 0.8MPa applied over a contact area of radius 142.5mm (1MPa=1N/mm^2) was analysed using *KENPAVE* software for pavement analysis.

4.2 MATERIALS USED

In the present study, soil samples were collected from various sites adjacent to the existing National Highway, close to the National Institute of Technology Karnataka, Surathkal. The soil samples were obtained from predominantly strong lateritic subgrades prepared for widening of the existing highway along a distance of 15km. The soil sample with the strongest characteristics was identified and designated as *100%L+0%S*. Similarly, *lithomargic* soil samples characterized by high silt content and pale white colour were obtained from a site close to Kavur, in Mangalore and were designated as *0%L+100%S*.

4.2.1 Lateritic Soil

Lateritic constitutes weathered soils formed by the concentration of hydrated oxides of iron and aluminium (Thagesen, 1996). The name *"Lateritic "* was given to the brick coloured soil by Buchanan in 1807 for soils observed in the Coast of Malabar. *Lateritic* soils appear in a variety of shades varying from reddish brown to red, yellow, and ivory (off-white). *laterites* are fine-grained cemented residual with nodular gravels (Lambe and Whitman, 1979).

The behaviour of *lateritic* soils in pavements mainly depend upon the particle-size characteristics, strength and stiffness of the soil and gravel, the degree of compaction of the soil, loading on soils due to movement of traffic, and the environmental conditions (Gidigasu, 1976). Well-graded *lateritic* soils are strong enough to be used as material for road subgrades. However, lateritic soils tend to contain high amount of *silty* fines and lesser amount of sandy particles that result in breakdown of softer coarse particles, reducing the stiffness of the soil (Thagesen, 1996).

Lateritic soils cover a total area of about 248000 sq km, especially in the southern peninsular region of India. Lateritic soils are predominantly encountered in the hills of the Deccan, Dakshina Kannada district of Karnataka, Kerala, Madhya Pradesh, the Eastern Ghats, regions of Orissa, Maharashtra, Malabar (North Kerala), and Assam.

4.2.2 Lithomargic Soil

Lithomargic soils occur in the layers below *lateritic soils*, and are seen to occur over extensive non-alluvial tracts of peninsular India. Lateritic and *lithomargic soils* are formed in regions where soluble minerals are leached out of soils exposed to rainfall, and are characterized by an increased proportion of oxides of iron showing a reddish hue. The heavily leached red-to-yellow soils are encountered in high-rainfall areas of the Western Ghats, and the Deccan peninsular region of India. See **Fig.4.1a**.

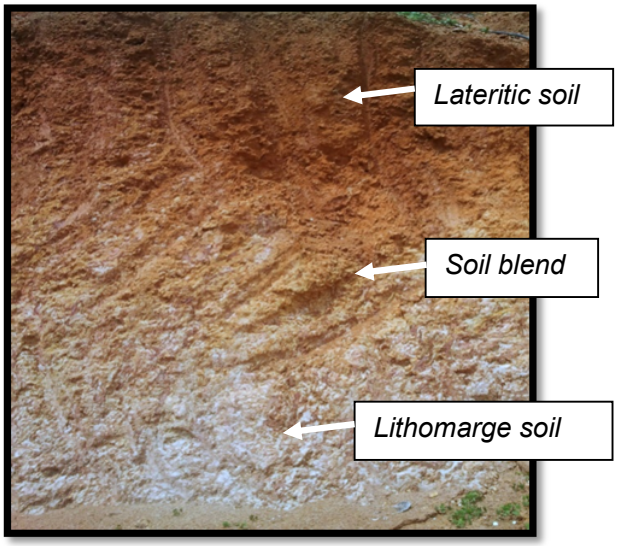

Fig.4.1a Soil Profile Showing Laterite Layer at the Top and Partially Lithomargic Soil Layer at Bottom for a Highway Cutting near Mulki, Dakshina Kannada

4.3 PREPARATION OF BLENDED SOIL SAMPLES

Along the coastal region of Dakshina Kannada of Dakshina Kannada and Udupi, engineers frequently come across soil intermixed with *lateritic* and *lithomargic* constituents in various proportions. *Lateratic soils* in southern region mainly comprise *lateritic lithomarge* (with 25%-50% latertic content), and *lithomargic laterite* (with 50-90% *latertite* content).

4.4 LABORATORY TESTS ON INDEX PROPERTIES FOR VARIOUS BLENDS

It was planned to perform laboratory tests such as the tests for, specific gravity, Atterberg's limits, particle-size distribution, optimum moisture content (OMC), maximum dry density (MDD) based on Proctor density (Modified compaction test), permeability, triaxial compression test and the unconfined compressive strength test(UCS). Subsequently, tests for determining the resilient modulus and soil stiffness were performed using the portable Falling Weight Deflectometer (PFWD), and the dynamic cone penetrometer (DCP).

4.4.1 Tests for Specific Gravity

The tests for specific gravity were conducted according to Sec.1 of **IS: 2720 Part III (1964)** for various soil blends. See **Table 4.1**.

Table 4.1 Results of the Tests for Specific Gravity for Various Soil Blends

Sl No.	Soil Blend Tested	Specific Gravity
1	100%L+0%S	2.58
2	75%L+25%S	2.54
3	50%L+50%S	2.50
4	25%L+75%S	2.44
5	0%L+100%S	2.37

4.4.2 Tests for Determination of Atterberg's Limits

Tests for Atterberg's limits that include tests for the liquid limit, plastic limit and the shrinkage limit were conducted on various blends of soils. The test procedure adopted is explained below:

a. *Test for liquid limit*: The *liquid limit* is defined as the minimum water content at which a groove made by a standard tool on a soil cake flows together for a distance of 12mm under the impact of 25 blows provided using Casagrande's apparatus. The tests for *liquid limit* were performed for various soil blends according to IS 2720 Part V (1985).
b. *Tests for plastic limit:* The *plastic limit* is defined as the minimum water content at which soil just begins to crumble when rolled into the form of a thin thread of approximately 3mm diameter. The tests for *plastic limit* were performed for various soil blends according to IS 2720 Part V (1985).
c. *Tests for shrinkage limit:* The *shrinkage limit* is defined as the water content at which soil changes from a semi solid state to a solid state when subjected to drying. The tests for *shrinkage limit* were performed for various soil blends according to IS 2720 Part VI (1972). Oven dried soil samples passing through a 425 micron-size sieve were used in this experiment. See Table 4.2.

4.4.3 Tests for Particle Size Distribution

The tests for particle-size distribution were performed according to IS: 2720 Part IV (1985) using the sieve analysis method (for soil fractions above 75 micron size), and the hydrometer method (for soil fractions of size lesser than 75 micron). Table 4.3 provides details on the classification of various soil blends into gravel, sand, and fines based on the above tests. Similarly, Fig.4.1b provides the grain size distribution based on results obtained

using the above methods. The soil classifications for each blend was identified according to IS: 1498 (1970) and also based on Casagrande's Chart (Casagrande, 1932). See Fig.4.1c.

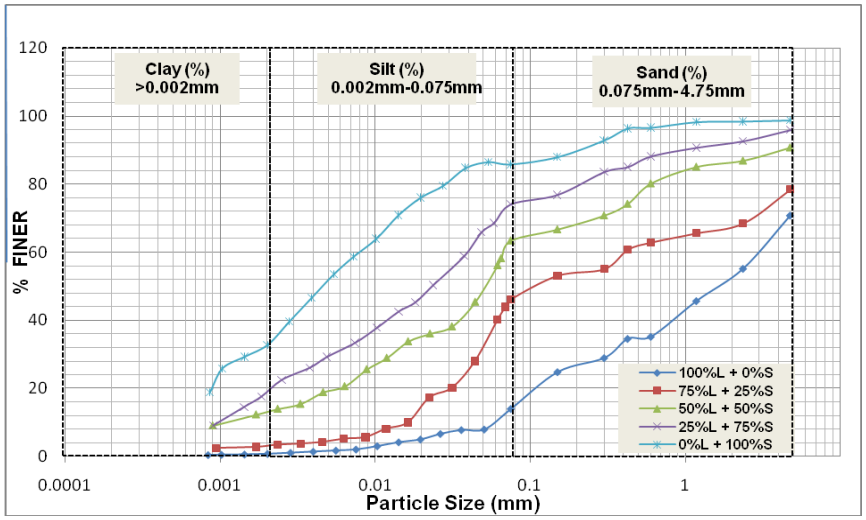

Fig.4.1b Particle Size Distribution for Various Soil Blends Tested

4.4 DETERMINATION OF MDD AND OMC USING MODIFIED PROCTOR COMPACTION

The Modified Proctor compaction method was adopted to determine the OMC and MDD for various soil blends. The tests were performed according to IS: 2720 Part VIII (1983). The Proctor density mould has an internal diameter of 4 inches (101.5 cm), having a height of 4.6 inches (117 mm) with a capacity of 945 ml. The soil was compacted in 5 layers with 25 blows using a standard hammer of 4.89 kg falling through a height of 450 mm. See Table 4.4.

Table 4.4 Results of the Tests for OMC and MDD using Modified Proctor Compaction Method

Sl. No.	Soil Blends	MDD (g/cc)	OMC (%)
1	100%L+0%S	1.97	13.8
2	75%L+25%S	1.86	14.6
3	50%L+50%S	1.82	16.2
4	25%L+75%S	1.75	17.7
5	0%L+100%S	1.67	20.4

4.5 DETERMINATION OF PERMEABILITY FOR VARIOUS SOIL BLENDS

Also, the results of the tests for permeability performed according to IS: 2720 Part 17 (1986) are provided in Table 4.5. According to IS Specifications, soil with more than 50% sand content has to be tested using the *constant head method*, while sand with less than 50% sand has to be tested with the *variable head method*. Hence for 100%L+0%S and

75%L+25%S soil blends; the *constant head* method was adopted while for and other blends permeability was calculated using the *variable head* method.

In the test for permeability, the soil samples were prepared at OMC based on the result obtained from the Modified proctor compaction test. To ensure full saturation of the soil specimen, the same was subjected to immersion in water for 24 hours as per IS 2720 Part 17 (1986). .

4.6 TESTS FOR *CALIFORNIA BEARING RATIO* (CBR) FOR BLENDED SOILS

The tests for CBR values were performed using moulds of 150 mm diameter, and 125 mm height according to IS: 2720 Part-16 (1987) for various blends of soils and for various moisture contents. Tests were performed on samples soaked for 4 days, and on unsoaked soil specimens. See Table 4.6. Also see Fig. 4.2a to Fig. 4.2j.for CBR Charts for various soil blends. Fig.4.2k and Fig. 4.2l shows the tests for CBR performed in the laboratory and soaking of sample.

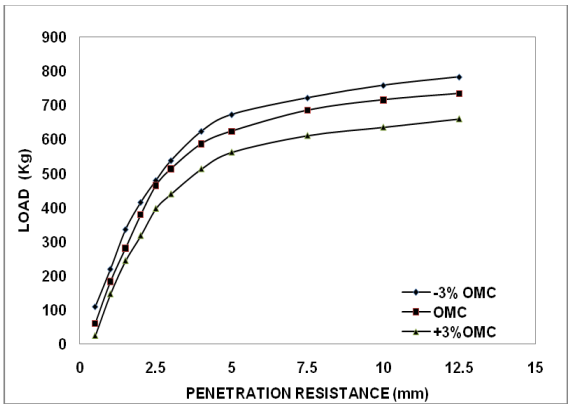

Fig.4.2a CBR Charts for Various Moisture Contents: Unsoaked (100%L+0% S)

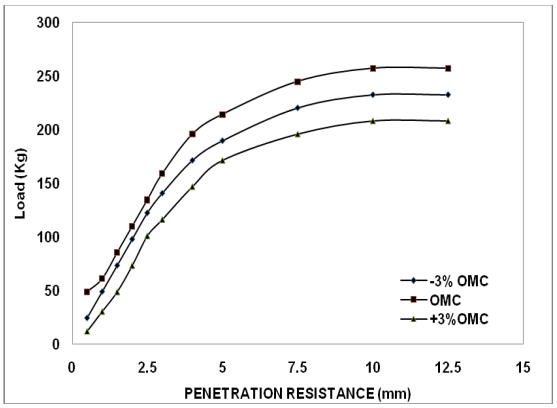

Fig.4.2b CBR Charts for Various Moisture Contents: Soaked (100%L+0%S)

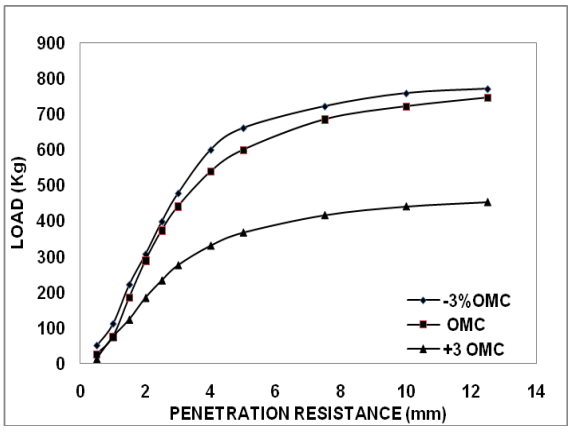

Fig.4.2c CBR Charts for Various Moisture Contents: Unsoaked (75%L+25%S)

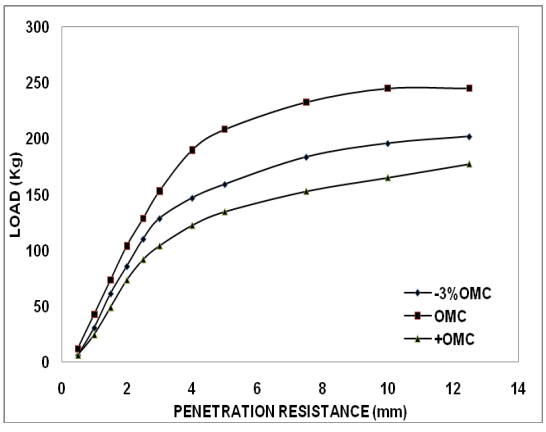

Fig.4.2d CBR Charts for Various Moisture Contents: Soaked (75%L+25%S)

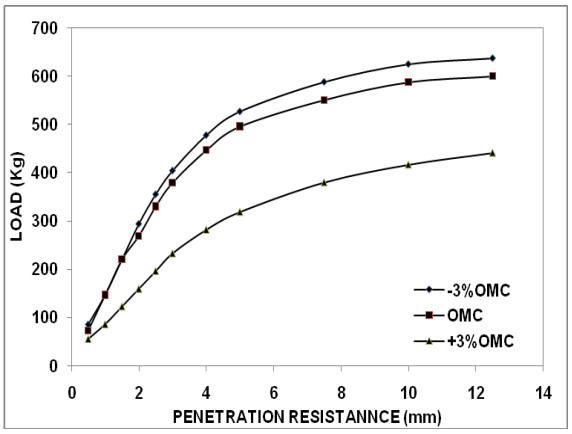

Fig.4.2e CBR Charts for Various Moisture Contents: Unsoaked (50%L+50%S)

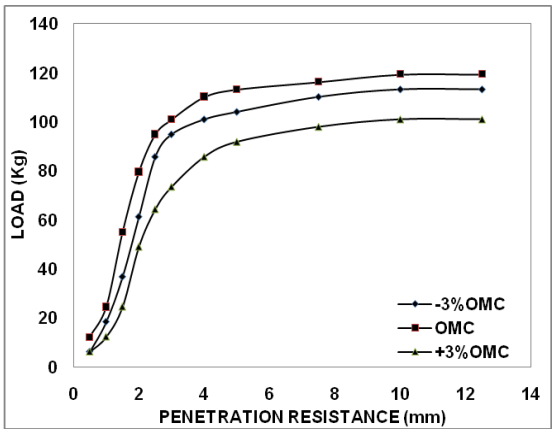

Fig.4.2f CBR Charts for Various Moisture Contents: Soaked (50%L+50%S)

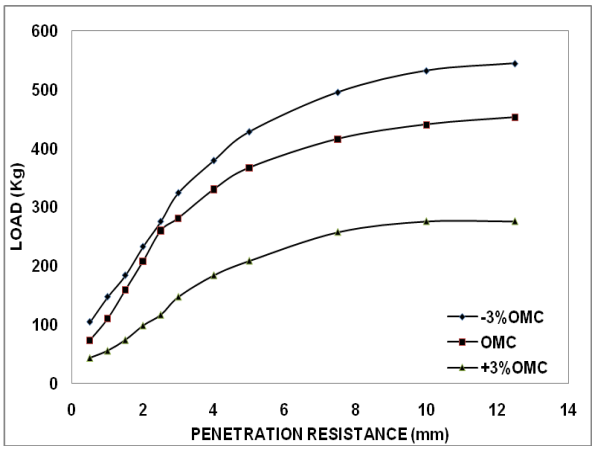

Fig.4.2g CBR Charts for Various Moisture Conten Unsoaked (25%L+75%S)

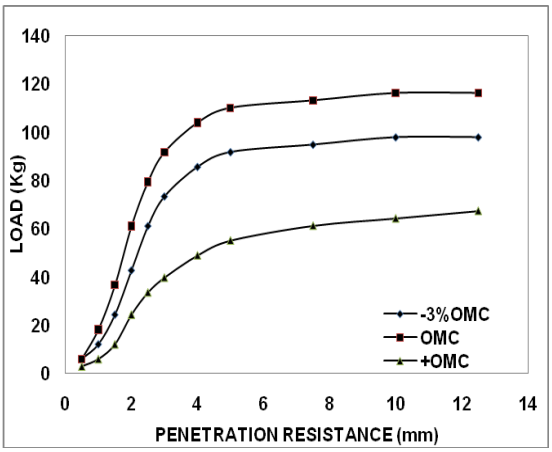

Fig.4.2h CBR Charts for Various Moisture Contents: Soaked (25%L+75%S)

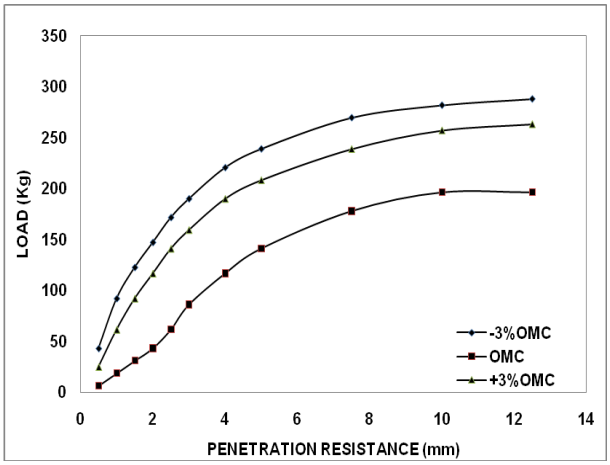

Fig.4.2i CBR Charts for Various Moisture Contents: Unsoaked (0%L+100%S)

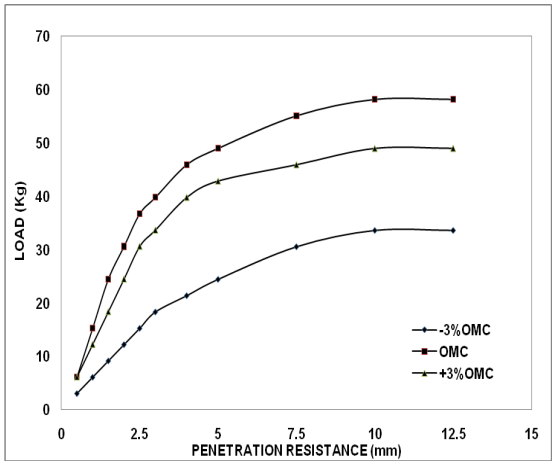

Fig.4.2j CBR Charts for Various Moisture Contents: Soaked (0%L+100%S)

Fig.4.2k Test setup for CBR Performed in the Laboratory: Unsoaked

Fig.4.2l Soaking of the CBR Mould in a Bucket of Water

4.7 TESTS FOR UNCONFINED COMPRESSIVE STRENGTH (UCS)

Tests for unconfined compressive strength (UCS) were performed according to IS: 2720 Part X (1973). The test for UCS is a special case of the triaxial test, where the cell pressure or confining pressure is considered to be zero. The investigations were performed on remoulded soil samples of 100 mm diameter with 200 mm height, and for samples of 38 mm diameter with 76 mm height for various soil blends and moisture contents. Fig.4.5a and Fig.4.5b show the variations for stresses and strains at OMC conditions for 38 mm diameter and 100 mm diameter samples for various blends. Fig.4.6a and Fig.4.6b shows the Fig. of the tests for UCS performed in the laboratory.

It may be observed that the diameter of the soil sample tested must be larger than 8 times the size of the largest particle size in the soil tested. Since various blends of lateritic soils were tested, it was considered ideal to perform test using both 38 mm and 100 mm diameter soil samples.

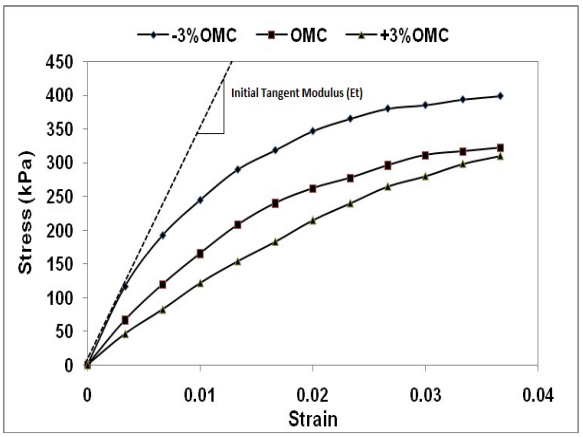

Fig.4.3a Stress-Strain Graphs for UCS using 38mm Diameter Sample: 100%L + 0%S

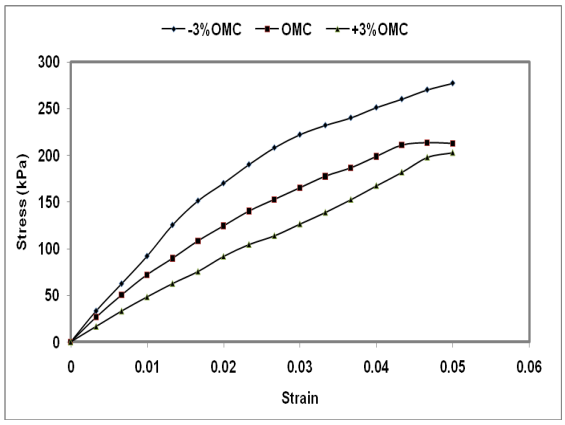

Fig.4.3b Stress-Strain Graphs for UCS using 38mm Diameter Sample: 75%L + 25%S

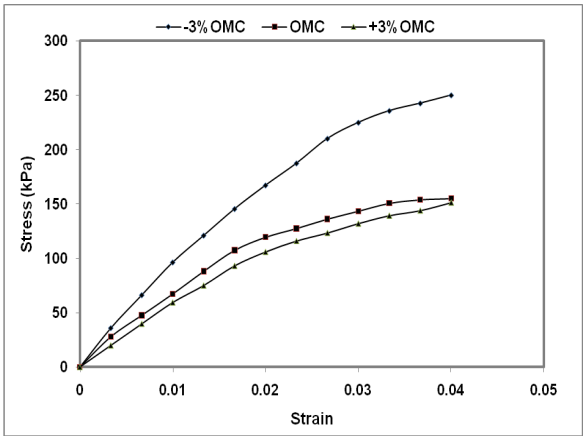

Fig.4.3c Stress-Strain Graphs for UCS using 38mm Diameter Sample: 50%L + 50%S

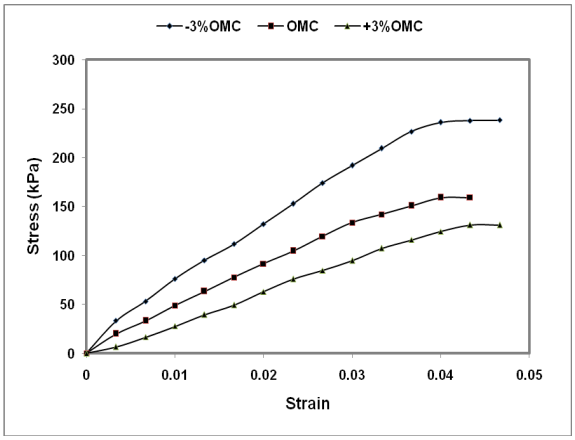

Fig.4.3d Stress-Strain Graphs for UCS using 38mm Diameter Sample: 25%L + 75%S

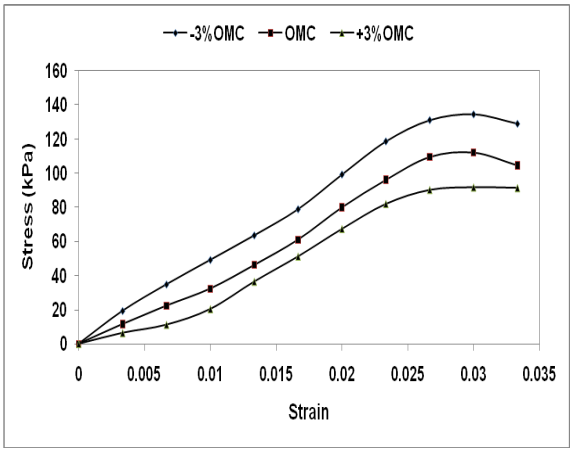

Fig.4.3e Stress-Strain Graphs for UCS using 38mm Diameter Sample: 0%L + 100%S

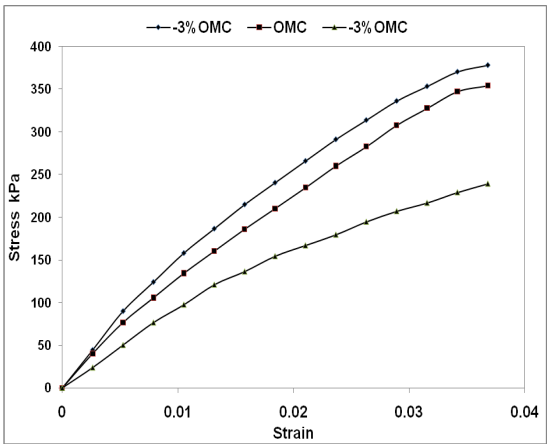

Fig.4.4a Stress-Strain Graphs for UCS using 100mm Diameter Sample: 100%L + 0%S

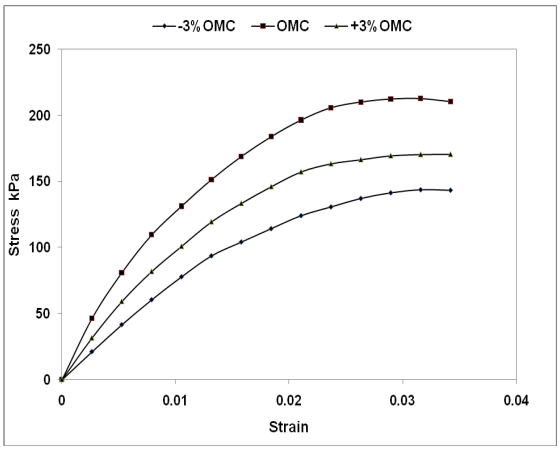

Fig.4.4b Stress-Strain Graphs for UCS using 100mm Diameter Sample: 75%L + 25%S

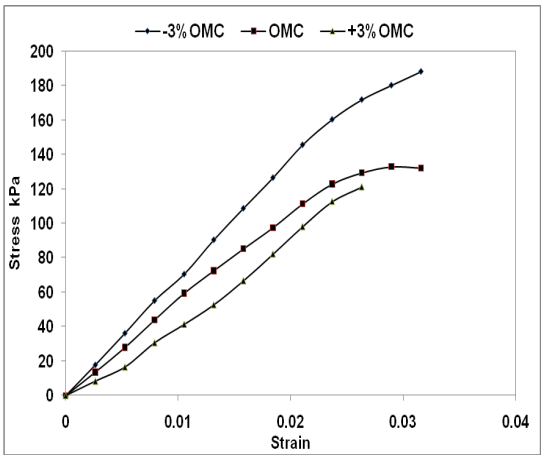

Fig.4.4c Stress-Strain Graphs for UCS using 100mm Diameter Sample: 50%L + 50%S

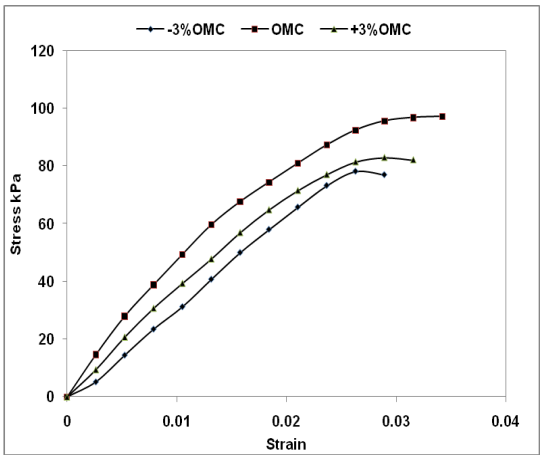

Fig.4.4d Stress-Strain Graphs for UCS using 100mm Diameter Sample: 25%L + 75%S

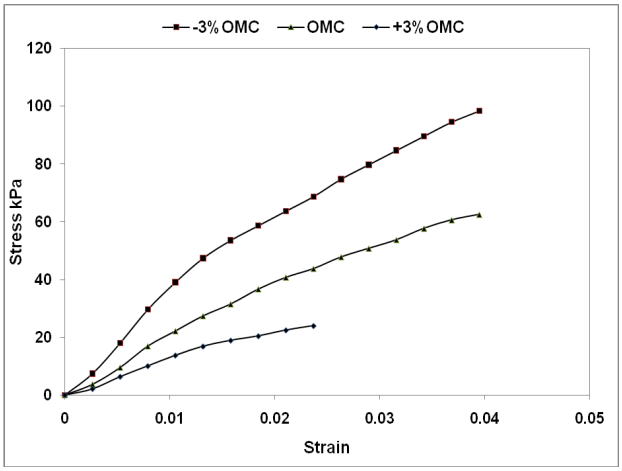

Fig.4.4e Stress-Strain Graphs for UCS using 100mm Diameter Sample: 0%L + 100%S

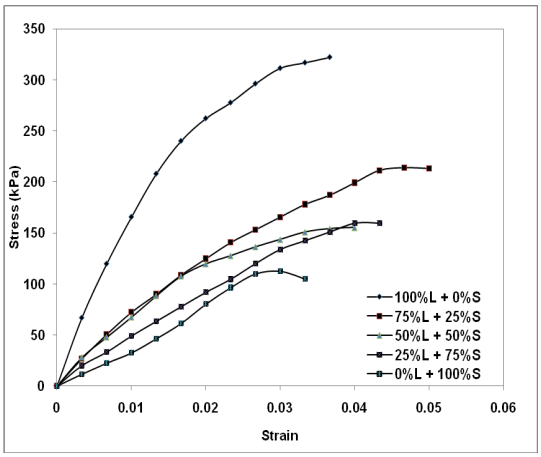

Fig.4.5a Stress-Strain @ OMC for 38mm Specimen

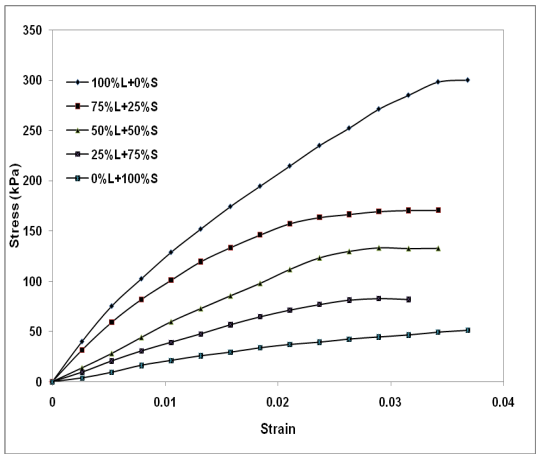

Fig.4.5b Stress-Strain @ OMC for 100mm Specimen

4.8 STATIC TRIAXIAL TESTS FOR VARIOUS BLENDS

In a number of investigations conducted in the US, and in other countries, and according to George et al. (2009), the *initial tangent modulus* obtained at a cell/ lateral pressure of 0.14 MPa can be used to estimate the *modulus of elasticity* of embankment material. Hence in this study, the modulus of elasticity was determined for tests conducted at a cell pressure of 0.14MPa (or 1.4 kg/cm^2) in addition to tests at cell pressures of 0.1MPa (or 1.0 kg/cm^2), 0.14MPa (or 1.4 kg/cm^2), 0.15MPa (or 1.5 kg/cm^2), and 0.2MPa (or 2.0 kg/cm^2). In the present study, triaxial tests were performed for un-consolidated and un-drained (UU) soil samples according to IS: 2720 Part XII (1981).

Tests on Un-consolidated and Un-drained Samples (UU)

In this test, the remolded samples of 100 mm diameter with 200 mm height, and samples of 38mm diameter with 76 mm height were prepared for various soil blends and for various moisture contents. The soil of each blend was filled in 5 layers in a split-mold. Each of the remolded soil samples was covered with a rubber membrane, and subjected to triaxial test. The proving-ring setup and a dial gauge were then fixed to measure the deviator load (or normal load P) and the deformation respectively. The deviator load (P) displayed by the proving ring was noted for deformations at every 25th division shown on the deformation dial gauge of 0.01 mm least count.

The results obtained from tests on unconsolidated undrained triaxial (UU test) test samples will be of use in situations where the loading of soil takes place rapidly, such that there is insufficient time for the induced pore-water pressure to get dissipated. Here, the consolidation

does not take place as the loading takes place faster. This happens usually in subgrades subjected to road traffic loads.

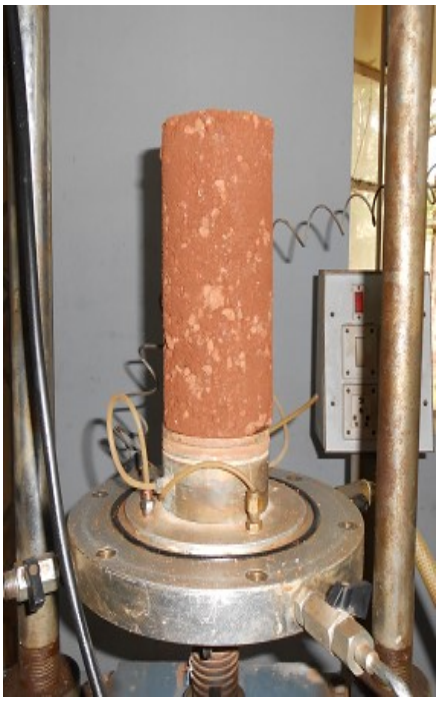

Fig.4.7a Triaxial Test Sample

Fig.4.7b Triaxial Test Setup

4.9 TESTS USING THE DYNAMIC CONE PENETROMETER (DCP)

The *Dynamic Cone Penetrometer,* was developed in 1956 in South Africa as an in situ pavement evaluation technique for evaluating soil strength (Scala 1956). This device, originally known as the Scala penetrometer, consists of a steel rod with a steel penetration cone of 60 degrees cone-angle and 20 mm diameter attached at one end. See Fig. 4.8. The equipment measures the strength of the subgrade soils in terms of the penetration resistance offered. The *penetration-index* is computed as the penetration of the DCP probe measured in mm per blow. The assistance of two persons is required in order to perform tests using the DCP - one to hold the hammer, and the other, to record the depth of penetration.

4.10 *FEM* BASED ANALYSES USING *PLAXIS-2D* FOR INFLUENCE DEPTHS BASED ON IMPACT STRESSES AND DEFORMATIONS APPLIED USING THE PFWD FOR CYLINDERICAL SPECIMENS

This section provides details on the later stage of the study focused on an *FEM* based analysis of stresses and deformations using *Plaxis–2D* software for cylindrical specimens of various blends of *lateritic* and *lithomargic* soils compacted at MDD. Section 4.10.1 and 4.10.2 provide the necessary theoretical foundations for computing the influence depth and the influence width of the mould in which the PFWD can be used to test the soil sample. From the descriptions in Section 4.10, it can be inferred that the influence depth and influence width can be assumed to be 360mm and 420mm. The cylindrical mould for testing the soil samples was designed based on these considerations with a height of 450mm, and a diameter of 450mm. Section 4.10.3 provides a description on the use of the *FEM* technique in computing the stresses and deformations at various points on the soil cross-section for lateritic and lithomargic blends, while Section 4.11 provides an explanation on performing tests using the PFWD on various soil blends.

4.10.1 Computation of Impact Stresses under the Loading Plate of the PFWD

In a portable falling weight deflectometer (PFWD), it is assumed that the force generated due to the impact of a falling weight is synonymous to the force applied due to a static load falling over a predetermined height while the subgrade is considered to posses uniform elastic property. The fall of the static load over a given height results in the dynamic loading of the soil subgrade.

4.10.2 Computation of Vertical Stresses, and Determination of Influence Depth Using Boussinesq's Equation for Impact Loads Applied Using the PFWD

The vertical stress (σ_z) at a depth of z vertically below a point load, and at a horizontal distance r from the point load can be computed using the following expression according to Boussinesq (1885):

$$\sigma_z = q \{1- [1/ (1+(r/z)^2) ^{5/2}]\} \quad \text{Eq. 4.1}$$

Also, for a uniformly loaded circular plate, the distribution of vertical stresses at a depth of z below a circular loaded plate of radius r can be computed using the following expression (Boussinesq, 1885):

$$\sigma_z = q \{1- [1/ (1+(r/z)^2) ^{3/2}]\} \quad \text{Eq. 4.2}$$

It must also be kept in mind that the stresses developed under a loading plate of 200 mm diameter is only 50% of that produced under loading plates of 140 mm diameter. Thus, in the case of PFWD loads applied using loading plates of 140 mm and 200 mm diameters, the influence depths are computed as 360 mm, and 380 mm respectively. Thus, the compacted depths of the cylindrical specimens were maintained at 450 mm. Nazzal (2003) also estimated that influence depths for experiments using the PFWD varied between 280 mm and 380mm depending on the soil-strength.

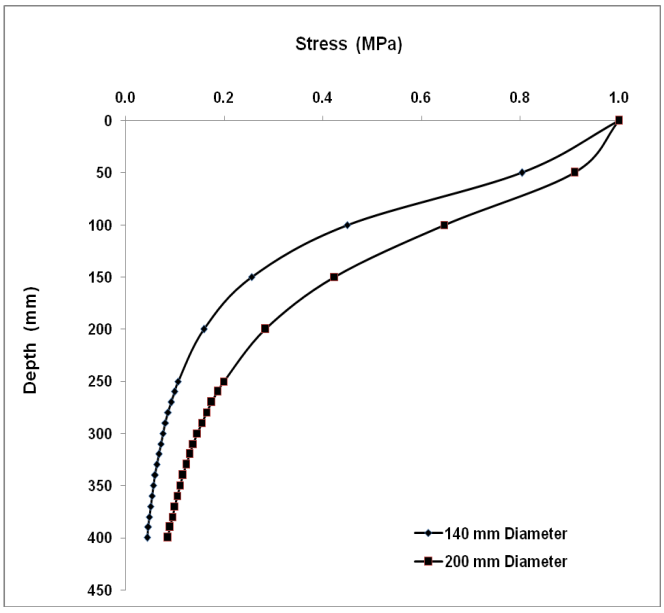

Fig.4.9 Boussinesq's Vertical Stress Distribution for 140 mm and 200 mm Diameter Loading Plates

Jurgenson (1934) states that for soil elements spread over a width of 3 times the radius of the loading plate, the percentage of stress experienced is lesser than $0.1q$ or 10% of the stress applied on the soil surface. Based on this premise, for load stresses distributed by circular loading plates of 140 mm diameter, the stress experienced at a horizontal distance of 3 times the diameter of the loading plate or 420 mm will be only 10% of the stress applied n the soil surface. Hence, the diameters of the compacted cylindrical specimens were maintained at 450 mm. In the case of stresses applied using a loading plate of 200 mm diameter, it must be observed that the effect is equivalent to only 50% of the stresses induced by a loading plate of 140 mm diameter. Moreover, loading plates of 200 mm are used only for testing weaker soils. Thus, in the case of PFWD loads applied using loading plates of 140 mm diameters, the influence width was considered to be 420 mm for testing of lateritic soils.

Based on the above discussions, it can be seen that for investigations using the PFWD with a falling weight of 10 kg falling over a height of 800 mm on to loading plates of 140 mm diameter, the influence depth is 360 mm and the influence width is 420 mm. The investigations using the PFWD were thus performed on compacted cylindrical specimens of 450 mm depth and 450 mm height. See **Fig.4.10**.

4.10.3 FEM Based Analyses Using *Plaxis-2D* for Impact Stresses Using the PFWD

Further analyses using the FEM were then performed for the specimens of compacted lateritic samples prepared in cylindrical moulds considering an impact loading of 0.51 MPa as derived in the above section. In this exercise, the properties of various soil blends determined in the initial stages of the study were compiled as in Table 4.11 and used as input in the modelling of the cylindrical specimens. Fig.4.11a illustrates the geometry of the cylindrical model analyzed in *Plaxis 2D*.

Table 4.11 Properties of the Soil Modeled

Soil blends	γ_{unsat}	γ_{sat}	$K_y = K_x$	E	υ	C	φ	ψ	*Load*
100%L+0%S	19.32	21.64	1.79×10^{-7}	19200	0.3	30.2	35.90	5.90	87.72
75%L+25%S	18.25	21.08	1.44×10^{-7}	15400	0.3	36.7	26.5	-	78.33
50%L+50%S	17.85	20.71	0.94×10^{-8}	12950	0.3	64	25.8	-	71.36
25%L+75%S	17.17	20.12	0.64×10^{-8}	5000	0.3	78	20.4	-	40.60
0%L+100%S	16.38	19.48	1.54×10^{-9}	3250	0.3	100	11	-	30.81

Note:

γ_{unsat} *or* γ_d = maximum dry density (kN/m^3) obtained based on IS Modified Proctor Compaction test;
γ_{sat} = saturated density (kN/m^3) computed using the basic relationship $\gamma_{sat} = (G+e)*\gamma_w /(1+e)$;
where e = voids ratio = $\{ G*\gamma_w/ \gamma_d \} -1$; γ_w = unit weight of water (9.81kN/m^3); G = specific gravity of soil; $K_y = K_x$ = co-efficient of permeability (m/s) computed based on lab tests; E = Young's Modulus (kPa) of soil determined using the triaxial test; υ = Poisson's ratio of the soil (generally assumed as 0.3); c = cohesion (kPa) of soil computed based on triaxial tests; Φ = angle of internal friction (degrees) determined using triaxial tests;
Ψ = dilatancy angle (Φ -30^o), used only when Φ is greater than 30^o; and q = stress on subgrade (kN/m^2) determined using *KENPAVE* (3-layer pavement analysis) for the design wheel load of 5100kg.

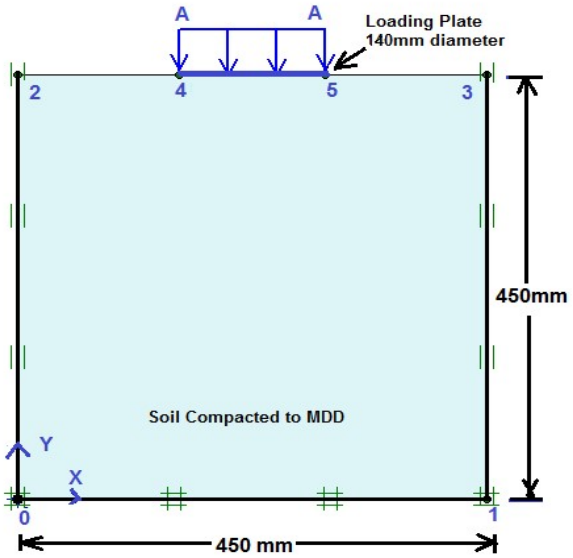

Fig.4.11a Geometry of the Cylindrical Soil Specimen with a Compacted Height of 450mm and an Internal Diameter of 450mm

The stress contours, and the deformations for pure *lateritic* soils as analyzed using *Plaxis-2D* for the blend *100%L+0%S* are shown in Fig.4.11b and Fig.4.11c respectively. Similarly, for pure lithomargic soils, the stress contours and deformations for the blend *0%L+100%S* are shown in Fig.4.11d and Fig.4.11e respectively. Fig.4.12a to Fig.4.12f illustrates details on the stress contours and deformations for other soil blends. Table 4.12 provides a summary of the results obtained using the FEM analysis on various blends of lateritic and lithomargic soils tested.

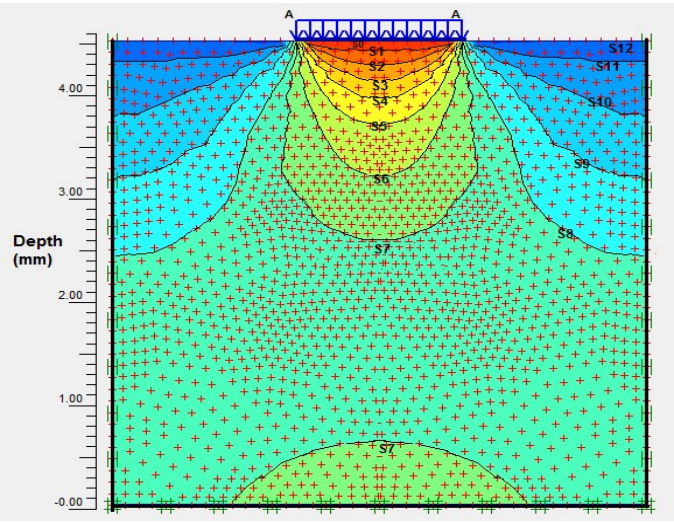

Fig.4.11b Stress Distributions Determined Using *Plaxis-2D* for Cylindrical Soil Specimen: 100%L+0%S

Note: S0 = -480 kN/m^2; S1 = -440 kN/m^2; S2 = -400 kN/m^2; S3 = -360 kN/m^2; S4 = -320 kN/m^2; S5 = -280 kN/m^2; S6 = -240 kN/m^2; S7 = -200 kN/m^2; S8 = -160 kN/m^2; S9 = -120 kN/m^2; S10 = -80 kN/m^2; S11 = -40 kN/m^2; and S12 = 0 kN/m^2.

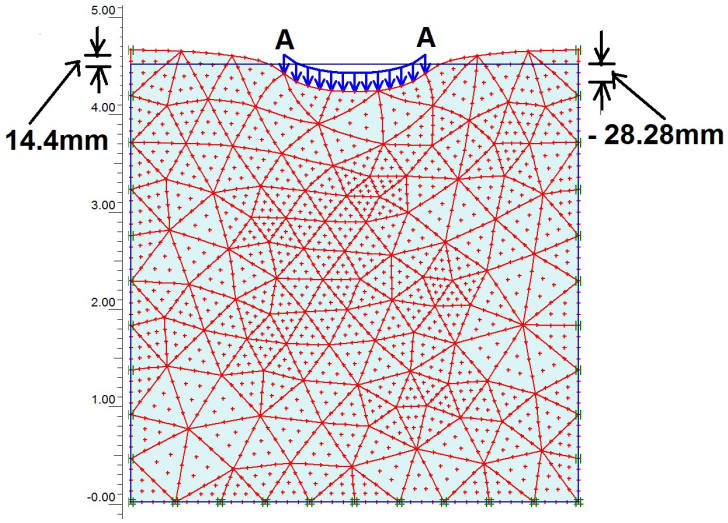

Fig.4.11c Deformation Determined Using *Plaxis-2D* for Lateritic Cylindrical Soil Specimen: 100%L+0%S

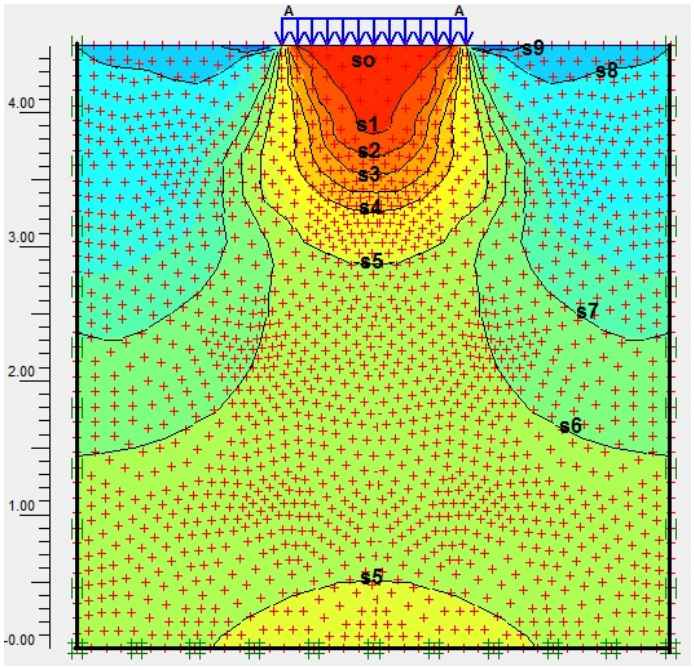

Fig.4.11d Stress Distribution Determined Using *Plaxis-2D* for *Lithomargic* Cylindrical Soil Specimen: 0%L+100%S

Note: S0 = -400 kN/m^2; S1 = -350 kN/m^2; S2 = -300 kN/m^2; S3 = -250 kN/m^2; S4 = -200 kN/m^2; S5 = -150 kN/m^2; S6 = -100 kN/m^2; S7 = -50 kN/m^2; S8 = 0 kN/m^2; S9 = 50 kN/m^2

It was found that the stresses predicted using the FEM-based analyses did not agree with the theoretical values computed using the Boussinesq's approach. This is due to the reason that the Boussinesq's formula provides stresses for static loading conditions, whereas, in this study, the computations were made considering the dynamic impact load due to the falling

weight. Moreover, the Boussinesq's approach did not consider soil properties such as such as soil density, cohesion, and angle of internal friction.

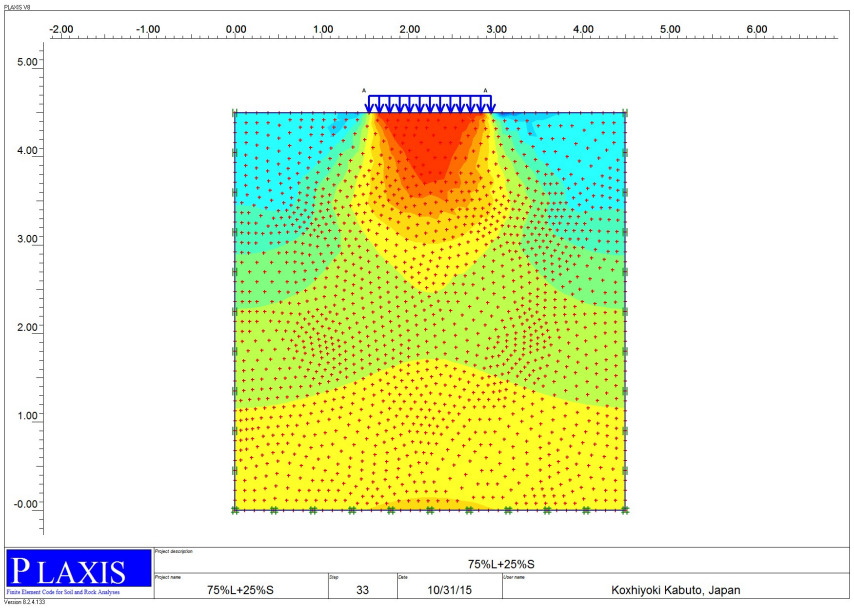

Fig. 4.12a Stress Distribution Determined Using *Plaxis-2D* for Cylindrical Soil Specimen: 75%L+25%S

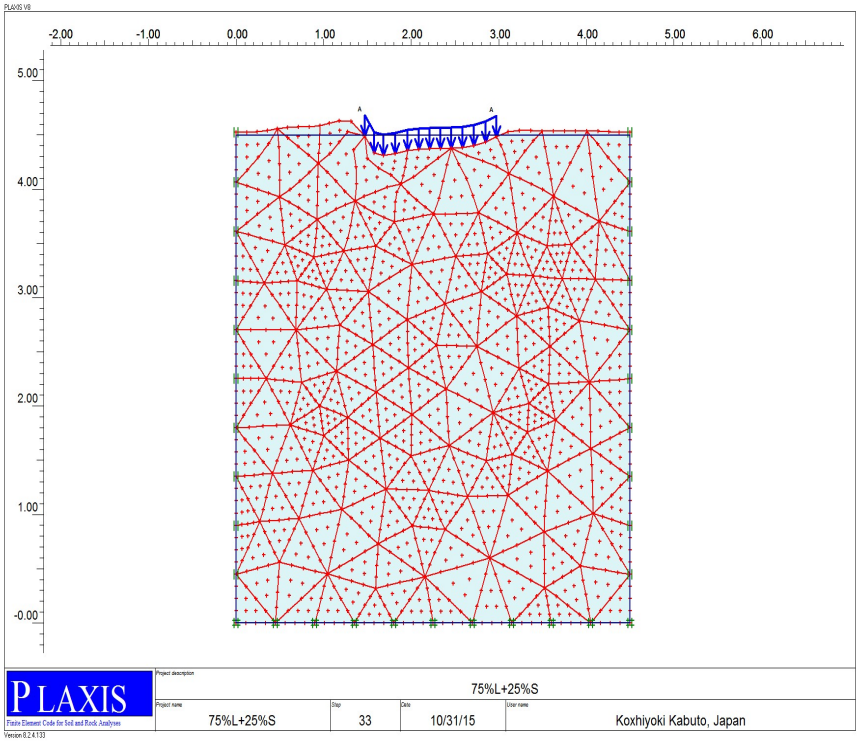

Fig. 4.12b Deformation Determined Using *Plaxis-2D* for Cylindrical Soil Specimen: 75%L+25%S

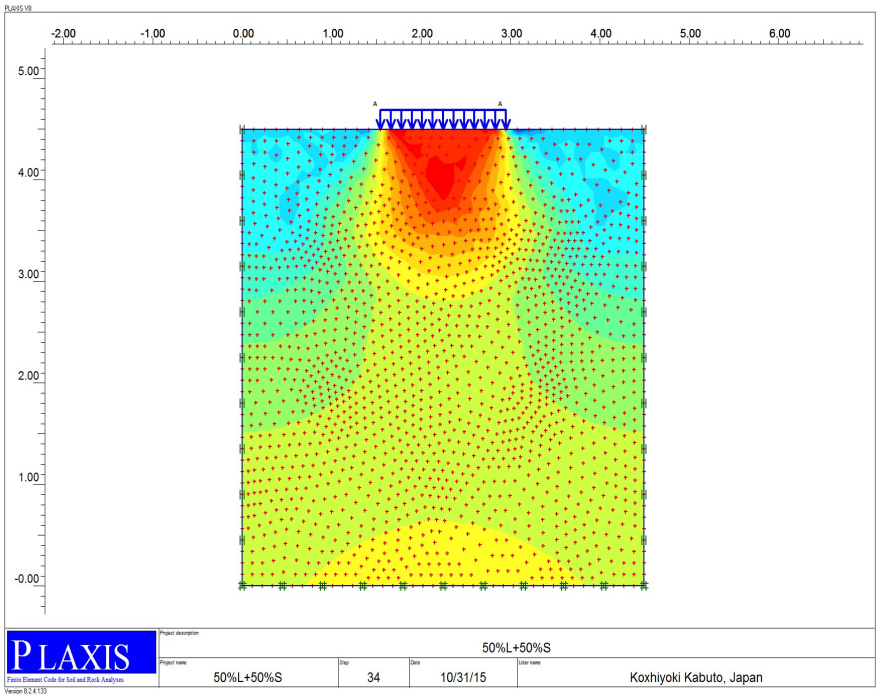

Fig. 4.12c Stress Distribution Determined Using *Plaxis-2D* for Cylindrical Soil Specimen: 50%L+50%S

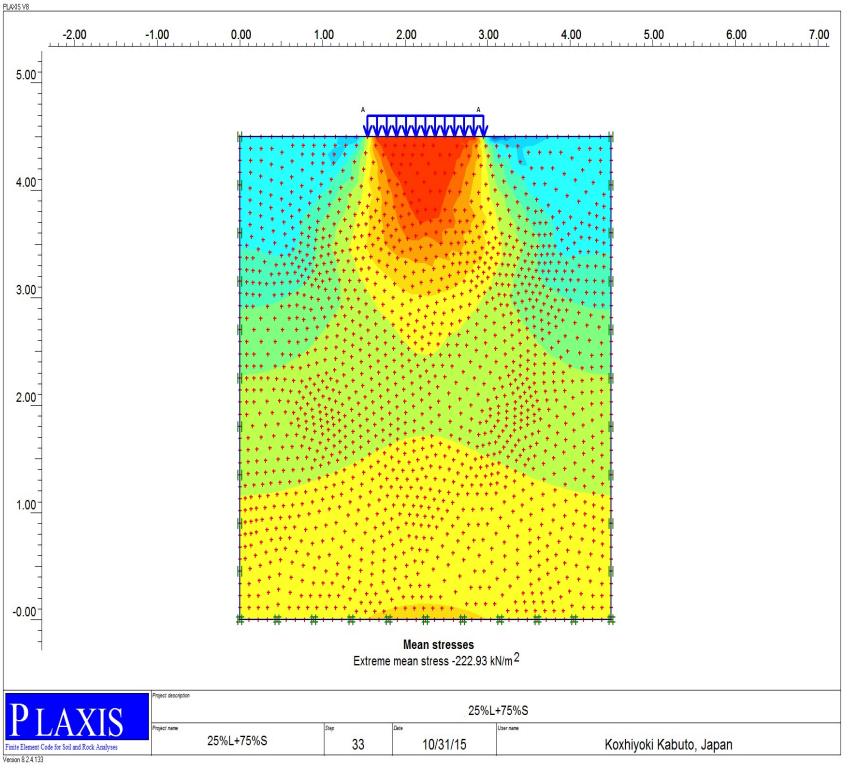

Fig. 4.12e Stress Distribution Determined Using *Plaxis-2D* for Cylindrical Soil Specimen: 25%L+75%S

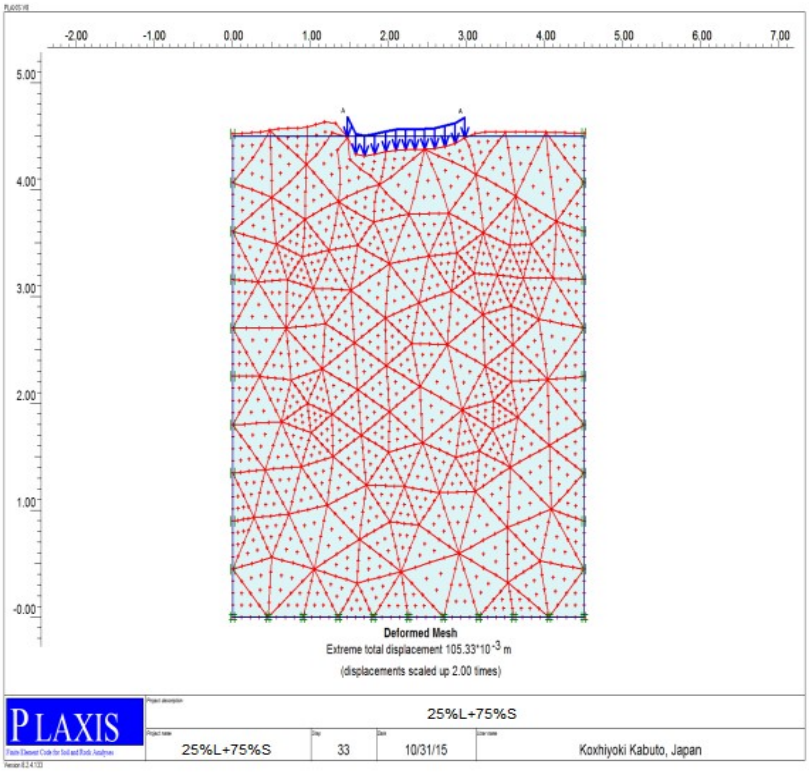

Fig. 4.12f Deformation Determined Using *Plaxis-2D* for Cylindrical Soil Specimen: 25%L+75%S

Table 4.12 Summary of Results of *FEM* Analyses on Predicted Deformations for

4.11 TESTS FOR RESILIENT MODULUS ON CYLINDERICAL SPECIMENS USING THE PFWD FOR VARIOUS BLENDS

The PFWD was used in determining the resilient modulus of soil subgrades and pavements. The main components of the equipment are enclosed in a hollow aluminium tube 1200 mm long, with a square cross-section of 100 mm side. It consists of a falling weight of 10 kg (22 lb) weight that drops over a height of 800 mm (31.5 inches) onto a loading plate fixed to the bottom of the tube. The falling weight is held in place by holding magnets. An accelerometer is attached to the falling weight in order to measure the deflection, and the rebound deflection. The *modulus of resilience* of the soil is estimated automatically by the embedded software in the PWFD, based on the deflection of the soil, and is displayed on the LCD screen immediately after each test. The display also provides details on the deflection, the rebound-deflection, and the impulse duration.

Loading plates of 200 mm diameter are used for investigations on soft soils where the *modulus of resilience* is estimated to be lesser than 10 MPa, while loading plates of 140 mm diameter are used for soils with *modulus of resilience* varying from 0 to 1200 MPa. The device is capable of applying a surface pressure of 730 to 1500 kPa below the loading plates. It can measure deflections from 0.1 to 5 mm (Englo, 2004). See Fig.4.13.

The tests were performed for various blends of soils and for various moisture contents, and the *Young's modulus of elasticity* or the *modulus of resistance* (E*pfwd*) was determined. Each blend of soil was compacted in 5 layers to a thickness of 350 mm at MDD for the OMC, wet-side of OMC (OMC+3%), and the dry-side of OMC (OMC-3%) in a cylindrical mild steel test box of inner diameter of 450 mm, and a total height of 450 mm. The experiments were performed in the laboratory. Details on the cylindrical mould used were provided in Fig.4.12 in the previous section. Table 4.13a and Table 13b; provide details on the test results for unsoaked and soaked samples respectively.

CHAPTER V

STUDIES ON SOIL STIFFNESS, AND MODULUS OF RESILIENCE USING CYCLIC TRIAXIAL TESTS

5.0 INTRODUCTION

It may be seen that preliminary standard tests on soils, including tests for index properties, and OMC were performed in the previous phase. Moreover, tests were performed on blended soils to obtain the CBR values, and the UCS. Investigations were also conducted using the static triaxial equipment to obtain the values of cohesion and internal friction for various soil blends, in addition to tests using the DCP and the PFWD.

The present chapter provides details on the second phase of experiments using the cyclic triaxial test equipment in order to determine the modulus of resilience. This chapter also provides details on the experimental procedure adopted in this study.

5.1 MEASUREMENT OF *RESILIENT MODULUS* USING THE CYCLIC TRIAXIAL TEST EQUIPMENT: GENERAL CONSIDERATIONS

The experimental setup for the determination of the *resilience modulus* using the cyclic triaxial test equipment consists of a loading frame with a crosshead mounted on a hydraulic actuator. Fig. 5.1 provides a schematic diagram of a soil specimen placed in a triaxial chamber.

The specifications regarding the size of the specimen and the method of preparation of the test specimen have undergone a number of changes as stipulated by AASHTO 307-99 for tests for *resilient modulus*. Accordingly, the soil specimens for fine-grained soils are required to have a diameter of 2.8 inches (71.1 mm) to 4.0 inches (101.6 mm), while for coarse grained soils, a diameter of 4.0 inches (101.6 mm) to 6.0 inches (152.4 mm) is specified with a diameter to length ratio of 1:2.

The specimens are housed in a triaxial cell where confining pressure was applied. A load cell is attached to the actuator to measure the applied load, and is mounted outside the triaxial chamber as specified by AASHTO T 307-99 (AASHTO, 2003). As the actuator applies the repeated load, the soil specimen undergoes deformation, which is measured by a set of *linear variable deflection transducers* (LVDT's).. The load cycle duration, for the hydraulic loading device is 1 second, which includes a 0.1 second loading duration, and an unloading period of 0.9 seconds. AASHTO T 307 specifies the use of a haversine-shaped loading waveform as shown in Fig.5.2.The repeated axial load is applied on top of the

cylindrical specimen under a confining pressure. Compressed air is used to build-up the confining pressure. The total recoverable axial deformation response of the specimen is measured and is used to calculate the *resilient modulus*. A data acquisition system records all output data generated while testing.

In a repeated load triaxial test, the *resilient modulus* is defined as the ratio of the deviator stress to the recoverable strain, and is expressed as follows:

$M_r = (\sigma_1 - \sigma_3) / \varepsilon_r$, or

$M_r = \sigma_d / \varepsilon_r$ Eq. 5.1

Where M_r = resilient modulus; ε_r = resilient strain (recoverable axial strain); σ_1 = total axial stress (or major principal stress) applied; σ_3 = confining stress (or radial stress on the sample); and σ_d = deviator stress (cyclic stress in excess of confining pressure due to the vertical load); and where $\sigma_1 = \sigma_d + \sigma_3$. This is further illustrated in Fig.5.3

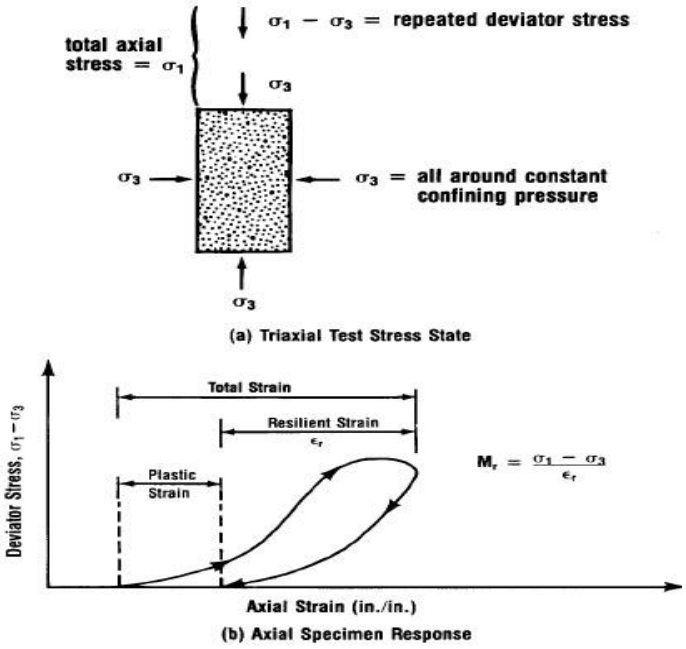

Fig. 5.3 Illustration for Resilient Modulus (Barksdale, 1993)

5.2 PROCEDURE FOR DETERMINATION OF RESILIENT MODULUS OF SOILS USING CYCLIC TRIAXIAL TEST EQUIPMENT

The repeated load triaxial test equipment consists of a loading frame powered by either a pneumatic or electro-hydraulic loading system. The apparatus is capable of generating a haversine or rectangular loading waveform for cyclically loading a soil specimen at a predefined frequency. The study using the cyclic triaxial test equipment for determining the *resilient modulus* for pure and blended lateritic and lithomargic soil blends was performed at Siddaganga Institute of Technology, Tumkur.

5.2.1 Preparation of the Soil Specimen

The optimum moisture content (OMC) for the soil sample was initially obtained based on modified Proctor tests performed as per IS:2720 Part VIII (1983), where 5 layers of soil, each compacted with 25 blows of a rammer of 4.9 kg falling through a height of 45cm. The density of the soil at OMC, and the dry density determined using the modified Proctor tests were used in preparing the soil specimens for the cyclic triaxial tests. Moulds of 50mm diameter, and 100mm height were used to prepare the soil specimens. Oven dried soil maintained between 100-110 °C for 24 hours was added with the required quantity of water for OMC in the preparation of the soil specimens. The various steps involved in the preparation of the soil specimen are illustrated in Fig. 5.4a to Fig. 5.4d

Fig. 5.4a Mixing of Dry Soil with Water

Fig. 5.4b Using the Rammer of the Kneading Compactor to Compact Soil to the Desired Density

Preparation of the Soil Specimen

5.2.2 Mounting the Soil Specimen on to the Cyclic Triaxial Test Equipment

A filter paper was placed at the top and the bottom surfaces of the soil specimen prepared as mentioned above, and a porous stone was placed above and below the specimen as specified in (IS 2720 Part XII -1981). A thin rubber membrane was then slipped over the specimen using a metal jacket of 54 mm diameter, and the O-rings were slipped into position at the top and at the bottom. The load-cell attachment along with a pore-pressure applying/ measuring lead were then placed over the prepared specimen, and a cylindrical glass chamber (as used in triaxial tests) was clamped over the setup. The entire assembly was then sealed. See Fig. 5.4e – Fig. 5.4L. Proper care was taken so as to seal the joints using vaseline or grease.

The connecting tap at the centre of the above assembly, through which the confining pressure (or cell-pressure) was to be applied, was connected to the compressor. The cylindrical glass chamber was then filled with water through the tap at the top-centre. The entire assembly was mounted on the loading platform of the cyclic triaxial testing machine. Two LVDTs (linear variable deflection transducers) used in measuring the deflections were then attached to the assembly. The data cable was then connected to the computer based measurement system. See Fig. 5.4m –Fig. 5.4s.

5.2.3 Application of Repeated Loads for Cyclic Triaxial Tests on the Soil Specimens

The *hydraulic pump*, the electronic control system, and the computer system attached to the machine were switched on. See Fig. 5.5a and Fig. 5.5b.The software named *Cyclic System Console V1.0.0* was then activated so as to function in the *Dynamic test* mode. See Fig. 5.5c.

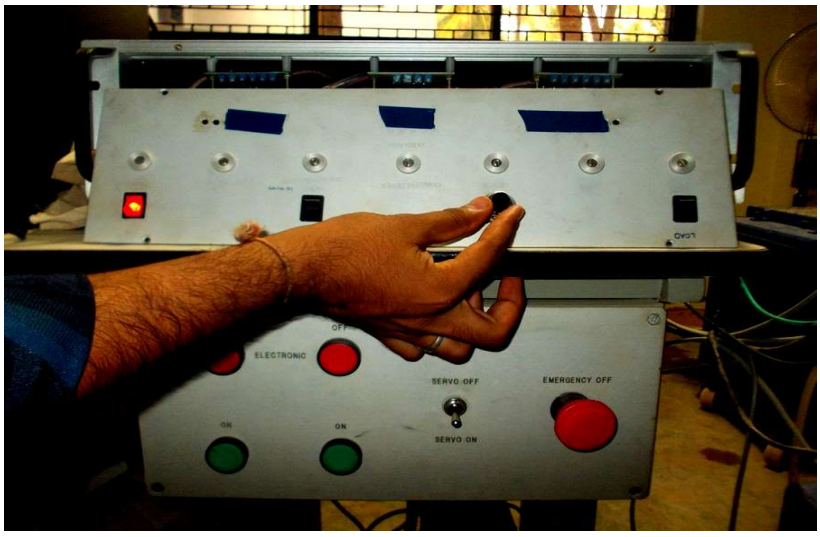

Fig. 5.5a Switch Panel for Hydraulic Pump and Electronic System

Fig. 5.5b Switch Panel for Hydraulic Pump with Cyclic Triaxial Test System

5.3 RESULTS OF TESTS USING THE CYCLIC TRIAXIAL TEST EQUIPMENT

The results of the repeated load triaxial test on pure and blended lithomarge and lateritic soil compacted at maximum dry density at optimum moisture content are presented below. The values for the *resilient modulus* were computed as the ratio between the deviatoric stress to the recoverable strain for the 96^{th}, 97^{th}, 98^{th}, 99^{th}, and the 100^{th} loading cycles, and the *mean resilient modulus* of the soil specimen was determined and reported.

5.3.1 Test Results: 100%L + 0%S: OMC

In each sequence of test, on the completion of 100 loading cycles, the stop button in the display software was pressed. The output generated for these 100 loading cycles was then automatically saved in the form of a *.txt* file by the system. The *.txt* file was converted to a *spread-sheet* form for further computation.

In the above mentioned figure, it is possible to visually identify the point corresponding to the maximum load in the 1^{st} loop of the plot. This load is considered as the *actual maximum axial load* that the specimen is subjected to in the 96^{th} cycle, from which

actual applied cyclic stress can be obtained, based on which the *resilient modulus* (M_r) for 96th cycle is computed.

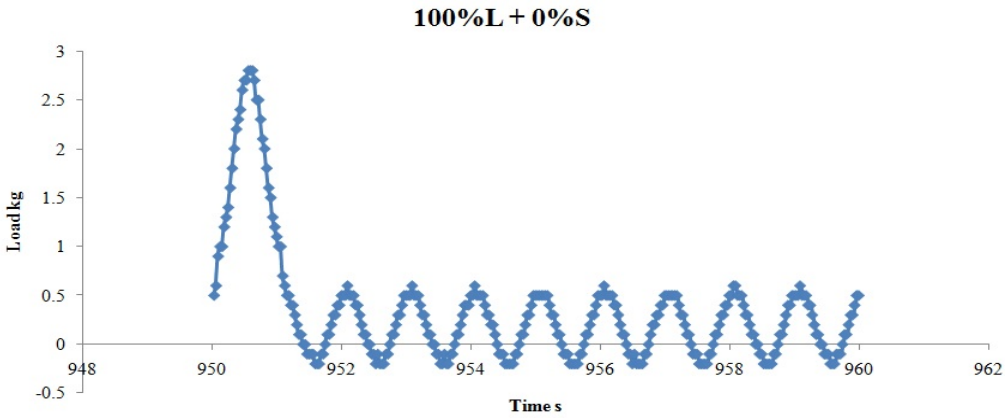

Fig.5.6a Load Vs Time Relationships: 100%L+0%S: *Cp*=0.41 kg/cm^2 D_L=0.25 kg for 96th Cycle: OMC

At the end of each 100 cycle of loading, the .txt file generated by the system is analysed. A typical output generated by the system is shown in Fig.5.6b. The stress and strain values, for each data point, can be computed using a *spread-sheet* application based on the corresponding data on load and displacement.

The typical *cyclic stress Vs strain* graph is plotted based on 320 data points for each cycle. The values corresponding to the first 32 data points represent the stress and strain values for the *loading sequence*, while the rest of the data points represent the *unloading sequence*. The curve ABC in Fig.5.6c; represents the cyclic stress-strain behaviour considering the first 40 data points for the 96th cycle for a confining pressure (*Cp) of* 0.41 kg/cm^2, and a deviator load (D_L) of 0.25 kg.

```
Data Points,Cycle,Time (ms),Load,Displacement,Conff Pressure,
Pore Pressure,Volume Change,Back Pressure,External Disp,Bender Element
1,1,.00,1.2,00.139,0.40,00.02,-3.2,0.02,00.00,-3.8
2,1,31.25,1.2,00.143,0.41,00.02,-3.1,0.02,00.00,-3.6
3,1,62.50,1.2,00.133,0.41,00.03,-3.1,0.02,00.00,-3.6
4,1,93.75,1.0,00.146,0.40,00.01,-3.1,0.02,00.00,-3.6
5,1,125.00,0.9,00.139,0.40,00.02,-3.1,0.02,00.00,-3.6
6,1,156.25,1.1,00.139,0.40,00.02,-3.1,0.02,00.00,-3.6
7,1,187.50,1.3,00.139,0.40,00.02,-3.2,0.03,00.00,-3.6
8,1,218.75,1.3,00.138,0.40,00.02,-3.2,0.02,00.00,-3.6
9,1,250.00,1.5,00.139,0.40,00.02,-3.2,0.02,00.00,-3.6
10,1,281.25,1.8,00.139,0.40,00.02,-3.2,0.02,00.00,-3.5
11,1,312.50,1.9,00.141,0.40,00.02,-3.2,0.02,00.00,-3.5
12,1,343.75,2.0,00.140,0.40,00.02,-3.1,0.02,00.00,-3.5
13,1,375.00,2.3,00.139,0.41,00.03,-3.1,0.03,00.00,-3.5
14,1,406.25,2.4,00.135,0.40,00.02,-3.1,0.03,00.00,-3.5
15,1,437.50,2.5,00.140,0.40,00.02,-3.1,0.03,00.00,-3.5
16,1,468.75,2.7,00.135,0.40,00.02,-3.1,0.02,00.00,-3.6
17,1,500.00,2.7,00.140,0.40,00.02,-3.1,0.02,00.00,-3.6
18,1,531.25,2.8,00.137,0.40,00.02,-3.2,0.02,00.00,-3.6
19,1,562.50,2.8,00.139,0.41,00.03,-3.2,0.03,00.00,-3.6
20,1,593.75,2.9,00.137,0.41,00.02,-3.2,0.02,00.00,-3.6
21,1,625.00,2.8,00.138,0.40,00.02,-3.2,0.03,00.00,-3.6
22,1,656.25,2.6,00.145,0.41,00.03,-3.2,0.02,00.00,-3.5
```

Fig.5.6b Data generated by the System: 100%L+0%S: *Cp*=0.41 kg/cm^2 D_L=0.25 kg for 96th Cycle: OMC

The point where the strain reaches a constant value (corresponding to point C) represents the plastic strain (ε_P) that occurs at the *unloading sequence*. The difference between the *maximum strain* (ε_{max}) and the *plastic strain* (ε_P) gives the *recoverable axial strain* or *resilient strain* (ε_r) based on which the modulus of resilience M_r is can be calculated. The first row in Table 5.4a provides details on the observations made for the 96th cycle. In a similar manner, the remaining rows provide details on the computations for the *resilient strain* for the 97th, 98th, 99th, and 100th loading cycles.

Based on the maximum axial load obtained using the *load vs time* relationship as shown in Fig.5.6a, it is possible to compute the actual contact load as 0.1 times the maximum axial load. The actual cyclic load, the maximum axial stress, the actual contact stress, and the actual cyclic stress are then computed as shown in Table 5.4b. Based on data compiled for the 96th, 97th, 98th, 99th and 100th loading cycles. The *modulus of resilience* of the soil sample for the given deviator stress, and for the given confining stress, is then computed as the average of the observations made for the last 5 loading cycle. Appendix A3 provides details on computations for other confining pressures and blends. Fig.5.6d provides details on the variations between the *resilient modulus Vs* the *deviator stresses* for various confining stresses.

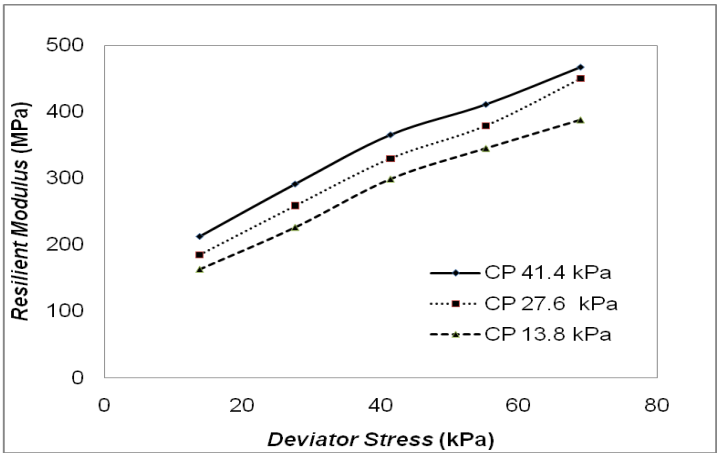

Fig.5.6d Resilient Modulus Vs Deviator Stress Relationships: 100%L+0%S: OMC

5.3.2 Test Results: 75%L + 25%S

In each sequence of test, on the completion of 100 loading cycles, the stop button in the display software was pressed. The output generated for these 100 loading cycles was then automatically saved in the form of a *.txt* file by the system. The *.txt* file can be converted to a *spread-sheet* form for further computation.

From the above mentioned figure, it is possible to visually identify the point corresponding to the maximum load in the 1st loop of the plot. This load is considered as the *actual maximum axial load* that the specimen is subjected to in the 96th cycle, from which *actual applied cyclic stress* can be obtained. This *applied cyclic stress* value is required for calculating the value of the resilient modulus (M_r) for 96th cycle.

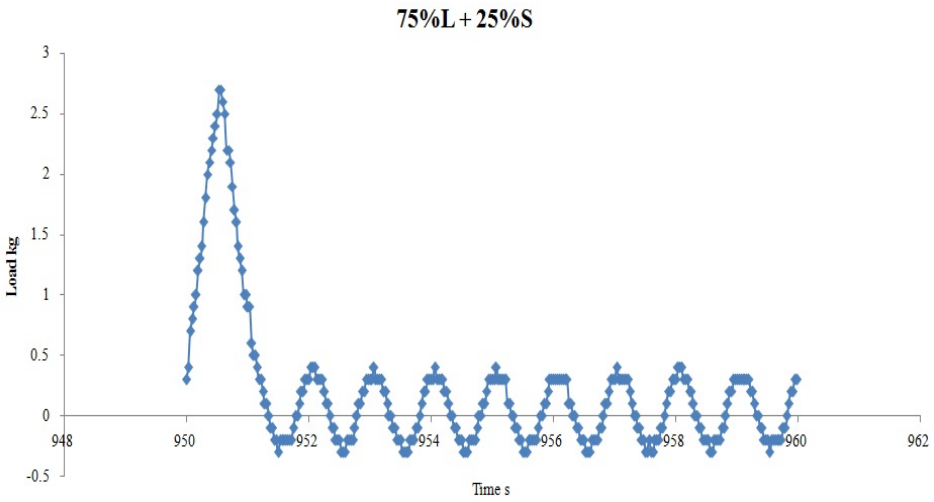

Fig.5.6e Load Vs Time Relationships: 75%L+25%S: *Cp*=0.41 kg/cm^2 D_L= 0.25 kg for 96th Cycle: OMC

The typical *cyclic stress Vs Strain graph* is plotted based on 320 data points for each cycle. The values corresponding to the first 32 data points represent the stress and strain values for the *loading sequence*, while the rest of the data points represent the *unloading sequence*. The curve ABC in Fig.5.6f represents the cyclic stress-strain behavior considering the first 40 data points for the 96th cycle for a confining pressure (*Cp) of* 0.41 kg/cm^2, and a deviator load (D_L) of 0.25 kg.

In the above mentioned in Fig.5.6g, the highest point on the abscissa (corresponding to point B) for the curve ABC represents the maximum value of strain (ε_{max}) that occurs at the *loading sequence*. The point where the strain reaches a constant value (corresponding to point C) represents the plastic strain (ε_P) that occurs at the *unloading sequence*. The difference between the *maximum strain* (ε_{max}) and the *plastic strain* (ε_P) gives the *recoverable axial strain* or *resilient strain* (ε_r) based on which the modulus of resilience *Mr* is can be calculated. The first row in Table 5.5a provides details on the computation of the *resilient strain* for the 96th cycle. In a similar manner, the computations of the *resilient strain* for the 97th, 98th, 99th, and 100th loading cycles were performed.

Based on the maximum axial load obtained using the load vs time relationship shown in Fig.5.6e, it is possible to compute the actual contact load as 0.1 times the maximum axial load. The actual cyclic load, the maximum axial stress, the actual contact stress, and the actual cyclic stress are then computed as shown in Table 5.5b based on data compiled for the 96th, 97^{th}, 98^{th}, 99^{th}, and 100^{th} loading cycles. The *modulus of resilience* of the soil sample for the given deviator stress, and for the given confining stress, is then computed as the average of the observations made for the last 5 loading cycle. Fig. 5.6f provides details on the variations between the *resilient modulus Vs* the *deviator stresses* for 75%L+25%S of at various confining pressures.

5.3.3 Test Results: 50%L + 50%S

Tests were performed for the blend at 50%L + 50%S at OMC, OMC+3%, and OMC-3% moisture conditions. The relation between resilient modulus vs deviator stress are provided Fig. 5.6g. Similarly, the tables showing details on computations for resilient strain, and computations for resilient modulus, are provided in Table 5.6a and Table 5.6b.

5.3.4 Test Results: 25%L + 75%S

Tests were performed for the blend at OMC, OMC+3%, and OMC-3% moisture conditions. The resilient modulus vs deviator stress relationships are provided Fig. 5.6h. Similarly, the tables showing details on computations for resilient strain, and computations for resilient modulus, are provided vide Table 5.7a and Table 5.7b.

Fig. 5.6h Resilient Modulus Vs Deviator Stress Relationships: 25%L + 75%S: OMC

5.3.5 Test Results: 0%L + 100%S

Tests were performed for the blend at at OMC, OMC+3%, and OMC-3% moisture conditions. The resilient modulus vs deviator stress relationships are provided in Fig. 5.6i. Similarly, the tables showing details on computations for resilient strain, and computations for resilient modulus, are provided vide Table 5.a. and Table 5.8b.

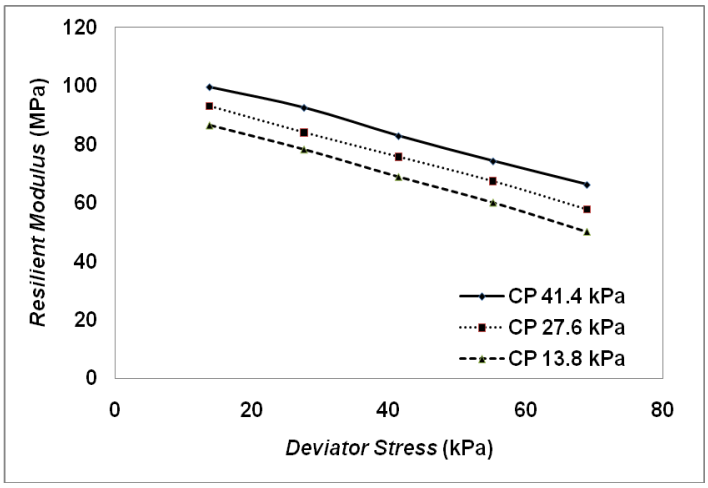

Fig. 5.6i Resilient Modulus Vs Deviator Stress Relationships: 0%L + 100%S: OMC

5.3.6 Summary of Results from the Cyclic-Triaxial Tests

See Table 5.9 for details on final computed values for resilient moduli for various blends tested at -3%OMC, at OMC and +3%OMC.

`

CHAPTER VI

DEVELOPMENT OF REGRESSION MODELS BASED ON RESULTS FOR PHASE I AND PHASE II, AND DISCUSSIONS

6.0 INTRODUCTION

The soil in the Southern Peninsular region of India, including the coastal areas of Dakshina Kannada, and Malabar (Northern Kerala) mainly comprises of lateritic characteristics. Engineers of these regions encounter situations where road subgrades and embankments need to be constructed over *laterite soils* intermixed with weak *silty-fines* (locally known as 'shedi' soils). The presence of hard *laterite* soils are generally confined to the top 2 to 3 meters in these regioins (Ahn, 1970; Yaji, 1993) whereas the layers below consist mainly of *silty (*or *Shedi*) soils characterized by high silt content, and low strengths (Nye, 1955; Gidigasu, 1976).

The soils with *lateritic* constituents ranging from 25 to 50% are generally known as *lateritic-lithomarges*, while soils with *lateritic* constituents ranging from 50 to 75% are known as *lithmargic-laterites.*

Based on the above studies, it is possible to develop regression equations that can help engineers correlate various soil properties to soil stiffness. This chapter provides details on the regressions developed using the Statistical Package for Social Sciences (SPSS). The best possible regressions were identified based on the *R*-square values, the adjusted *R*-square values, the standard error of estimate, the *F-test* value, the *t-test* value, and the level of significance also known as the *p* value (indicated as 'Sig F' in the tables included in this chapter).

6.1 DEVELOPMENT OF CORRELATIONS BASED ON TESTS ON INDEX PROPERTIES, GRAIN SIZE DISTRIBUTION, PERMEABILITY, MDD, AND OMC

The following sub-sections provide details on the regressions developed based on investigations on index properties, grain-size distribution, permeability, maximum-dry-density (MDD), and optimum moisture content (OMC).

The regressions were developed using the *Statistical Package for Social Sciences* (SPSS), for the five blends of *lateritic* and *lithomargic* soils tested. Table 6.1 provides details on the summarized results obtained based on standard tests performed on lateritic soils of Dakshina Kannada region.

`

6.1.1 Effect of percentages of *fines* on the *OMC*, *MDD*, Specific Gravity, Grain-size Distribution, Permeability, and Atterberg's Limits

Based on Table 6.1, it may be noted that as the fines content increases, the *OMC* increased from 13.8 to 20.4 percent. This is due to the reason that the addition of silty-fines to laterite soils increases the proportion of smaller sized particles resulting in an increase in the *total surface-area* of the soil particles. Also, the increase in the percentage of fines has resulted in a corresponding decrease in the proportion of gravel and sand from 30.2 to 2 % and from 55.8 to 12% respectively. This has also resulted in a decrease in the MDD from 1.97 g/cc to 1.67 g/cc. Moreover, an increase in the fines content has consequently resulted in a decrease in the permeability 1.79×10^{-7} to 1.54×10^{-9} m/sec. The above mentioned variations are graphically represented in Fig.6.1. Similar observations were made by Hicks and Monismith (1971). Omotosho (2004) also provides similar observations based on studies conducted on laterite soils of Nigeria.

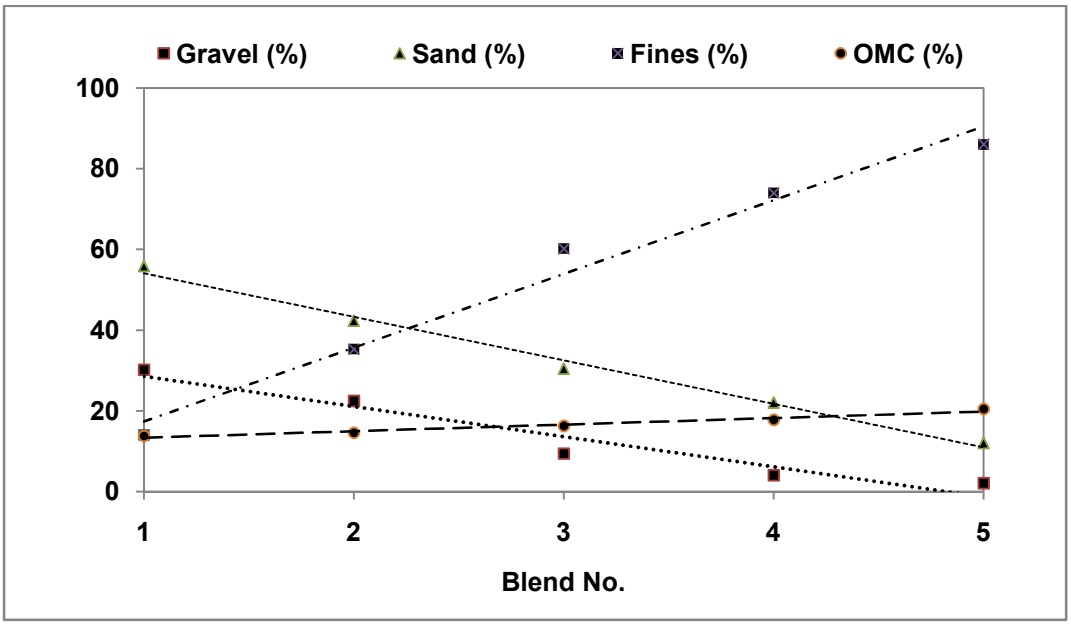

Fig. 6.1 Effect of Variations in Percentages of Fines, Gravel and Sand on OMC

It may also be observed that an increase in the fines content has resulted in a decrease in the specific gravity from 2.58 to 2.37. However, since the Atterberg's limits depend to a large extent on the presence of clays or soil fractions lesser than 2 microns, and since the proportion of soil fractions lesser than 2 microns has not changed significantly with the increase in the

`

percentage of silty-fines, no significant change in the values of Atterberg's limits were observed for various blends of soils. Similar studies on silty soils were performed by Wong et al. (2017).

6.1.1.1 Correlation between *Fines* (%) and the *Specific Gravity* for Various Soil Blends

From Table 6.1, it may be noted that for the lateritic soil blends 100%+0%S, *75%L+25%S, 50%L+50%S, 25%L+75%S* and 0%L+100%S, the increase in the fines content has been accompanied by a decrease in the specific gravity.

6.1.1.2 Correlation between *Fines* (%) and *MDD* for Various Soil Blends

It is also seen in Table 6.1 that for the lateritic soil blends 100%+0%S, *75%L+25%S, 50%L+50%S, 25%L+75%S* and 0%L+100%S compacted to OMC, the increase in the fines content is related to a decrease in the values of *MDD*.

A regression between the percentages of *fines* vs *MDD* as shown in Eq 6.2 was developed. The scatter plot for the same is given in Fig. 6.1b. The relationship developed indicates that the *percentage of fines* and the *MDD* are correlated linearly with an R-square value of 0.962, an adjusted R-square value of 0.94, a standard error of 6.29, and *F-test* and *t test* values of 50.46 and 9.83 respectively at a significance of 0.003 for a confidence level of 99.99%.

$$Fines\ (\%) = -242(MDD) + 496.3 \qquad \text{Eq.6.2}$$

6.1.1.3 Correlation between *Fines* (%) and *Optimum moisture content*, *OMC* (%) for Various Soil Blends

It is also seen in Table 6.1 that for the lateritic soil blends 100%+0%S, *75%L+25%S, 50%L+50%S, 25%L+75%S* and 0%L+100%S compacted to OMC, the increase in the fines content is related to a increase in the percentage of *OMC*.

$$Fines\ (\%) = 10.52\ (OMC) - 119.98 \qquad \text{Eq.6.3}$$

`

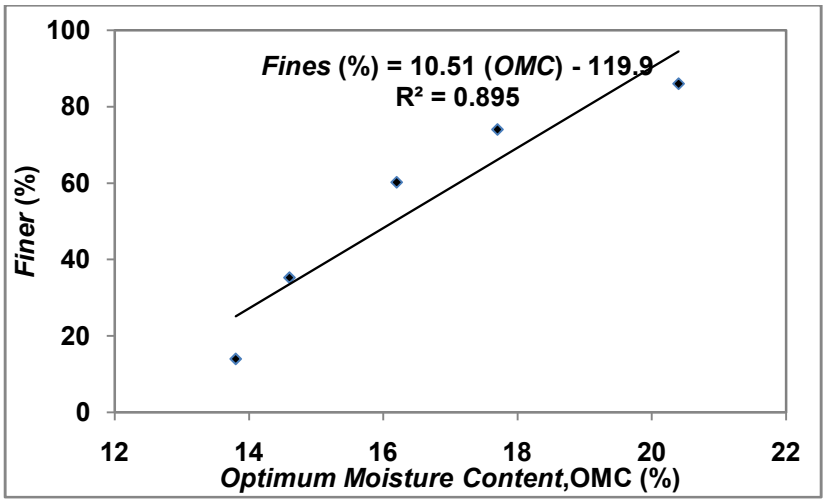

Fig.6.1c Correlation between Fines (%) and Optimum moisture content, *OMC* (%)

A regression between the percentages of *fines* vs *OMC* as shown in Eq 6.3 was developed. The scatter plot for the same is given in Fig. 6.1c. The relationship developed indicates that the *percentage of fines* and the *OMC* are correlated linearly with an R-square value of 0.895, an adjusted R-square value of 0.86, a standard error of 10.92, and *F-test* and *t test* values of 25.57 and -3.45 respectively at a significance of 0.014 for a confidence level of 99.99%. This relationship holds good for OMC values ranging between 13 and 21% for lateritic soils.

6.1.1.4 Correlation between *Fines* (%) and *Permeability Constant*, k (m/sec) for Various Soil Blends

In Table 6.1, it can also be observed that for the lateritic soil blends 100%+0%S, *75%L+25%S, 50%L+50%S, 25%L+75%S* and 0%L+100%S compacted to OMC, the increase in the fines content is related to a decrease in the values of permeability.

Fines (%) = 98.27- 44.69 (*k*) Eq. 6.4

A regression equation developed between the percentage of *fines* vs *permeability* (k) is shown in Eq.6.4 and scatter plot for the same is given in Fig. 6.1d. The relationship developed indicates that the percentage of fines and the *permeability* are correlated linearly with an R-square value of 0.975, an adjusted R-square value of 0.967, a standard error of 5.27, and *F-test* and *t test* values of 119.6 and 20.93 respectively for a confidence level of 99.99%.

`

6.1.1.8 Development of Multi-linear Regressions Relating Fines to MDD, Specific Gravity, Permeability, and Atterberg's Limits

Based on Tables 6.1, it was found that a multi-linear regression could be developed relating the fines content to the MDD, specific gravity, permeability, and the Atterberg's limits. The details of the various regressions developed (Eq. 6.1s to Eq.6.1f) along with the related statistical values including *R* square values, are provided in Table 6.2.

6.1.2 Effect of *Fines, Gravel, Sand, MDD, and Moulding water content* on *Unconfined Compressive Strength*

The *unconfined compressive strength* (q_u) is an important material parameter that indicates the strength and stiffness of soil subgrades. Tests for Unconfined Compressive Strength (q_u) were performed according to IS: 2720 Part X (1973). The investigations were performed on re-moulded soil samples of 38 mm diameter and 76 mm height for various soil blends and moisture contents.

The details on fines content for various lateritic soil blends as summarized in Table 6.1, and the results on the *UCS* values for various soil blends for samples tested for moisture contents *M1, M2,* and *M3* as available in Table 4.8a, can be further summarized as in Table 6.3. In this part of the study, the influence of fines, gravel, sand, *OMC*, and *MDD* is examined. Fig. 6.2a illustrates the variations in the *unconfined compressive strength* (q_u) across various lateritic soil blends for various compacting moisture contents *OMC-3%* (denoted as *M1*), *OMC* (denoted as *M2*), and *OMC+3%* (denoted as *M3*).

6.1.2.1 Correlations between Fines (%) and *UCS* for Various Soil Blends

Table 6.3 provides a summary of details on the values of q_u, for various blends of lateritic soil samples compacted to moisture contents for various blends B1 to B5 with fines content varying from 14% to 86%. The table also provides details on the molding moisture contents *M1*, *M2*, and *M3* for the soil samples tested.

It can be observed that for various blends of lateritic soils tested at molding moisture content of *M1* (*OMC-3%*), the *unconfined compressive strength* (q_u) decreased from 0.399 MPa to 0.129 MPa. Similarly, for molding moisture content of *M2* (*OMC*), the values of q_u decreased from 0.321 MPa to 0.105 MPa. Also, for molding moisture content *M3* (*OMC*+3%) the values of q_u decreased from 0.310 MPa to 0.091 MPa. Thus, it can be seen that the strength of the soil

`

decreases with increase in the fines content from 14 to 86% irrespective of the molding moisture contents.

6.1.2.2 Correlations between *Gravel* (%) and *UCS* of Various Soil Blends

Based on a summary of the details on values of q_u, for various blends of lateritic soil samples and for various molding moisture contents as shown in Table 6.3, regression equations were developed correlating the values of the *UCS* for various lateritic soil blends (*B1* to *B5*) to the percentage of gravel for soil samples tested at moisture contents *M1*, *M2*, and *M3* as shown in Table 6.5. The scatter plot for the same is provided in Fig. 6.2c.

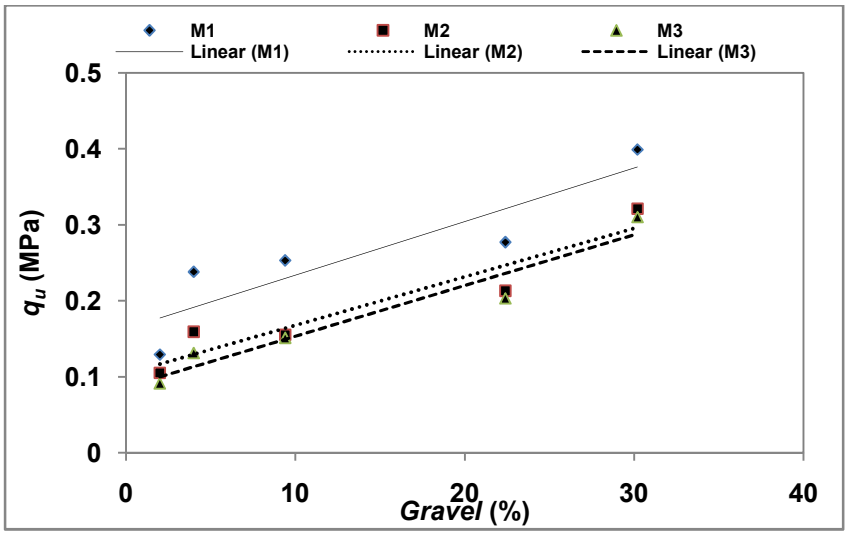

Fig.6.2c Correlation between *Gravel* (%) vs. *UCS* (q_u)

6.1.2.3 Correlations between *Sand* (%) and *UCS* of Various Soil Blends

Based on a summary of the details on values of q_u, for various blends of lateritic soil samples and for various molding moisture contents as shown in Table 6.3, regression equations were developed correlating the values of the *UCS* for various lateritic soil blends (*B1* to *B5*) to the percentage of sand for soil samples tested at compacted at moisture contents *M1*, *M2*, and *M3* as shown in Table 6.6. The scatter plot for the same is provided in Fig. 6.2d.

`

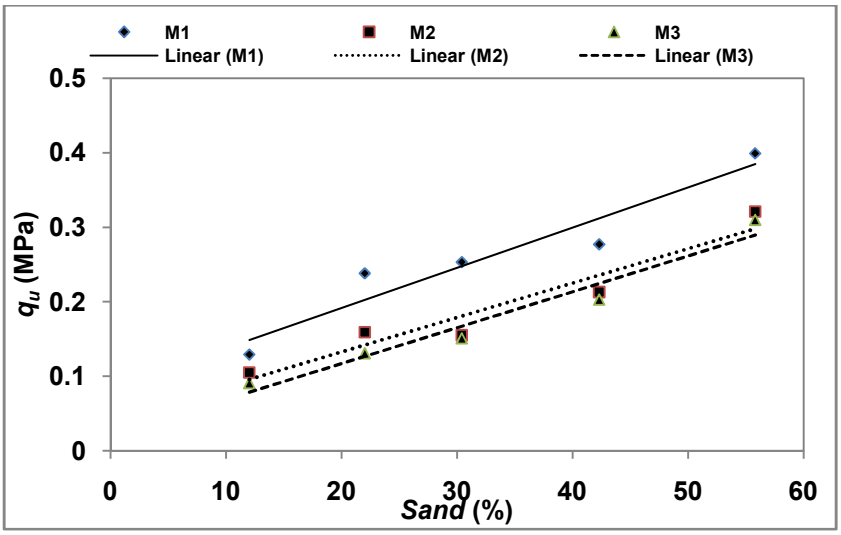

Fig. 6.2d Correlation between Sand (%) vs. UCS (q_u)

6.1.2.4 Correlations between *MDD* (Maximum Dry Density) and *UCS* of Various Soil Blends

Based on a summary of the details on values of q_u, for various blends of lateritic soil samples and for various molding moisture contents as shown in Table 6.3, regression equations were developed correlating the values of the *UCS* for various lateritic soil blends (*B1* to *B5*) to the *MDD* (maximum dry density) for soil samples tested at compacted at moisture contents *M1*, *M2*, and *M3* as shown in Table 6.7. The scatter plot for the same is provided in Fig. 6.2e.

`

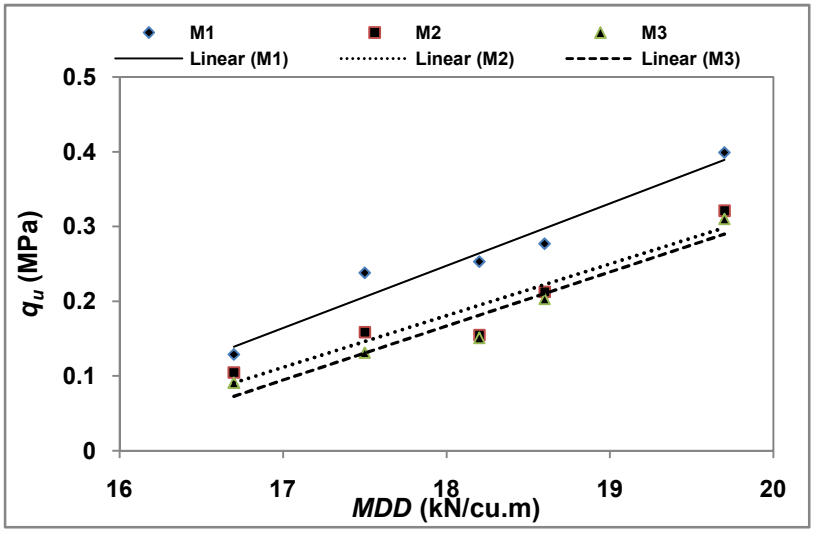

Fig.6.2e Correlation between *MDD* (kN/cu.m) *vs. UCS* (q_u)

6.1.2.5 Correlations between *moulding water content* and *UCS* for Soil Blends

Based on a summary of the details on values of q_u, for various blends of lateritic soil samples and for various molding moisture contents as shown in Table 6.3, regression equations were developed correlating the values of the *UCS* for various lateritic soil blends (*B1* to *B5*) to the moisture content for soil samples tested at compacted at moisture contents *M1*, *M2*, and *M3* as shown in Table 6.8. The scatter plot for the same is provided in Fig. 6.2f.

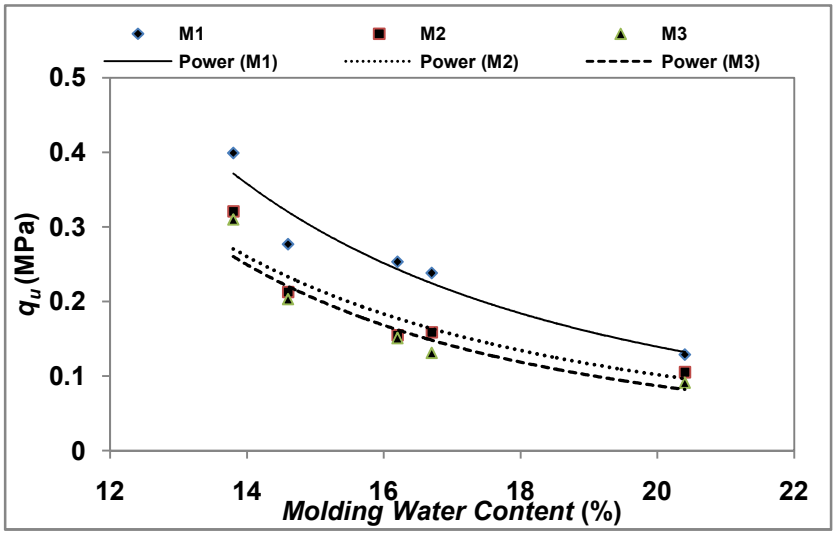

Fig.6.2f Correlation between *Moulding water content* (%) *vs. UCS* (q_u)

`

6.1.3 Effect of *Fines, Gravel, Sand, MDD, and Moulding water content* on Cohesion for Triaxial Tests on Various Soil Blends

The *cohesion* (*C*) is an important material parameter that indicates the shear strength of soil subgrades. Static *Triaxial* tests were performed according to IS: 2720 Part XI (1981) to determine the *cohesion* ($_C$) for various soil blends. The investigations were performed on re-molded soil samples of 38 mm diameter and 76 mm height for various soil blends and moisture contents.

The details on fines content for various lateritic soil blends as summarized in Table 6.1, and the results on the static *triaxial* tests for various soil blends for samples tested for moisture contents *M1, M2,* and *M3* as available in Table 4.9a, can be further summarized as in Table 6.9. In this part of the study, the influence of fines, gravel, sand, *MDD,* and *OMC* on *cohesion* is examined. Fig. 6.3a illustrates the variations in the values of *cohesion* (*c*) across various lateritic soil blends for various compacting moisture contents *OMC-3%* (denoted as *M1*), *OMC* (denoted as *M2*), and *OMC+3%* (denoted as *M3*).

A comparison on the variations in the values of *cohesion* for compacting moisture contents *M1, M2,* and *M3* indicate that the cohesion values are the highest at optimum moisture contents for each blend of lateritic soil sample. Kim and Kim (2006) also made similar observations. These observations also agree with the finding of Cokca et al. (2004) that the cohesion at the *drier side of optimum* will be lesser than that at *OMC* due to the *clay aggregation* phenomenon which gives rise to a granular texture to the soil mass, and the findings of Seed et al. (1961) that the cohesion on the wetter side of optimum is lesser than that at OMC due to formation of 'thicker water films' around clay particles in the 'clay-water system'.

6.1.3.1 Correlations between *Fines* (%) and *Cohesion* for Various Soil Blends

Table 6.9 provides a summary of details on the values of *cohesion* (*c*), for various blends of lateritic soil samples compacted to moisture contents for various blends *B1* to *B5* with fines content varying from 14% to 86%. The table also provides details on the molding compacted moisture contents *M1*, *M2*, and *M3* for the soil samples tested.

It can be observed that for various blends of lateritic soils tested at molding moisture content of *M1* (*OMC-3%*), the *cohesion* increased from 26.4 MPa to 71 MPa. Similarly, for molding moisture content of *M2* (*OMC*), the values of *c* increased from 30.2 MPa to 100MPa. Also, for molding moisture content *M3* (*OMC*+3%) the values of *C* increased from 13 MPa to 65

`

MPa. Thus, it can be seen that the cohesion of the soil increased with increase in the fines content from 14 to 86% irrespective of the molding moisture contents. This is graphically illustrated in Fig.6.3a which indicates that as the percentage of fines in the blended soil samples increases from blends *B1* to *B5*, an increase in *Cohesion* (*c*) is observed irrespective of the compaction moisture contents.

Regression equations were developed correlating the values of *cohesion* for various lateritic soil blends (*B1* to *B5*) to the values of *Fines* for samples compacted at moisture contents *M1, M2*, and *M3* as shown in Table 6.10. The scatter plot for the same is provided in Fig. 6.3b. Based on the trend-lines of regressions developed, it can be surmised that the increase in the proportion of silty soil from blends B_1 to B_5, resulted in a consequent decrease in the sand content and a consequent increase in the values of *cohesion* following an exponential relationship.

Based on a summary of the details on values of *c,* for various blends of lateritic soil samples and for various molding moisture contents as shown in Table 6.9, regression equations were developed correlating the values of the *c* for various lateritic soil blends (*B1* to *B5*) to the percentage of gravel for soil samples tested at compacted moisture contents *M1, M2*, and *M3* as shown in Table 6.11. The scatter plot for the same is provided in Fig. 6.3c. Here, it can be seen that an increase in the proportion of *silty* soils from blends *B1* to *B5*, resulted in a consequent decrease in the *gravel* content, and an increase in the *cohesion* following exponential expression.

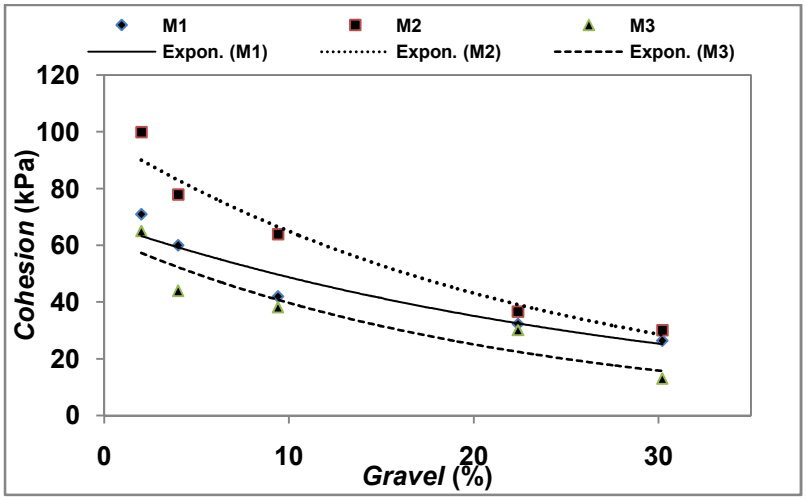

Fig.6.3c Correlation between of *Gravels* (*%*) vs. Cohesion *(c,kPa)*

`

6.1.3.3 Correlations between *Sand* (%) and *Cohesion* for Various Soil Blends

Based on a summary of the details on values of ***c,*** for various blends of lateritic soil samples and for various molding moisture contents as shown in Table 6.9, regression equations were developed correlating the values of the ***c*** for various lateritic soil blends (*B1* to *B5*) to the percentage of sand for soil samples tested at compacted moisture contents *M1*, *M2*, and *M3* as shown in Table 6.12. The scatter plot for the same is provided in Fig. 6.3d. Here, it can be seen that an increase in the proportion of *silty* soils from blends *B1* to *B5*, resulted in a consequent decrease in the *sand* content, and an increase in the *cohesion* following linear relationships.

6.1.3.4 Correlations between *MDD* and *Cohesion* for Various Soil Blends

Based on a summary of the details on values of *c,* for various blends of lateritic soil samples and for various molding moisture contents as shown in Table 6.9, regression equations were developed correlating the values of the ***c*** for various lateritic soil blends (*B1* to *B5*) to the *MDD* for soil samples tested at compacted moisture contents *M1*, *M2*, and *M3* shown in Table 6.13. The scatter plot for the same is provided in Fig. 6.3e. Here, it can be seen that an increase in the proportion of *silty* soils from blends *B1* to *B5*, resulted in a consequent decrease in the *sand* content, and an increase in the *cohesion* following linear relationships.

6.1.3.5 Correlations between *moulding water content* and *Cohesion* for Various Soil Blends

Based on a summary of the details on values of ***c,*** for various blends of lateritic soil samples and for various molding moisture contents as shown in Table 6.9, regression equations were developed correlating the values of the ***c*** for various lateritic soil blends (*B1* to *B5*) to the *moisture content* for soil samples tested at compacted moisture contents *M1*, *M2*, and *M3* shown in Table 6.14. The scatter plot for the same provided in Fig. 6.3f shows a linear trend. Here, it can be seen that an increase in the proportion of *silty* soils from blends *B1* to *B5*, resulted in an increase in the *total surface area* resulting in an increase in the *OMC*. Similar trends were observed in investigations made by George et al. (2009).

Here, it can be seen that the increase in the fines content from blends *B1* to *B5*, resulted in a decrease in the proportion of gravel and sand which has resulted in the increase in void- ratio, and a decrease in *MDD*. This conforms to studies made by Hicks and Monismith (1971), and Omotosho (2004). A similar observation was made above while comparing *MDD* to the values of *UCS*.

`

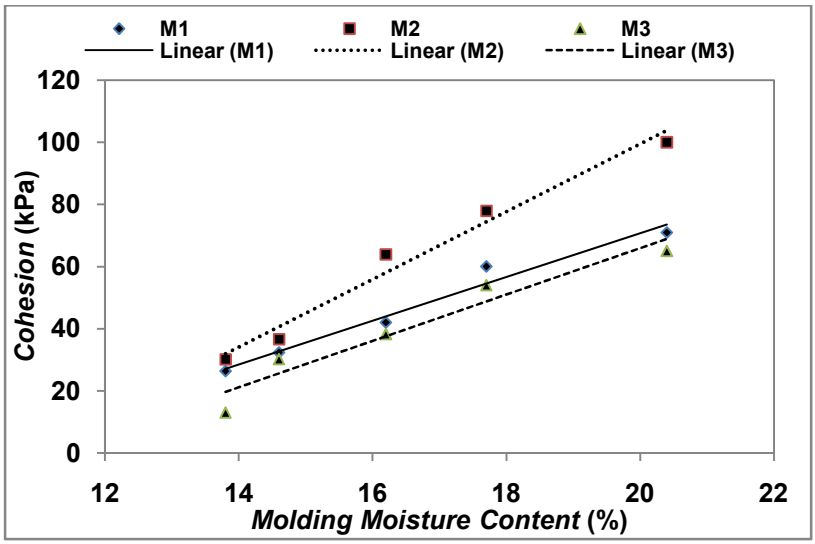

Fig. 6.3f. Correlation between Percentage of *Moulding water content* vs. *Cohesion* (*c*, kPa)

6.1.4 Effect of *Fines, Gravel, Sand, MDD, and Moulding water content* on *Angle of Internal Friction* for Triaxial Tests on Various Soil Blends

The *angle of internal friction* (Ø) is an important material parameter that indicates the shear strength of soil subgrades. Static *Triaxial* tests were performed according to IS: 2720 Part XI (1981) to determine the *angle of internal friction* (Ø) for various soil blends. The investigations were performed on re-molded soil samples of 38mm diameter and 76mm height for various soil blends and moisture contents.

A comparison on the variations in the values of the *angle of internal friction* (Ø) for compacting moisture contents *M1, M2,* and *M3* indicate that the values of *angle of internal friction* (Ø) decrease with the increase in the fines content. These observations conform to the findings of Toll (2000) that the presence of particles of larger effective sizes results in generating higher angles of friction.

In investigations performed by Kim and Kim (2006), it is observed that the *angle of internal friction* measured in triaxial tests is higher for samples moulded at optimum moisture content. Also, it is observed that as the moisture content further increases, the angle of internal friction reduces. This conforms to the findings of Cokca et al. (2004).

`

6.1.4.1 Correlations between *Fines* (%) and *Angle of Internal Friction* for Various Soil Blends

Table 6.9 provides a summary of details on the values of *angle of internal friction* (*C*), for various blends of lateritic soil samples compacted to moisture contents for various blends *B1* to *B5* with fines content varying from 14% to 86%. The table also provides details on the molding compacted moisture contents *M1*, *M2*, and *M3* for the soil samples tested.

Regression equations were developed correlating the values of the *angle of internal friction* for various lateritic soil blends (*B1* to *B5*) to the values of *fines* for samples compacted at moisture contents *M1, M2*, and *M3* as shown in Table 6.15. The scatter plot for the same is provided in Fig. 6.4b. Based on the trend-lines of regressions developed, it can be surmised that the increase in the proportion of silty soil from blends *B1* to *B5*, resulted in a consequent decrease in the sand content and a consequent decrease in the values of *angle of internal friction* following a linear relationship. This conforms to the findings of Adunoye (2014).

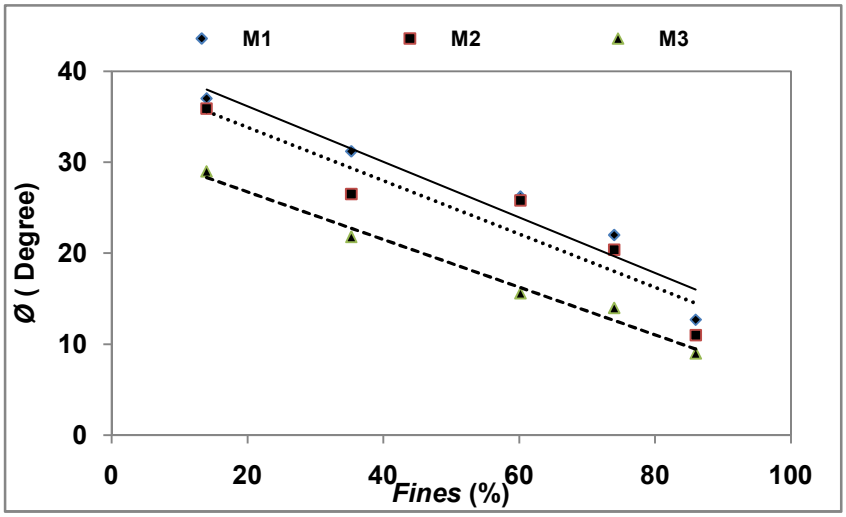

Fig.6.4b Correlation between of *Fines* vs. *Angle of Internal Friction* (ϕ, Degrees)

6.1.4.2 Correlations between *Gravel* (%) and *Angle of Internal Friction* for Various Soil Blends

Based on a summary of the details on values of *angle of internal friction,* for various blends of lateritic soil samples and for various molding moisture contents as shown in Table 6.9, regression equations were developed correlating the values of the *angle of internal friction,* for various lateritic soil blends (*B1* to *B5*) to the percentage of gravel for soil samples tested at compacted moisture contents *M1, M2*, and *M3* as shown in Table 6.16. The scatter plot for the

`

same is provided in Fig. 6.4c. Here, it can be seen that an increase in the proportion of *silty* soils from blends *B1* to *B5*, resulted in a consequent decrease in the *gravel* content, and a decrease in the *angle of internal friction* following linear expression.

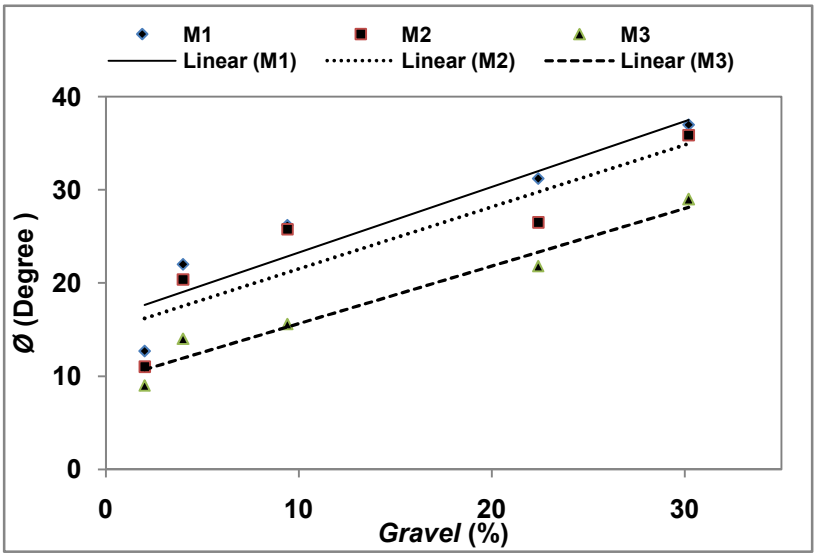

Fig.6.4c Correlation between of *Gravels* vs. *Angle of Internal Friction* (ϕ, Degrees)

6.1.4.3 Correlations between *Sand* (%) and *Angle of Internal Friction* for Various Soil Blends

Based on a summary of the details on values of *angle of internal friction,* for various blends of lateritic soil samples and for various molding moisture contents as shown in Table 6.9, regression equations were developed correlating the values of the *angle of internal friction* for various lateritic soil blends (*B1* to *B5*) to the percentage of *sand* for soil samples tested at compacted moisture contents *M1, M2*, and *M3* as shown in Table 6.17. The scatter plot for the same is provided in Fig. 6.4d. Here, it can be seen that an increase in the proportion of *silty* soils from blends *B1* to *B5*, resulted in a consequent decrease in the *sand* content, and a decrease in the *angle of internal friction* following linear expression.

6.1.4.4 Correlations between *MDD* and *Angle of Internal Friction* for Various Soil Blends

Based on a summary of the details on values of *angle of internal friction,* for various blends of lateritic soil samples and for various molding moisture contents as shown in Table 6.9, regression equations were developed correlating the values of the *angle of internal friction* for various lateritic soil blends (*B1* to *B5*) to the *MDD* for soil samples tested at compacted moisture

`

contents *M1*, *M2*, and *M3* shown in Table 6.18. The scatter plot for the same is provided in Fig. 6.4e.

Here, it can be seen that the increase in the fines content from blends *B1* to *B5*, resulted in a decrease in the proportion of gravel and sand which has resulted in the increase in void- ratio, and a decrease in *MDD*. This conforms to studies made by Hicks and Monismith (1971), and Omotosho (2004). A similar observation was made above while comparing *MDD* to the values of *UCS*.

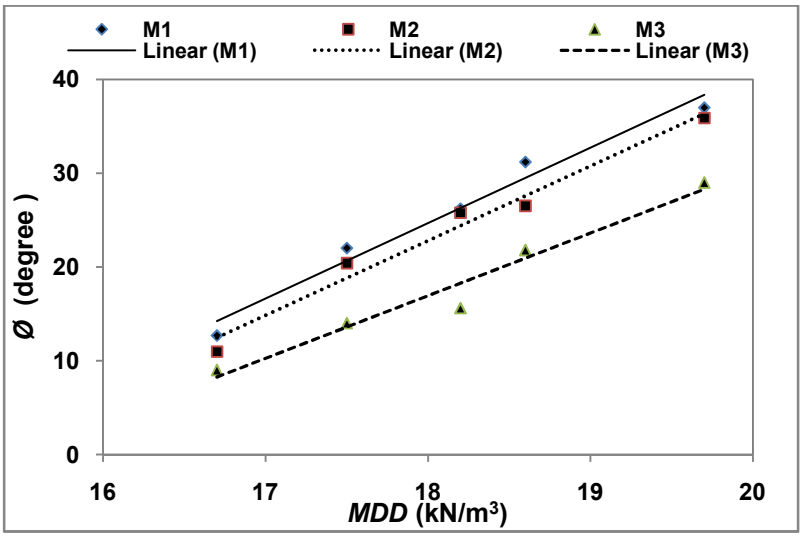

Fig. 6.4e Correlations between of *MDD vs. Angle of Internal Friction* (ϕ, Degrees)

6.1.4.5 Correlations between *Moulding water content* and *Angle of Internal Friction* for Various Soil Blends

Based on a summary of the details on values of *angle of internal friction,* for various blends of lateritic soil samples and for various molding moisture contents as shown in Table 6.9, regression equations were developed correlating the values of the *angle of internal friction* for various lateritic soil blends (*B1* to *B5*) to the *moulding moisture content* for soil samples tested at compacted moisture contents *M1*, *M2*, and *M3* shown in Table 6.19. The scatter plot for the same is provided in Fig. 6.4f. Here, it can be seen that an increase in the proportion of *silty* soils from blends *B1* to *B5*, resulted in an increase in the *total surface area* resulting in an increase in the *OMC*. Similar trends were observed in investigations made by George et al. (2007).

Here, it can be seen that the increase in the fines content from blends *B1* to *B5*, resulted in a decrease in the proportion of gravel and sand which has resulted in the increase in void- ratio, and a decrease in *MDD*. This conforms to studies made by Hicks and Monismith (1971), and

`

Omotosho (2004). A similar observation was made above while comparing *MDD* to the values of *UCS*.

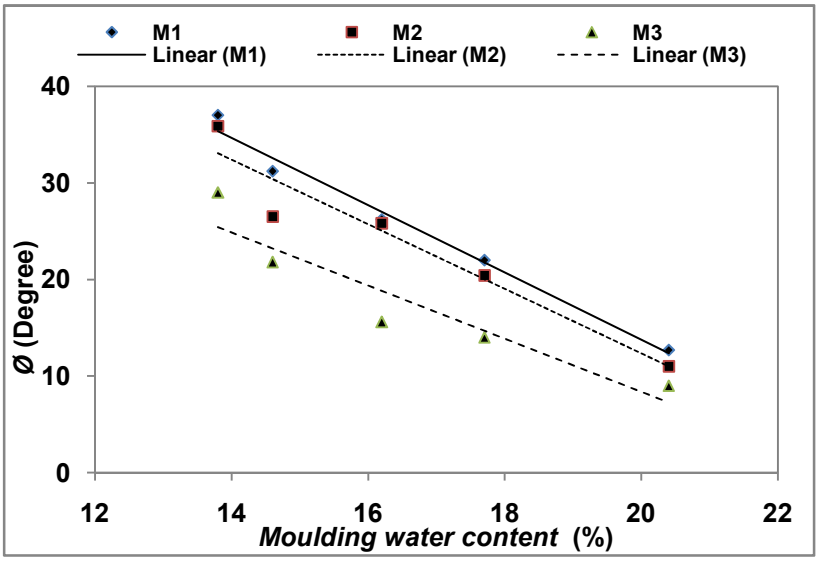

Fig. 6.4f Correlations between Percentage of *Moulding water content* vs. *Angle of Internal Friction* (ϕ, Degrees)

6.1.5 Effect of *Fines, Gravel, Sand, MDD, and Moulding water content* on *CBR* on Various Soil Blends

The most common parameter used in the evaluation of subgrade strength is the *California Bearing Ratio* (*CBR*). The tests for CBR values were performed using moulds of 150mm diameter, and 125mm height according to IS: 2720 Part-16 (1979). The penetration resistance or bearing resistance of soil (*CBR*) is commonly influenced by the presence of water content and the type of soil. Table 4.7 of Chapter IV provides details on the values of *CBR* for various blends of lateritic soil samples compacted to moisture contents *OMC-3%* (*denoted as M1*), *OMC* (*denoted as M2*), and *OMC+3%* (*denoted as M3*) at unsoaked (denoted as CBR_u) and soaked condition (denoted as CBR_s).

The details on fines content for various lateritic soil blends as summarized in Table 6.1, and the results on the *CBR* tests for various soil blends for samples tested for moisture contents *M1, M2,* and *M3* as available in Table 4.7, can be further summarized as in Table 6.20. In this part of the study, the influence of fines, gravel, sand, *MDD,* and *OMC* on the *California Bearing Ratio* is examined.

`

Also, it can be observed that in the case of unsoaked soil samples, the increase in the percentage of fines (and the reduction in the percentage of gravels) has resulted in a significant negative influence on the stiffness of soil. Also, it is seen that soils compacted to the drier-side of optimum have higher stiffness values. Similar observations were made by Thompson and Robnett (1979) where it was explained that the higher stiffness values at the drier-side of optimum was due to *capillary suction*.

Fig. 6.5b illustrates the variations in the values of *California Bearing Ratio* (*CBR*) for tests at soaked conditions (denoted as CBR_s) across various lateritic soil blends for various compacting moisture contents *M1, M2,* and *M3*.

However, in the case of CBR tests on soaked soils, it can be noted that the CBR value (CBR_s) for soil samples compacted to OMC (or M2) is higher than that for *M1* and *M3*. Soaked soils tested at *M1* tend to have a *flocculent structure*, while the same tested at *M3* tend to have a *dispersive structure,* due to which the loads supported by these soaked samples tend to be lesser than that supported at OMC conditions. Thus, soil samples compacted at OMC, are capable of taking higher loads in soaked conditions due to their improved alignment (Lambe and Whitman, 1979).

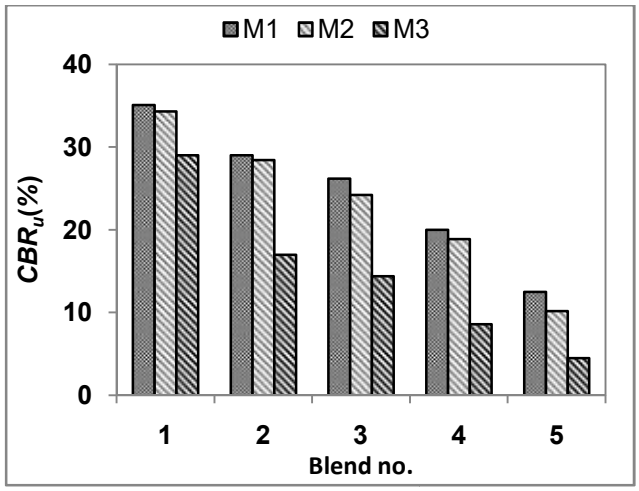

Fig.6.5a *CBR* Unsoaked (CBR_u) vs. *Moisture Content and Fines*

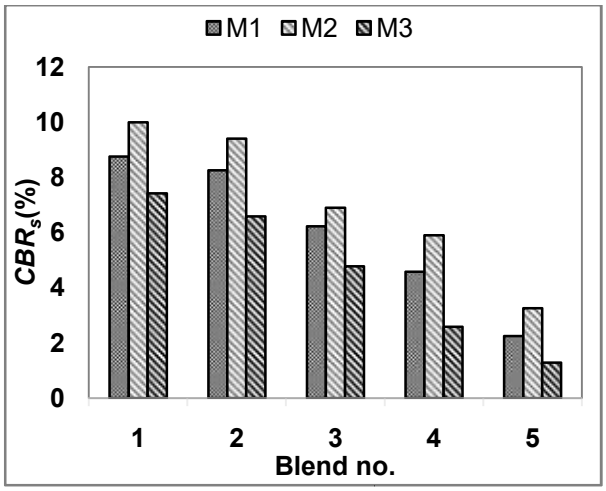

Fig.6.5b *CBR* Soaked (CBR_s) vs. *Moisture Content and Fines*

Additionally, it may be noted that the values of CBR_s at *M1* are slightly higher than that determined at *M3*. This is due to the presence of higher cohesive forces among *flocculent structures* of soil grains at *M1* when compared to lower cohesive forces among *dispersive*

`

structures of soil-grains at *M3* (Lambe and Whitman, 1979). Fredlund and Rahardjo, (1993) also report similar findings that indicate that the shear strength is influenced by *capillary suction* in unsoaked/ unsaturated compacted specimens.

6.1.5.1 Correlations between *Fines* (%) and *CBR* for Various Soil Blends

Table 6.20 provides a summary of details on the values of *California Bearing Ratio* at unsoaked condition (CBR_u), for various blends of lateritic soil samples compacted to moisture contents for various blends *B1* to *B5* with fines content varying from 14% to 86%. The table also provides details on the molding compacted moisture contents *M1*, *M2*, and *M3* for the soil samples tested.

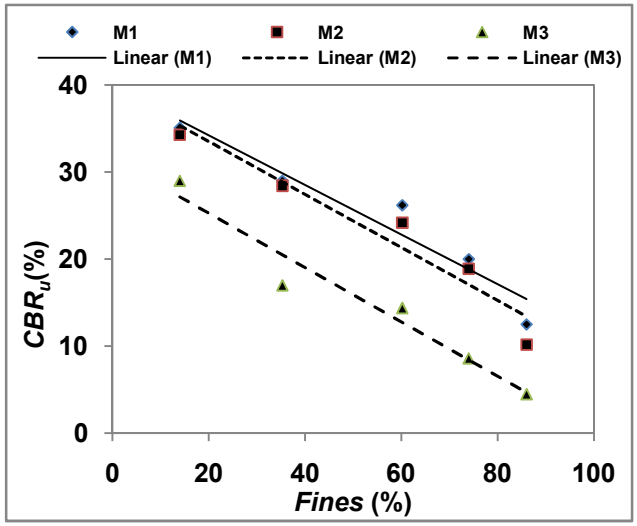

Fig. 6.5c Variations in Percentage of *Fines* vs. *CBR* for Unsoaked Conditions

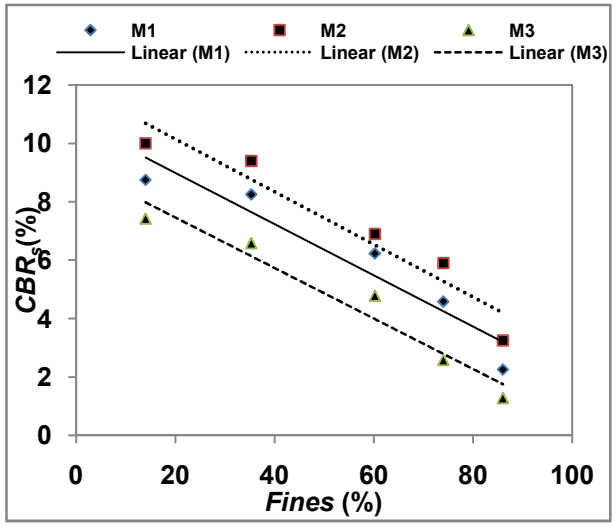

Fig. 6.5d Variations in Percentage of *Fines* vs. *CBR* for Soaked Conditions

Regressions for Soaked Soils

Similarly it can be observed that for tests on soaked soils, the CBR_s various blends of lateritic soils tested at molding moisture content of *M1*, the values of CBR_s decreased from 8.75% to 2.2 %, and for molding moisture content of *M2*, the values of CBR_s decreased from 10.0 % to 3.2%. Also, for molding moisture content *M3*, the values of CBR_s decreased from 7.4% to 1.2%. Thus, it can be seen that the values of CBR_s decrease with increase in the fines content from 14% to 86% irrespective of the molding moisture contents. Also, the increase in the

`

percentage of fines has resulted in a reduction in the soil strength as explained in the above section

However, the values of CBR_u at *OMC* conditions (denoted by *M2*) are higher than that at the drier-side of optimum (*OMC-3*% denoted as *M1*), and that at the wetter-side of optimum (*OMC+3*% denoted as *M3*). Also, the CBR_s at *M1* are slightly higher than that determined at *M3*. The reasons for the same were explained in previous section.

Regression equations were developed correlating the values of CBR_s for various lateritic soil blends (*B1* to *B5*) to the values of the percentage of *Fines* for samples compacted at moisture contents *M1, M2*, and *M3* as shown in Table 6.22. The scatter plot for the same is provided in Fig. 6.5d.

6.1.5.2 Correlations between *Gravel* (%) and *CBR* for Various Soil Blends

Based on a summary of the details on values of the *California Bearing Ratio* at unsoaked soil conditions (CBR_u) for various blends of lateritic soil samples (*B1* to *B5*) and for various molding moisture contents *M1, M2*, and *M3* as shown in Table 6.20, regression equations were developed correlating the values of CBR_u, to the percentage of *gravel* as shown in Table 6.23. The scatter plot for the same is provided in Fig. 6.5e.

Similarly, based on the results of the tests using the *CBR* equipment on soaked soil conditions, regression equations were developed correlating the values of CBR_s, for various lateritic soil blends (*B1* to *B5*) to the percentage of gravel for soil samples tested at compacted moisture contents *M1, M2*, and *M3* as shown in Table 6.24. The scatter plot for the same is provided in Fig. 6.5f.

Table 6.24 Regressions for *CBR* Based on Percentage of *Gravel* (%): Soaked

Moisture conditions	Regression equations	R^2	R^2adj	SEE	F	t	Sig F
M1	$CBR_s = 1.972(\%Gravel)^{0.466}$	0.92	0.90	0.179	35.17	5.93	0.010
M2	$CBR_s = 2.890(\%Gravel)^{0.380}$	0.93	0.90	0.141	38.06	6.16	0.009
M3	$CBR_s = 0.970(\%Gravel)^{0.627}$	0.96	0.95	1.168	72.95	8.52	0.003

Here, it can be seen that an increase in the proportion of *silty* soils from blends *B1* to *B5*, resulted in a consequent decrease in the *gravel* content, and a decrease in the values of CBR in unsoaked and soaked conditions following a *power* expression.

`

6.1.5.3 Correlations between *Sand* (%) and *CBR* for Various Soil Blends

Based on a summary of the details on values of the *California Bearing Ratio* at unsoaked soil conditions (CBR_u) for various blends of lateritic soil samples (*B1* to *B5*) and for various molding moisture contents *M1, M2*, and *M3* as shown in Table 6.20, regression equations were developed correlating the values of CBR_u to the percentage of *sand* as shown in Table 6.25. The scatter plot for the same is provided in Fig. 6.5g.

6.1.7.1 Correlations between *Fines* (%) and E_{pfwd} for Various Soil Blends

Table 6.42 provides a summary of details on the values *modulus of resilience* of soil (E_{pfwd}), for various blends of lateritic soil samples compacted to moisture contents for various blends *B1* to *B5* with fines content varying from 14% to 86%. The table also provides details on the molding compacted moisture contents *M1*, *M2*, and *M3* for the soil samples tested.

Regressions for Unsoaked Soils

It can be observed that for various blends of lateritic soils tested at molding moisture content of *M1*, at unsoaked conditions, the values of E_{pfwdu} decreased from 163 MPa to 44.7 MPa. Similarly, for molding moisture content of *M2*, the values of E_{pfwdu} decreased from 154MPa to 36 MPa. Also, for molding moisture content *M3*, the values of E_{pfwdu} decreased from 141 MPa to 26.5 MPa. Thus, it can be seen that the values of E_{pfwdu} decrease with increase in the fines content from 14% to 86% irrespective of the molding moisture contents. Also, the increase in the percentage of fines has resulted in a reduction in the soil strength as explained in the previous section.

Regression equations were developed correlating the values of E_{pfwdu} for various lateritic soil blends (*B1* to *B5*) to the values of the percentage of *fines* for samples compacted at moisture contents *M1, M2*, and *M3* as shown in Table 6.43. The scatter plot for the same is provided in Fig. 6.7c.

Regressions for Soaked Soils

Similarly it can be observed that for tests on soaked soils, the E_{pfwds} various blends of lateritic soils tested at molding moisture content of *M1*, the values of E_{pfwds} decreased from 47.3 MPa to 15.7Mpa, for molding moisture content of *M2*, and the values of $DCPI_s$ decreased from 50.7 MPa to 22.0MPa . Also, for molding moisture content *M3*, the values of $DCPI_s$ decreased

`

from 46.7 MPa to 7 MPa. Thus, it can be seen that the values of E_{pfwds} decrease with increase in the fines content from 14% to 86% irrespective of the molding moisture contents. Also, the increase in the percentage of fines has resulted in a reduction in the soil strength as explained in the above section.

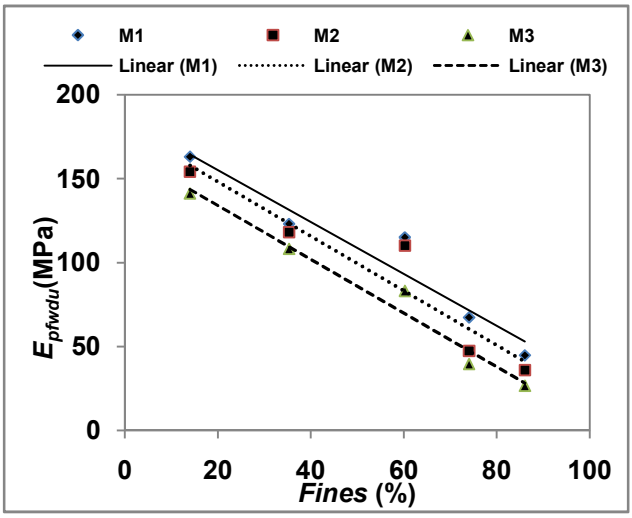

Fig.6.7c Variations in Percentage of *Fines* vs. *Modulus of Resilience* for Unsoaked Conditions

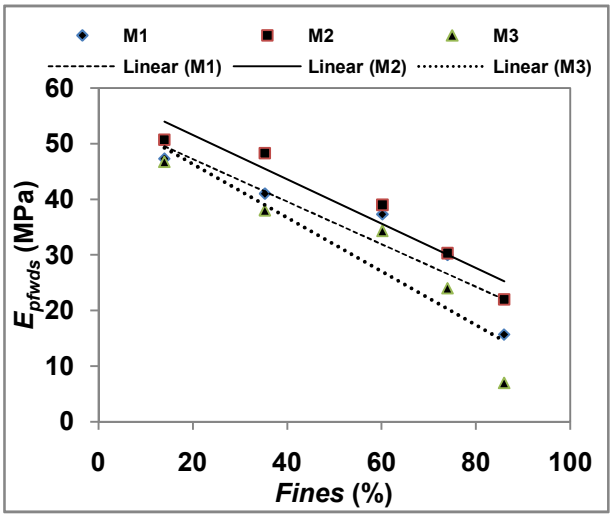

Fig.6.7d Variations in Percentage of *Fines* vs. *Modulus of Resilience* for Soaked Conditions

However, the values of E_{pfwds} at *OMC* conditions (denoted by *M2*) are higher than that at the drier-side of optimum (*OMC-3%* denoted as *M1*), and that at the wetter-side of optimum (*OMC+3%* denoted as *M3*). Also, the E_{pfwds} at *M1* is slightly higher than that determined at *M3*. The reasons for the same were explained in previous section.

Regression equations were developed correlating the values of E_{pfwds} for various lateritic soil blends (*B1* to *B5*) to the values of the percentage of *Fines* for samples compacted at moisture contents *M1, M2*, and *M3* as shown in Table 6.44. The scatter plot for the same is provided in Fig. 6.7d.

Based on the trend-lines of regressions developed, it can be surmised that the increase in the proportion of silty soil from blends *B1* to *B5*, resulted in a consequent decrease in the sand content and a consequent decrease in the values E_{pfwd} following a *linear* relationship.

6.1.7.2 Correlations between *Gravel* (%) and E_{pfwd} for Various Soil Blends

Based on a summary of the details on values of the *modulus of resilience* of soil (E_{pfwd}), for various blends of lateritic soil samples (*B1* to *B5*) and for various molding moisture contents

`

M1, M2, and *M3* as shown in Table 6.42, regression equations were developed correlating the values of E_{pfwdu} to the percentage of *gravel* as shown in Table 6.45. The scatter plot for the same is provided in Fig. 6.7e.

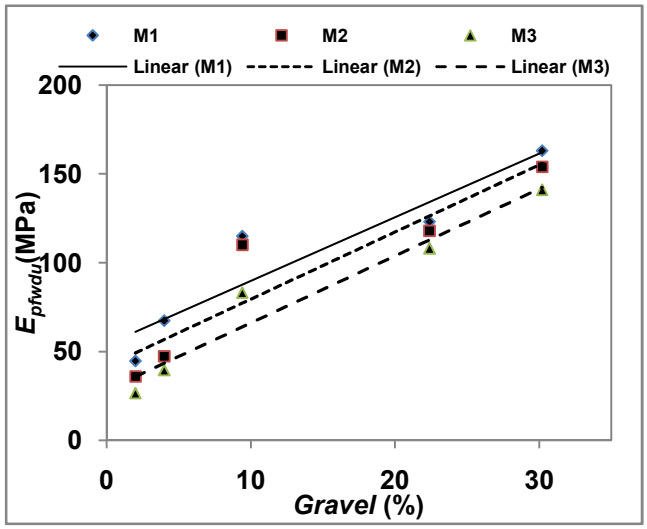

Fig.6.7e Variations in Percentage of *Gravel* vs. *Modulus of Resilience* for Unsoaked Conditions

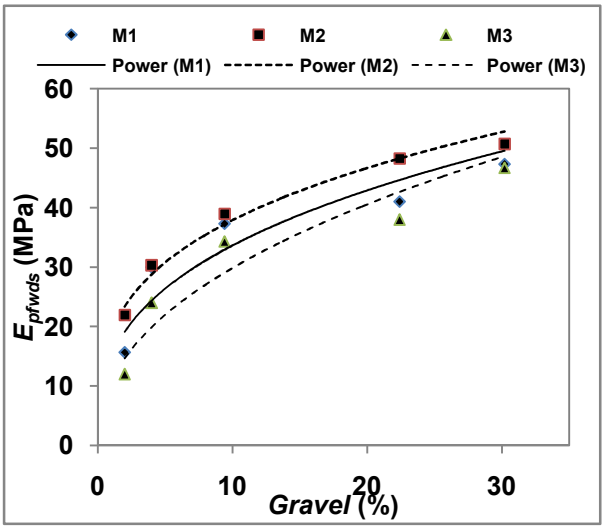

Fig.6.7f Variations in Percentage of *Gavel* vs. *Modulus of Resilience* for Soaked Conditions

Similarly, based on the results of the tests using the E_{pfwd} equipment on soaked soil conditions, regression equations were developed correlating the values of E_{pfwds}, for various lateritic soil blends (*B1* to *B5*) to the percentage of gravel for soil samples tested at compacted moisture contents *M1, M2*, and *M3* as shown in Table 6.46. The scatter plot for the same is provided in Fig. 6.7f.

Here, it can be seen that an increase in the proportion of *silty* soils from blends *B1* to *B5*, resulted in a consequent decrease in the *gravel* content, and a decrease in the values of $\boldsymbol{E_{pfwd}}$ in unsoaked and soaked conditions following *linear* and expression related to *power* equations.

6.1.7.3 Correlations between *Sand* (%) and E_{pfwd} for Various Soil Blends

Based on a summary of the details on values of the *modulus of resilience* of soil (E_{pfwd}), at unsoaked soil conditions (E_{pfwdu}) for various blends of lateritic soil samples (*B1* to *B5*) and for various molding moisture contents *M1, M2*, and *M3* as shown in Table 6.42, regression equations were developed correlating the values of E_{pfwdu}, to the percentage of *sand* as shown in Table 6.47. The scatter plot for the same is provided in Fig. 6.7g.

`

Similarly regression equations were developed correlating the values of the *modulus of resilience* of soil *(E_{pfwd})*, at soaked condition (E_{pfwds}) for various lateritic soil blends (*B1* to *B5*) to the percentage of *sand* for soil samples tested at compacted moisture contents *M1, M2*, and *M3* as shown in Table 6.48. The scatter plot for the same is provided in Fig. 6.7h.

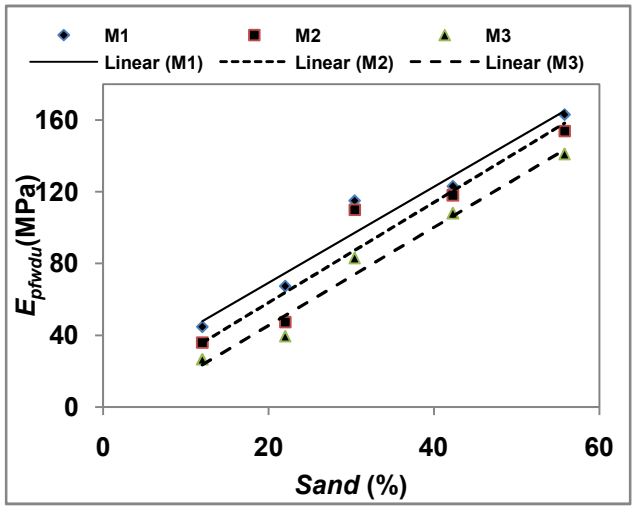

Fig.6.7g Variations in Percentage of *Sand* vs. *Modulus of Resilience* for Unsoaked Conditions

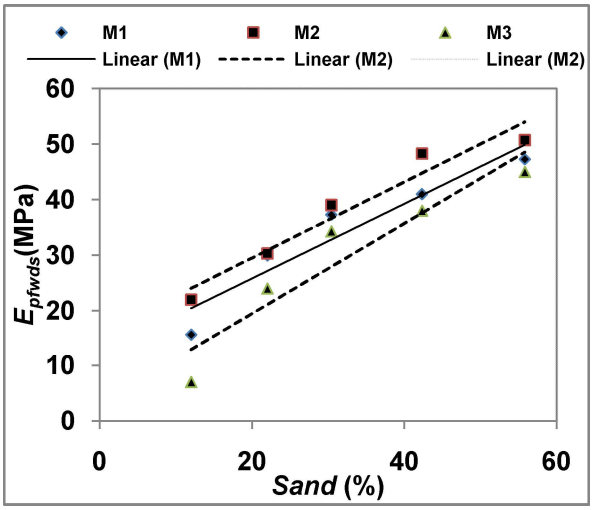

Fig.6.7h Variations in Percentage of *Sand* vs. *Modulus of Resilience* for Soaked Conditions

6.1.7.4 Correlations between *MDD* and the E_{pfwd} for Various Soil Blends

Based on a summary of the details on values of the *modulus of resilience* of soil *(E_{pfwd})*, at unsoaked soil conditions (E_{pfwdu}) for various blends of lateritic soil samples (*B1* to *B5*) and for various molding moisture contents *M1, M2*, and *M3* as shown in Table 6.42, regression equations were developed correlating the values of E_{pfwdu}, to the values of *MDD* as shown in Table 6.49. The scatter plot for the same is provided in Fig. 6.7i.

`

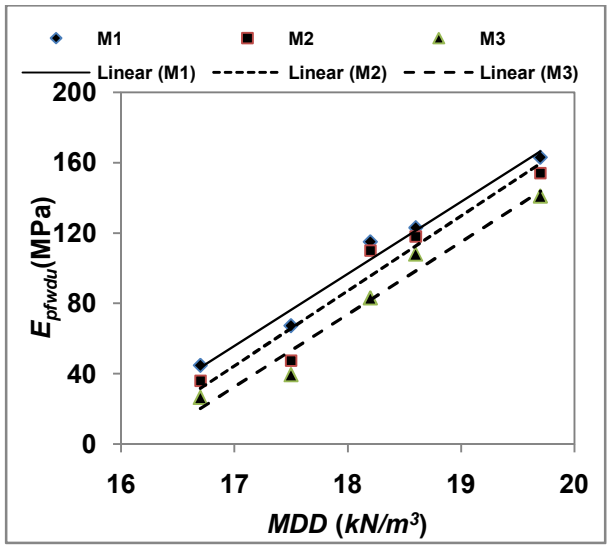

Fig. 6.7i Variations in *MDD* vs. *Modulus of Resilience* for Unsoaked Conditions

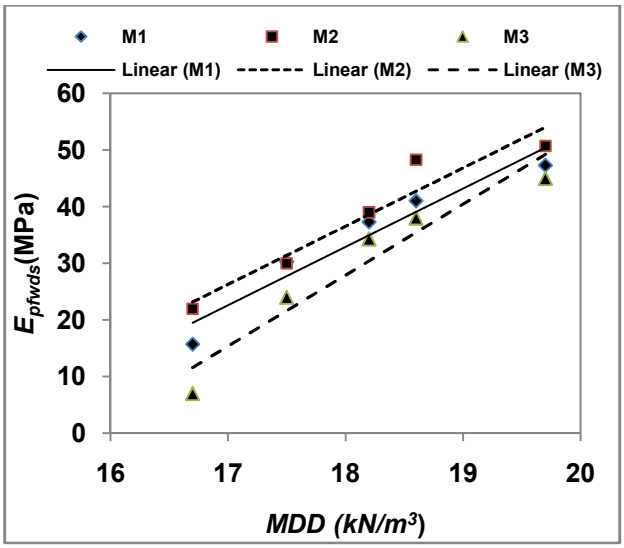

Fig. 6.7j Variations in *MDD* vs. *Modulus of Resilience* for Soaked Conditions

Similarly regression equations were developed correlating the values of the *modulus of resilience* of soil *(E_{pfwd})*, at soaked condition (E_{pfwds}) for various lateritic soil blends (*B1* to *B5*) to the values of *MDD* for soil samples tested at compacted moisture contents *M1, M2*, and *M3* as shown in Table 6.50. The scatter plot for the same is provided in Fig. 6.7j.

6.1.7.5 Correlations between *Moulding water content* (%) and the E_{pfwd} for Various Soil Blends

Based on a summary of the details on values of the *modulus of resilience* of soil *(E_{pfwd})* for various blends of lateritic soil samples (*B1* to *B5*) and for various molding moisture contents *M1, M2*, and *M3* as shown in Table 6.42, regression equations were developed correlating the values of E_{pfwdu}, to the values of *OMC* as shown in Table 6.49. The scatter plot for the same is provided in Fig. 6.7k.

`

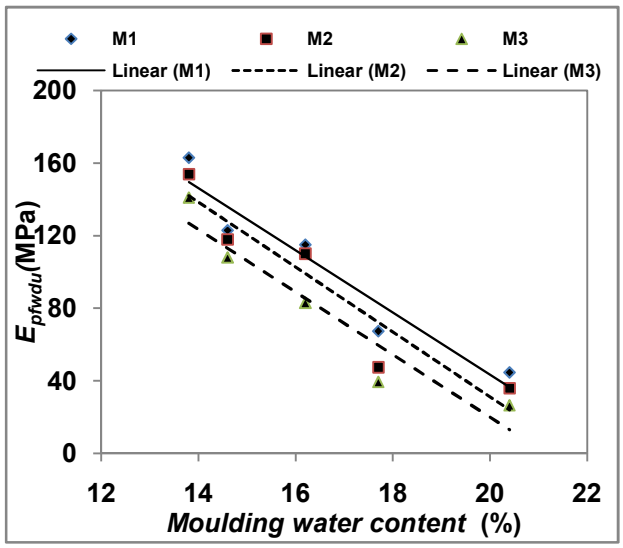

Fig. 6.7k Variations in *Moulding water content* vs. *Modulus of Resilience* for Unsoaked Conditions

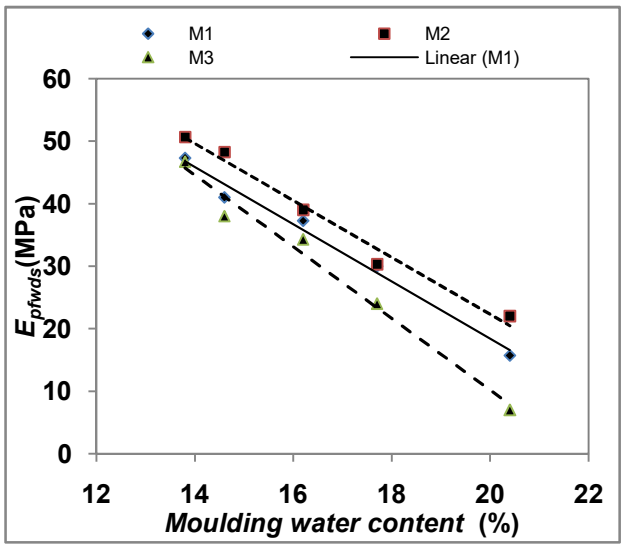

Fig. 67l Variations in *Moulding water content* vs. *Modulus of Resilience* for Soaked Conditions

6.1.8 Effect of *Fines, Gravel, Sand, MDD, and moulding water content* on *Modulus of Resilience* of Soil (M_r) Using *Cyclic Triaxial* Test for Various Soil Blends

The *cyclic triaxial* test equipment is designed to determine the *resilient modulus* (M_r) of soil blends. Table 5.9 of Chapter V provides details on the values of M_r for various blends of lateritic soil samples compacted to moisture contents *OMC-3%* (*denoted as M1*), *OMC* (*denoted as M2*), and *OMC+3%* (*denoted as M3*) at unsoaked soil conditions (denoted as M_r).

The details on fines content for various lateritic soil blends as summarized in Table 6.1, and the results on the tests using the *cyclic triaxial* test equipment for various soil blends for samples tested for moisture contents *M1, M2,* and *M3* as available in Table 5.9, can be further summarized as in Table 6.53. In this part of the study, the influence of fines, gravel, sand, *MDD,* and *OMC* on the M_r is examined.

Fig. 6.8a illustrates the variations in the values of the *modulus of resilience* of soil (M_r) for tests on unsoaked soil conditions (denoted as M_r) across various lateritic soil blends for various compacting moisture contents *M1, M2,* and *M3*. A comparison on the variations in the values of the M_r for compacting moisture contents *M1, M2,* and *M3* indicate that the increase in moisture content has resulted in a decrease in the M_r at unsoaked soil conditions.

`

According to the findings made by Kato et al. (2005), and Kizza et al. (2014) on triaxial tests performed on undrained soils, it was observed that the shear strength of soil compacted to the dry side of optimum will be lower than that of soil compacted to OMC.

The investigations performed as part of this study also confirms the above observations. It is felt that soil strength determined at optimum moisture content (OMC) on undrained soils using the triaxial test equipment is higher due to the reason that in triaxial tests, the soil strength is measured based on the combined effect of the deviator stress (or major principal stress), and the cell pressure (or minor principal stress), and the resistance offered by the effect of *cohesion* and the *angle of internal friction* of the soil sample.

In contrast, in the case of tests on unsoaked soil samples using equipment such as the CBR, the PFWD, and the DCP, the soil strength is mainly measured in terms of the stiffness offered to compressive stress applied, where it is seen that soils compacted to the drier-side of optimum have higher stiffness values as observed by Thompson and Robnett (1979).

6.1.8.1 Correlations between *Fines* (%) and the M_r for Various Soil Blends

Table 6.53 provides a summary of details on the values of *modulus of resilience* of soil *(M_r)* at unsoaked condition (M_r), for various blends of lateritic soil samples compacted to moisture contents for various blends *B1* to *B5* with fines content varying from 14% to 86%. The table also provides details on the molding compacted moisture contents *M1*, *M2*, and *M3* for the soil samples tested.

However, the values of M_r at *OMC* conditions (denoted by *M2*) are higher than that at the drier-side of optimum (*OMC-3*% denoted as *M1*), and that at the wetter-side of optimum (*OMC+3*% denoted as *M3*). Also, the M_r at *M1* is slightly higher than that determined at *M3*. The reasons for the same were explained in previous section.

Regression equations were developed correlating the values of M_r for various lateritic soil blends (*B1* to *B5*) to the values of the percentage of *Fines* for samples compacted at moisture contents *M1, M2*, and *M3* as shown in Table 6.54. The scatter plot for the same is provided in Fig. 6.8b.

`

Here, it can be seen that an increase in the proportion of *silty* soils from blends *B1* to *B5*, resulted in a consequent decrease in the *gravel* content, and a decrease in the values of M_r in unsoaked following *linear*

6.1.8.3 Correlations between *Sand* (%) and the M_r for Various Soil Blends

Based on a summary of the details on values of the *modulus of resilience* of soil *(M_r)*, at unsoaked soil conditions (M_r) for various blends of lateritic soil samples (*B1* to *B5*) and for various molding moisture contents *M1, M2*, and *M3* as shown in Table 6.53, regression equations were developed correlating the values of M_r, to the percentage of *sand* as shown in Table 6.56. The scatter plot for the same is provided in Fig. 6.8d.

Table 6.56 Regressions for M_r (MPa) Based on Percentage of *Sand*: Unsoaked

Moisture conditions	Regression equations	R^2	R^2adj	SEE	F	t	Sig F
M1	M_r= 18.503 + 5.178 (%*Sand*)	0.94	0.92	26.08	46.24	6.80	0.007
M2	M_r= 19.482 + 5.450 (%*Sand*)	0.94	0.92	27.46	46.24	6.80	0.007
M3	M_r= -14.445 + 5.094 (%*Sand*)	0.98	0.97	14.75	140.0	11.83	0.001

Here, it can be seen that an increase in the proportion of *silty* soils from blends *B1* to *B5*, resulted in a consequent decrease in the *gravel* content, and a decrease in the values of M_r in unsoaked conditions following *linear* expression.

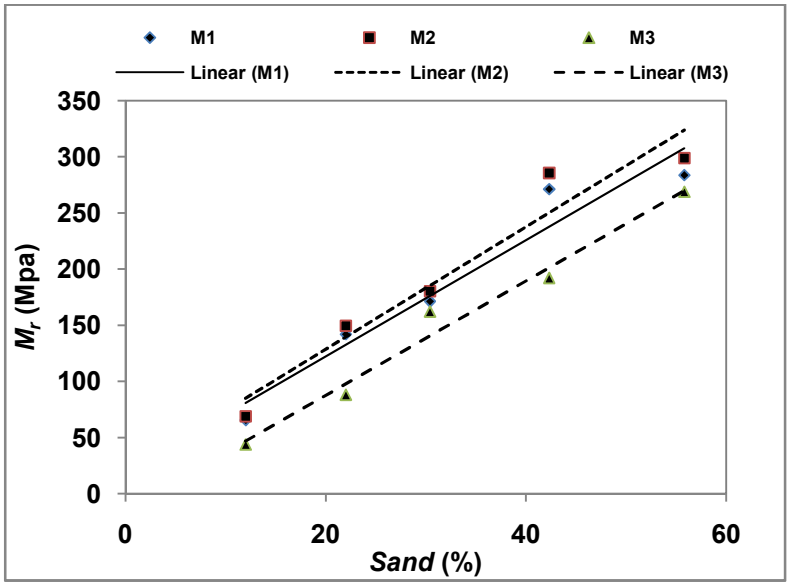

Fig. 6.8d Variations in Percentage of *Gravel* vs. *Modulus of Resilience*(M_r)for Unsoaked Conditions

`

6.1.8.4 Correlations between *MDD* and the M_r for Various Soil Blends

Based on a summary of the details on values of the *modulus of resilience* of soil *(M_r)*, at unsoaked soil conditions (M_r) for various blends of lateritic soil samples (*B1* to *B5*) and for various molding moisture contents *M1, M2*, and *M3* as shown in Table 6.53, regression equations were developed correlating the values of E_{pfwdu}, to the values of *MDD* as shown in Table 6.57. The scatter plot for the same is provided in Fig. 6.8e.

6.1.8.5 Correlations between *Moulding water content* (%) and the M_r for Various Soil Blends

Based on a summary of the details on values of the *modulus of resilience* of soil *(M_r)*, for various blends of lateritic soil samples (*B1* to *B5*) and for various molding moisture contents *M1, M2*, and *M3* as shown in Table 6.53, regression equations were developed correlating the values of M_r , to the values of *OMC* as shown in Table 6.58. The scatter plot for the same is provided in Fig. 6.8f.

Table 6.58 Regressions for M_r Based on *Moulding water content* (%): Unsoaked

Moisture conditions	Regression equations	R^2	R^2adj	SEE	F	t	Sig F
M1	M_r= 752.25 - 34.18 (-3%*OMC*)	0.96	0.95	20.12	79.78	-8.93	0.003
M2	M_r= 791.85 - 35.98 (%*OMC*)	0.96	0.95	21.17	79.78	-8.93	0.003
M3	M_r= 685.44 - 32.30 (+3%*OMC*)	0.93	0.90	27.55	37.99	-6.16	0.009

Here, it can be seen that the increase in the fines content from blends *B1* to *B5*, resulted in a decrease in the proportion of *gravel* and *sand* which has resulted in the increase in *void- ratio*, and a decrease in *MDD*. This conforms to studies made by Hicks and Monismith (1971), Omotosho (2004), George et al. (2007), Sivakumar et al. (2013) and Khoury Naji (2016). A similar observation was made while comparing *MDD* to the values of *UCS.* It may also be noted that the M_r values are sensitive to changes in moisture content as observed by studies in lateritic soils by Evans (1958) and Gidigasu (1976).

`

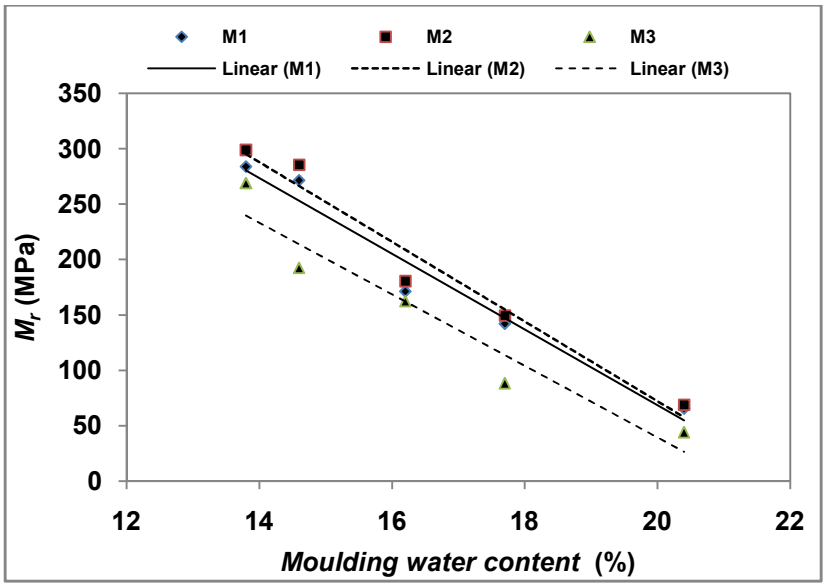

Fig. 6.8f Variations in *Moulding water content* vs. *Modulus of Resilience* for Unsoaked conditions

6.2 DEVELOPMENT OF CORRELATIONS FOR RESULTS BASED ON STATIC TRIAXIAL TESTS, AND *UCS* FOR 38 AND 100mm DIAMETER SAMPLES

Soil strength can be determined using the test for *unconfined compressive strength* (*UCS*) and the *triaxial* test equipment in addition to other tests. The results obtained based on these two tests are seen to be widely applied in estimating the soil strength. One of the important factors that influence the soil strength includes some aspects related to *geometry of the sample* (Lambe, 1951; Das, 2002; Haken and Rusen, 2015). Lambe (1951) suggested a *minimum geometry ratio* (or height/ diameter ratio) of 1.5. Das (2002) also suggested that the cylindrical specimen used for testing should have a diameter of 1.4 inches and a height/ diameter ratio of 2 to 3. Some of the standard codes for performing the *UCS* and triaxial tests specify a *geometry ratio* (or height/ diameter ratio) of 2.0 to 2.5 or a diameter of 1.3 to 2.0 inches according to ASTM (2002a). According to British Standards of testing (BSI, 1990), soil samples of diameter 35mm or 100mm can be used, while according to Indian standards, the geometry ratio can vary between 2 to 2.5 (IS 2720 Part x 1973).Thus, preparation of the soil sample of the required size is an important step in ensuring accuracy in determining the shear strength. The *size and shape* of the soil sample used in performing the tests must be such that the results obtained hold good over a wide range of soil characteristics.

Similar experimental investigations were carried out using the static triaxial test equipment for soil samples of 76 mm height and 38 mm diameter, and samples of 100 mm diameter and 200

`

mm height according to IS: 2720 Part XII (1981) for un-consolidated un-drained (UU) soil specimens.

6.2.1 Regression between Tests for *UCS* for 38mm Vs 100mm dia. Samples

Based on a summary of the details on values of the *Unconfined Compression Strength* (q_u), for various blends of lateritic soil samples (*B1* to *B5*) and for various molding moisture contents *M1, M2*, and *M3* as shown in Table 6.59, a regression was developed correlating the values of *UCS* for 38 mm diameter samples (or q_{u38}) against the values of *UCS* for 100 mm diameter samples (q_{u100}) using 10 sets of data as shown in Eq. 6.19. The scatter plot for the same is given in Fig. 6.9a. The R^2 value for the regression was 0.906 and the adjusted R^2 was 0.90. The standard error of estimation (SE) was found to be 0.026, while the values for F-test, and t-test were 77.73 and 3.78 respectively at significance level of 0.01.

$$q_{u38} = 0.946 q_{u100} - 0.066 \qquad \text{Eq 6.19}$$

The regression equation developed was validated using five sets of data for q_{u38} and q_{u100} set apart for the same. The scatter plot for the validation performed is shown in Fig. 6.9b. The regression line of the scatter plot satisfied an R^2 value of 0.846 coinciding satisfactorily with the theoretical line of equality, at a negligible intercept of 0.00. This shows that the values of q_{u38} of soil blends can be effectively predicted using q_{u100} values for tests conducted on samples of larger diameter.

6.2.2 Regression between Triaxial Tests for 38mm Vs 100mm dia Samples

A regression between the values of *cohesion* for 38mm dia samples (c_{38}) and *cohesion* for 100mm dia samples (c_{100}) was developed from the results of the triaxial tests as shown in Eq. 6.20 based on the scatter plot as given in Fig. 6.10a. The R^2 value for the regression was 0.928 and the adjusted R^2 was 0.92. The *standard error of estimation* (SE) was found to be 6.07, while the values for F-test, and t-test were 104.45 and 10.22 respectively at a significance level of 0.01.

$$c_{38}\,(\text{MPa}) = 1.269\, c_{100}\,(\text{MPa}) - 3.771 \qquad \text{Eq. 6.20}$$

The regression equation developed was validated using the data for c_{38} and c_{100} set apart for the same. The scatter plot for the validation performed is shown in Fig. 6.10b. The regression line of the scatter plot satisfied an R^2 value of 0.982 coinciding satisfactorily with the theoretical line of equality, at a negligible intercept of 9.814. This shows that the values of c_{38} of soil blends can be effectively predicted using c_{100} values for tests conducted on samples of larger diameter.

`

The regression equation developed was validated using the data for $Ø^{\circ}_{38}$ and $Ø^{\circ}_{100}$ set apart for the same. The scatter plot for the validation performed is shown in Fig 6.11b. The regression line of the scatter plot satisfied an R^2 value of 0.971 coinciding satisfactorily with the theoretical line of equality, at a negligible intercept of 1.241. This shows that the values of $\Phi°_{38}$ of soil blends can be effectively predicted using $\Phi°_{100}$ values for tests conducted on samples of larger diameter.

6.3 DEVELOPMENT OF CORRELATIONS FOR RESULTS BASED ON STATIC TRIAXIAL TESTS, CBR, AND UCS

This section focuses on the development of correlations for observations made based on the *CBR*, *UCS* and *triaxial tests*. A summary of the results obtained based on the tests for CBR, *UCS* and the *triaxial tests* are provided in Table 6.60. From the results compiled in the above mentioned table, data pertaining to a stratified sample of 10 rows of the table were used to develop regression equations. The data pertaining to the remaining 5 rows (for blend Vs. moisture content combinations *B1M1*, *B2M2*, *B3M3*, *B4M1*, and *B5M2*) were used for validating the regressions.

6.3.1 Regression between the Test Results for *CBR* and *UCS* (q_u)

A regression between CBR_u and *UCS* (q_u) was developed as shown in Eq 6.22 and a scatter plot for the same is given in Fig. 6.12a. The R^2 value for the regression was 0.67 and adjusted R^2 was 0.63. Standard error of estimation (SE) was found to be 5.916, while the values of F-test, and t-test was 16.49 and 0.399 respectively and confidence level of 99%.

$$CBR_u = 87.30(q_u) + 1.962 \qquad \text{Eq.6.22}$$

From Fig.6.12b, it is observed that the *observed CBR* and the *predicted CBR* values agree with each other. The regression line of the scatter plot satisfied an R^2 value of 0.88 coinciding satisfactorily with the theoretical line of equality, at a negligible intercept of -3.09. The results show that the values of CBR_u of soil blends can be effectively predicted using q_u values for tests conducted on unsoaked samples.

Similarly, a regression between CBR_s and *UCS* (q_u) was developed as shown in Eq. 6.23, and the scatter plot for the same is given in Fig.6.12c with an R^2 value of 0.80 and an adjusted R^2 value of 0.78. The *standard error of estimation* (SE) was found to be 1.485, while the values of F-test, and t-test were 32.43 and 1.233 respectively at a confidence level of 99%.

`

CBR_s=30.73 (q_u) - 0.745 Eq. 6.23

From Fig. 6.12d, it is seen that the *observed* CBR_s and the *predicted* CBR_s values agree with each other. The regression line of the scatter plot satisfied an R^2 value of 0.89 coinciding satisfactorily with the theoretical line of equality, at a negligible intercept of 1.68. The results show that the values of CBR_s of soil blends can be effectively predicted using q_u values for tests conducted on soaked samples.

6.3.2 Regression between the Test Results for *CBR* and *Cohesion* (c)

A regression between CBR_u and *cohesion* (*c*) was developed as shown in Eq. 6.24 and the scatter plot for the same is given in Fig.6.13a. The R^2 value for the regression was 0.66 and the adjusted R^2 was 0.62. Standard error of estimation (SE) was found to be 6.01, while the values of F-test, and t-test was 15.68 and 5.50 respectively and confidence level of 99%.

From Fig. 6.13b, it is observed that the *predicted* CBR_u and the *observed* CBR_u values agree with each other. The regression line of the scatter plot satisfied an R^2 value of 0.929 coinciding satisfactorily with the theoretical line of equality, at a negligible intercept of -7.646. The results show that the values of CBR_u of soil blends can be effectively predicted using *cohesion* values for tests conducted on unsoaked samples.

Similarly, a regression between CBR_s and *cohesion* (*c*) was developed as shown in Eq. 6.25 and the scatter plot for the same is given in Fig. 6.13c. The R^2 value for the regression was 0.73 and the adjusted R^2 was 0.70. The *standard error of estimation* (SE) was found to be 1.66, while the values of F-test, and t-test were 21.53 and 8.00 respectively at a confidence level of 99%.

From Fig. 6.13d, it is observed that the *predicted* CBR_s and the *observed* CBR_s values agree with each other. The regression line of the scatter plot satisfied an R^2 value of 0.944 coinciding satisfactorily with the theoretical line of equality, at a negligible intercept of 0.134. The results show that the values of CBR_s of soil blends can be effectively predicted using *cohesion* values for tests conducted on soaked samples

`

6.3.3 Regression between the Test Results for *CBR* and *Angle of Internal friction* (ϕ)

A regression between CBR_u and the *angle of internal friction* (ϕ) was developed as shown in Eq. 6.26 and the scatter plot for the same is given in Fig. 6.14a. The R^2 value for the regression was 0.869 and the adjusted R^2 was 0.85. The *standard error of estimation* (SE) was found to be 3.749, while the values of F-test, and t-test was 53.00 and -0.086 respectively and confidence level of 99%.

$$CBR_u = 0.841\ (\phi°) + 0.265 \qquad \text{Eq.6.26}$$

From Fig. 6.14b it is observed that the *predicted* CBR and the *observed* CBR values agree with each other. The regression line of the scatter plot satisfied an R^2 value of 0.922 coinciding satisfactorily with the theoretical line of equality, at a negligible intercept of -0.577. The results shows that the values of CBR of soil blends can be effectively predicted using the *angle of internal friction* for tests conducted on unsoaked samples.

Similarly, a regression between CBR_s and the *angle of internal friction* (ϕº) was developed as shown in Eq. 6.27 and the scatter plot for the same is given in Fig.6.14c. The R^2 value for the regression was 0.88 and the adjusted R^2 was 0.86. The *standard error of estimation* (SE) was found to be 1.121, while the values of F-test, and t-test were 57.29 and -0.944 respectively at a confidence level of 99%.

$$CBR_s = 0.261(\phi°) - 0.870 \qquad \text{Eq.6.27}$$

From Fig. 6.14d it is observed that the *predicted CBR* and the *observed CBR* values agree with each other. The regression line of the scatter plot satisfied an R^2 value of 0.942 coinciding satisfactorily with the theoretical line of equality, at a negligible intercept of 2.326. The results show that the values of *CBR* of soil blends can be effectively predicted using the *angle of internal friction* for tests conducted on soaked samples.

`

6.4 DEVELOPMENT OF CORRELATIONS FOR RESULTS BASED ON *CBR*, *PFWD*, *DCP* AND *CYCLIC TRIAXIAL* TESTS

This section focus on development of relationship between the observations made from the experimental results of the *CBR*, *PFWD*, and the *DCP* in addition to the results on the *modulus of resilience* (M_r) obtained using the c*yclic triaxial* test equipment. The results obtained from this section will be very useful for the engineers dealing with subgrade soil and pavement evaluation.

Experiments were conducted on soil blends of 75% *laterite* + 25% *lithomarge* (designated as *B2*, or *75%L+25%S*), 50% *laterite* + 50% *lithomarge* (designated as *B3*, or *50%L+50%S*), and 25% *lateritie* + 75% *lithomarge* (designated as *B4* or *25%L+75%S*), in addition to pure *lateritic soils* (designated as *B1* or 100%L+0%S), and pure *lithomargic soils* (designated as *B5* or 0%L+100%S) obtained from various sites.

6.4.1 Regression between the Test Results for *CBR* and E_{pfwd}: Unsoaked

A regression between the values of CBR_u and E_{pfwdu} was developed as shown in Eq. 6.28a, based on the scatter plot as given in Fig. 6.15a for the results compiled in Table 6.61a. The R^2 value for the regression was 0.86 and the adjusted R^2 was 0.842. The standard error of estimation (SE) was found to be 3.87, while the values for F-test, and t test were 49.0 and 0.994 respectively at a significance level of 0.01.

$$CBR_u = 0.194\ (E_{pfwdu}) + 2.783 \qquad \text{Eq.6.28a}$$

The regression equation developed was validated using the data for E_{pfwdu} and CBR_u set apart for the same. The scatter plot for the validation performed is shown in Fig. 6.15b. The regression line of the scatter plot satisfied an R^2 value of 0.895 coinciding satisfactorily with the theoretical line of equality, at a negligible intercept of 1.844. This shows that the values of CBR_u of soil blends can be effectively predicted using E_{pfwdu} values for tests conducted on unsoaked samples.

`

6.4.2 Regression between the Test Results for *CBR* and *DCPI*: Unsoaked

A regression between the values of CBR_u and the penetration resistance measured using DCP ($DCPI_u$) was developed as shown in Eq. 6.29a, and the scatter plot for the same is given in Fig. 6.16a for the results compiled in Table 6.61a. The R^2 value for the regression was 0.882 and the adjusted R^2 was 0.867. Standard error of estimation (SEE) was found to be 1.414, while the values of F-test, and t-test was 59.51 and 14.2 respectively and confidence level of 99%.

$$DCPI_u = -0.372(CBR_u) + 15.44 \qquad \text{Eq. 6.29a}$$

In this exercise it may be observed that the model developed in the present study for lateritic sub-grades of Dakshina Kannada, in India, follows a similar trend as that proposed by Riley et al (1987), and Rao et al.(2008). However, the scatter plot for observations made by Webster et al (1992) shows a slightly different trend with predicted CBR_u values ranging between 15 to 65%. This is due to the reason that Webster et al (1992) performed studies on granular and cohesive soils while the present study was confined to investigations on *c-ϕ* soils of lateritic nature.

The correlation between the CBR values and the DCPI for the laboratory compacted lateritic soils of Dakshina Kannada district followed a power model CBR = 246.2 $(DCPI)^{-1.34}$ with an R^2 value of 0.92, when compared to the transposed expression CBR = 47.32 $(DCPI)^{-0.7852}$ proposed by George et al. (2009a) for field samples of lateritic subgrades. The model also compares well with the transformed expression CBR = 25.11 $(DCPI)^{-0.55}$ proposed by Gabr et al. (2000) for tests conducted at Raleigh, North Carolina.

6.4.3 Regression between the Test Results for E_{pfwd} and *DCPI*: Unsoaked

A regression between the values of E_{pfwdu} and the penetration resistance measured using DCP ($DCPI_u$) was developed as shown in Eq. 6.30, and the scatter plot for the same is given in Fig. 6.17a for the results compiled in Table 6.61a. The R^2 value for the regression was 0.853 and the adjusted R^2 was 0.835. Standard error of estimation (SEE) was found to be 0.185, while the values of F-test, and t-test was 46.6 and 2.3 respectively and confidence level of 99%.

The regression equation developed was validated using the data for E_{pfwdu} and $DCPI_u$ set apart for the same. The scatter plot for the validation performed is shown in Fig. 6.17b. The regression line of the scatter plot satisfied an R^2 value of 0.779 coinciding satisfactorily with the theoretical line of equality, at a negligible intercept of 2.427. This shows that the values of

`

$DCPI_u$ of soil blends can be effectively predicted using E_{pfwdu} values for tests conducted on unsoaked samples.

The trend shown by the regression model of the form $DCPI = 130.6\ E_{pfwd}^{-0.66}$ for the prediction of E_{pfwd} developed for laboratory compacted lateritic soils of the District of Dakshina Kannada as described in this work was found to agree reasonably well with the transformed expression $DCPI = 12{,}859.9\ E_{FWD}^{-1.504}$ proposed by Chen et al. (2005) for the modulus of resilience (EFWD) measured using the FWD for roads in Texas. The model also compares well with the transformed model $DCPI = 312.27\ E_{pfwd}^{-0.9708}$ formulated by George et al. (2009b) for laboratory samples for unsoaked lateritic specimens. See Fig. 6.17c.

6.4.4 Regression between the Test Results for *CBR* and M_r: Unsoaked

A regression between the values of CBR_u and *modulus of resilience* (M_r) was developed as shown in Eq. 6.31, and the scatter plot for the same is given in Fig. 6.18a for the results compiled in Table 6.61a. The R^2 value for the regression was 0.945, and adjusted R^2 of 0.938 Standard error estimation (SEE) was found as 5.563, while F-test and t-test was 153.46 and 12.388 respectively at a confidence level of 99%.

$M_r = 8.795\ (CBR_u) - 0.972$ Eq. 6.31

The regression equation developed was validated using the data for CBR_u and *modulus of resilience* (M_r) set apart for the same. The scatter plot for the validation performed is shown in Fig. 6.18b. The regression line of the scatter plot satisfied an R^2 value of 0.868 coinciding satisfactorily with the theoretical line of equality, at a negligible intercept of 22.87. This shows that the values of M_r of soil blends can be effectively predicted using CBR_u values for tests conducted on unsoaked samples.

6.4.5 Regression between the Test Results for E_{pfwd} and M_r: Unsoaked

A regression between the values of E_{pfwdu} and *modulus of resilience* ($\boldsymbol{M_r}$) was developed as shown in Eq. 6.32, and the scatter plot for the same is given in Fig. 6.19a for the results compiled in Table 6.61a. The R^2 value for the regression was 0.82,, and adjusted R^2 of 0.80

`

Standard error estimation (SEE) was found as 0.276, while F-test and t-test was 36.195 and 6.109 respectively at a confidence level of 99%.

M_r =1.661 (E_{pfwdu})-34.885 Eq. 6.32

The regression equation developed was validated using the data for E_{pfwdu} and *modulus of resilience* (M_r) set apart for the same. The scatter plot for the validation performed is shown in Fig. 6.19b. The regression line of the scatter plot satisfied an R^2 value of 0.88 coinciding satisfactorily with the theoretical line of equality, at a negligible intercept of 37.54. This shows that the values of M_r of soil blends can be effectively predicted using E_{pfwdu} values for tests conducted on unsoaked samples.

6.4.6 Regression between M_r and *DCPI*: Unsoaked condition

A regression between the values of *modulus of resilience* (M_r) and the penetration resistance measured using DCP ($DCPI_u$)was developed as shown in Eq. 6.33, and the scatter plot for the same is given in Fig. 6.20a for the results compiled in Table 6.58a. The R^2 value for the regression was 0.90, and the adjusted R^2 value was 0.896. The standard error estimation (SEE) was found to be 1.650, while the F-test and t-test values were 87.5 and 9.358 respectively at a confidence level of 99%.

$M_r = 1908\ (DCPI_u)^{-1.30}$ Eq. 6.33

The regression equation developed was validated using the data for the penetration resistance measured using DCP ($DCPI_u$) and *modulus of resilience* (M_r) set apart for the same. The scatter plot for the validation performed is shown in Fig. 6.20b. The regression line of the scatter plot satisfied an R^2 value of 0.819 coinciding satisfactorily with the theoretical line of equality, at a negligible intercept of 15.49. This shows that the values of M_r of soil blends can be effectively predicted using $DCPI_u$ values for tests conducted on unsoaked samples.

6.4.7 Regression between *CBR*, E_{pfwd} and *DCPI* (soaked condition)

Similarly, correlations for E_{pfwd} Vs *CBR*, *DCPI* Vs E_{pfwd}, and *DCPI* Vs *CBR* were developed for soaked soil specimens and validated as shown in Table 6.62. The regressions developed were validated and the R-square values obtained in the validation procedures (R^2_{valid})

`

were found to range between 0.88 and 0.91. The intercepts for the validation exercise (I_{valid}) were found to be negligible indicating a reasonably good fit between the actual and *predicted* values of the *dependent variables*.

6.4.8 Development of Multi-Variable Regressions

Based on the information compiled for the result on *CBR*, *UCS* (q_u), *Static Triaxial*, *DCPI*, *PFWD*, and *Cyclic Triaxial* test equipment compiled in the Table 6.61a and Table 6.61b above section. It is possible to develop multi-linear regression equation relating Unsoaked and Soaked values of *CBR* to values of q_u, *Cohesion*, *angle of internal friction*, *DCPI, PFWD* and M_r. The list of regression equation developed are provided in Table 6.63. The details regarding R^2 value, the adjusted R^2 value, the f-test values, the t-test values and the level of significance are also provided in the table.

In the above mentioned table it can be seen that the CBR_u can be predicted with high accuracy based on the values of $DCPI_u$, E_{pfwdu} and M_r with the R^2 value above 0.90. For soaked sample it was found that adjusted R^2 is around 0.80-0.85. Thus it is observed that CBR value can be reliably predicted using multi-linear regression equation developed above.

6.5 SUMMARY ON DEVELOPMENT OF RELATIONSHIPS

The above sections have focused in detail on exploring relationships connecting the observations made using various pavement evaluation approaches using the *Unconfined Compression test* (q_u), *Triaxial test*, *DCPI*, *PFWD*, *CBR* and the tests for *resilient modulus* using the *Cyclic Triaxial Test* (M_r) for investigations performed on blended *laterite* soil samples. The relationships developed are expected to be of special advantage in pavement design and evaluation.

Additionally, a number of multi-variable relationships were developed for the prediction of *CBR, DCPI,* E_{pfwdu}, and M_r in soaked and unsoaked condition. The results were found to be logically correct. The conclusions of the investigations conducted are reported in the next chapter.

CHAPTER VII

FEM-BASED ANALYSES USING *PLAXIS* FOR EMBANKMENT MODELS OF VARIOUS SOIL BLENDS

7.0 INTRODUCTION

Details on investigations on soil stiffness and modulus of resilience using cyclic triaxial test equipment, DCP, and the PFWD were discussed in the previous chapter in addition to details on regressions developed and the related discussions. The soil properties for various blends were observed from the results obtained in the previous chapters, and further investigations were performed using *FEM* to study the stability of embankment models for various soil blends using *PLAXIS*.

7.1 ANALYSIS OF EMBAKMENTS OF SUBGRADES OF VARIOUS BLENDS USING *FEM* BASED PLAXIS-2D SOFTWARE WITH INPUTS FROM *KENPAVE*

In the analytical studies on embankment models performed using *FEM*, the *PLAXIS-2D* Dynamic Analysis Module software was used. The following sub-sections provide details on the analysis of stresses using the *FEM*-based approach for embankments with trapezoidal cross-sections.

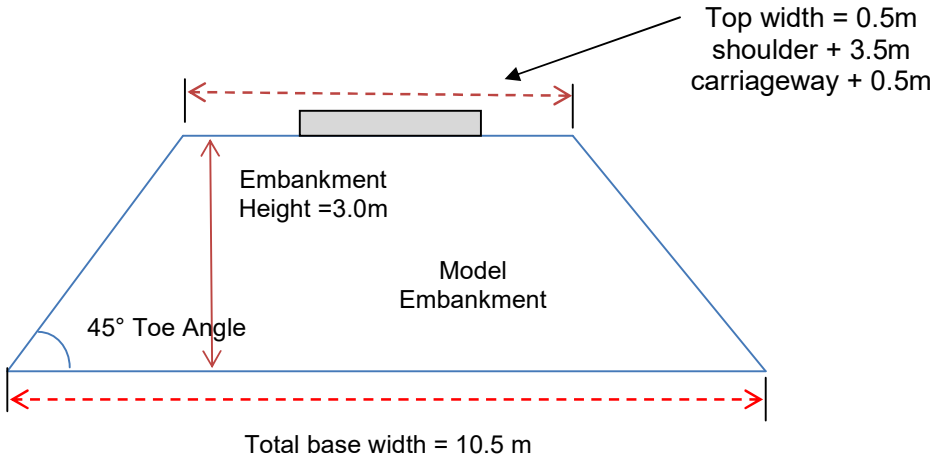

Fig.7.1a Cross-sectional Details of the Embankment Model

Plaxis-2D (Version 8.2) comprises the sub-modules such as, *Plaxis Input, Plaxis Calculations, Plaxis Output, Plaxis Curves,* and *Plaxis Manual*. The input data was provided using the *Plaxis Input* module. This is a front-end used for entering data such as, dimensions of the model to be tested, loading conditions of the subgrade, and the material properties of the soil tested. It is possible to give details on ground water table also, in case of analysis of soil structures. Fig.7.1a and Fig.7.1b provide details on the cross-section of the embankment.

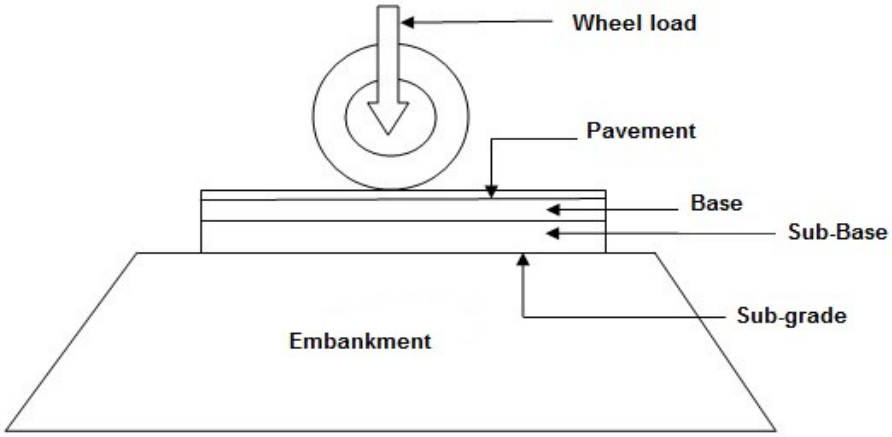

Fig.7.1b Cross-sectional Details of the Embankment Model

In the study of stresses, strains and displacements of various elements in pavement subgrades constructed on embankments, it is most often required to perform analyses for the following conditions:

i. *Considering the self weight of the embankment alone:*

The Geometry tool box and the line option are used to create the window showing the Geometry of the Model.

ii. *Considering a standard wheel load of 5100 kg (50 kN) applied at over the pavement constructed on the embankment in addition to the self weight of the embankment*:

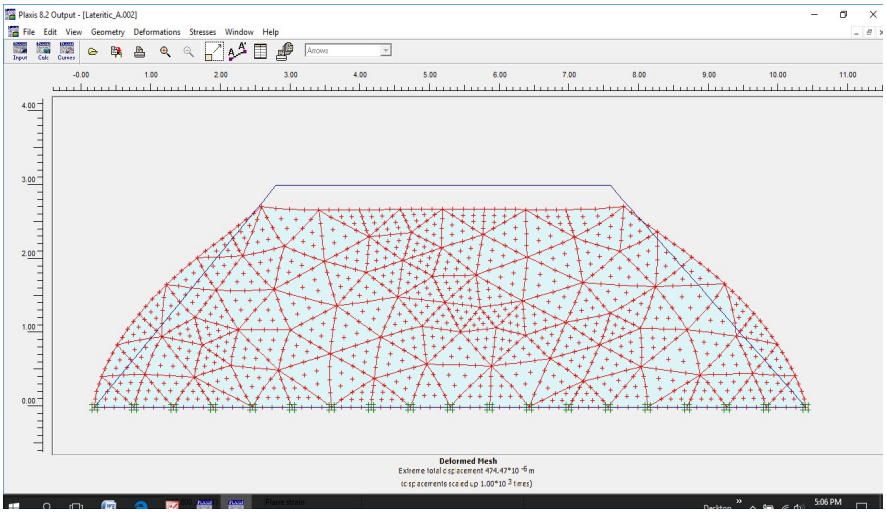

Fig.7.2 Output Window for Phase 1 for No Wheel Loads Applied

Similarly, the outputs with details on displacement without application of wheel loads are provided in Fig.7.3.

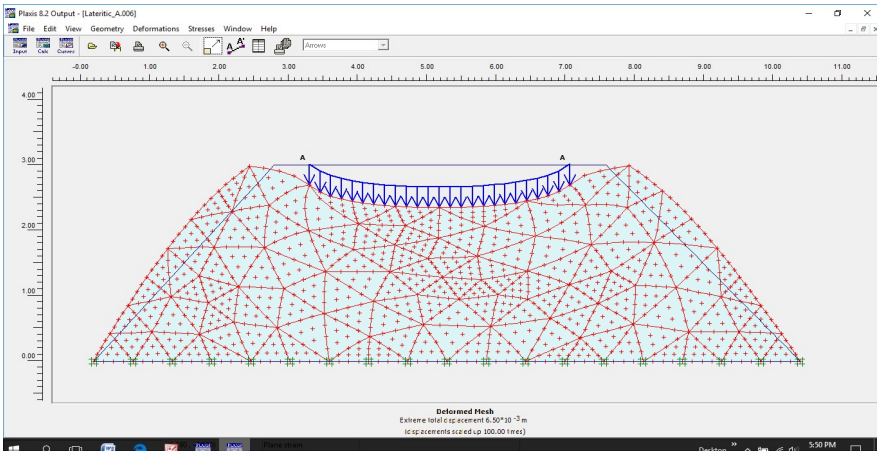

Fig.7.3 Output Window with Details on Displacements after Applying Wheel Loads

Additionally, the output details on effective stresses with and without application of wheel loads are provided in Fig. 7.4, and Fig.7.5.

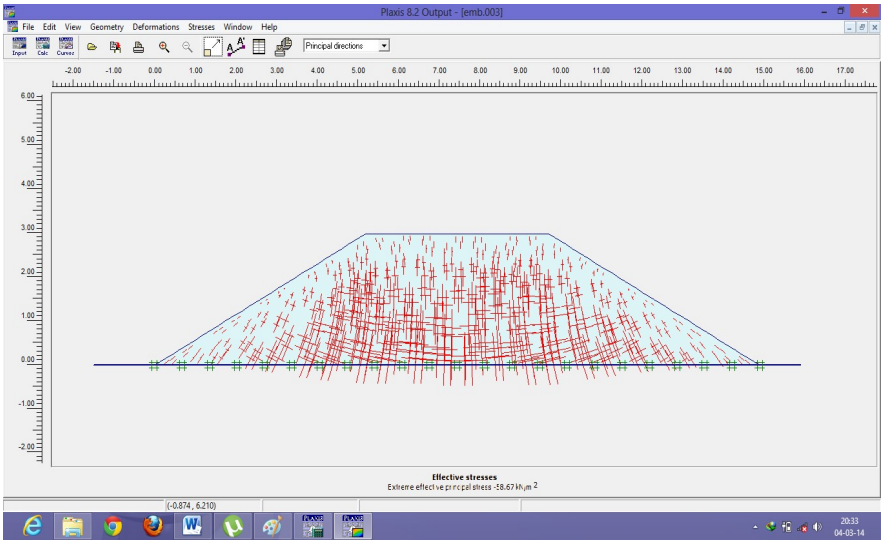

Fig.7.4 Output Window: Effective Stresses without Wheel Load Stresses

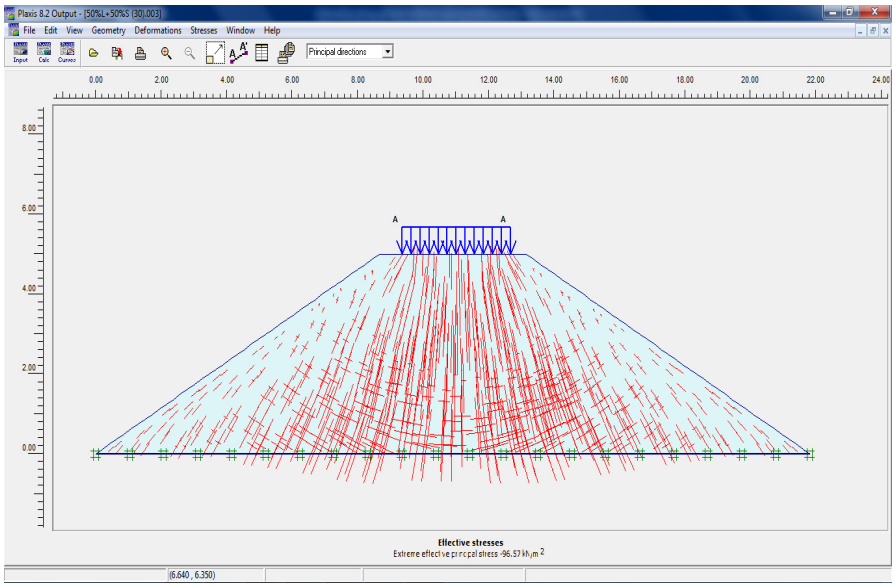

Fig.7.5 Output Window: Effective Stresses with Wheel Load Stresses

Table 7.2a and Table 7.2b provide details on the stresses, and strains along the *x* and *y* axes for coordinates of selected points on the boundary lines AB, AC, and CD of the embankment model of height 3 m and toe angle of 45 degrees for the soil blend *B1* (100%L+0%S), when tested without wheel loads and with wheel loads respectively.

Table 7.3a and Table 7.3b provide similar details for the embankment model of height 3m and toe angle of 45 degrees for the soil blend *B2* (75%L+25%S), when tested without wheel loads and with wheel loads respectively.

Appendix 5 provides details on computations for embankments with toe-angles of 30, 45, and 60 degrees for embankments heights of 3 m, 4 m and 5 m for various soil blends.

From the output generated by Plaxis-2D, for various tests performed on model embankments, the key observations on maximum effective stresses, total strains developed, and the maximum displacements are summarized in Table 7.4a, Table 7.4b and Table 7.4c respectively. Appendix 6 provides details on the output obtained for various soil blends.

CHAPTER VIII

CONCLUSIONS

8.0 INTRODUCTION

The design and construction of highway subgrades and embankments require a deeper understanding of the types of soil of the region, while due importance must be given on using locally available soil and construction material to optimize construction costs. The presence of *lateritic* and *lithomargic* soils in the region of Dakshina Kannada and other regions of peninsular India necessitate a proper study on their engineering properties. One of the advantages of lateritic soils is that these are not expansive in nature, and can be modified to some extent to take traffic loads. Embankments and subgrades help maintain the required gradient, ensure proper approaches to bridges, and prevent roads from being submerged during heavy rainfall. Failure of embankments is experienced due to poor subgrade strength, soil-structure interactions, and seismic vibrations. This is further worsened by increase in traffic loads far exceeding the projected growth (Tagore, 2003).

The *first phase* of this study on *lateritic* and *lithomargic* soils dealt with experimental investigations on 100%L+0%S , 75%L+25%S, 50%L+50%S, 25%L+75%S and 0%L+100%S soil blends, commencing with studies on index properties of soil based on specific gravity, Atterberg's limits, and particle size distribution. Tests for optimum moisture content (OMC) were performed for each soil blend using the modified Proctor tests and the maximum dry densities were determined. Test on permeability were also performed. Subsequently, the static tests for soil strength were performed using the *California bearing ratio* (CBR) method, followed by tests for *unconfined compressive strength* (UCS), and *static triaxial* tests. This was followed by studies on dynamic soil strength based on tests using the *portable falling weight deflectometer* (PFWD), and the *dynamic cone penetrometer* (DCP). Investigations on soil blends were performed at three moisture contents such as at the drier-side of optimum at OMC-3%, at OMC, and at the wetter-side of optimum at OMC+3%. The *second phase* of this study was focused on performing tests using the *cyclic triaxial* test equipment for various soil blends of *lateritic* and *lithomargic* soils for the determination of the *modulus of resilience*.

The *fourth phase* of this study dealt with performing further analyses on various configurations of the embankment models using *FEM*-based techniques. The following sections provide discussions on the results of investigation at various stages of work.

8.1 CONCLUSIONS ON THE *FIRST PHASE* OF THE PRESENT WORK

8.1.1 Important Observations on Specific Gravity, Atterberg's Limits, Grain-size Distribution, Compaction, and Permeability of Various Soil Blends

Based on the results of the tests for the determination of the in-situ-density, water-content, and dry-density and also based on the results of the heavy compaction (modified Proctor density) test, and the tests for particle-size distribution as shown in Table 4.1 to Table 4.4, the following important observations may be made:

- The results for the tests for *specific gravity* as shown in Table 4.1 indicate that the specific gravity for various blends varied between 2.58 to 2.37. However, it must be observed that the specific gravity values for lateritic soils in other regions as reported by Nanda and Krishnaramachari (1958), and Gidugasu (1976) were found to be higher. The lower values of specific gravity observed for the region of Dakshina Kannada indicate the presence of lesser amount of iron oxides and the increased amount of fines.
- The tests for Atterberg's limits as shown in Table 4.2 indicate that the *liquid limit* increases from 54.2 to 61.3, the plastic limit increases from 29.4 to 31.4, and the shrinkage limit increases from 20.1 to 23.4 as the fines content increases from 14.0% for blend B1 (100%L+0%S) to 86.0% for blend B5 (0%L+100%S).

8.1.2 General Conclusions on Tests for CBR

The tests for CBR were performed for unsoaked and soaked soil samples compacted at three different moisture contents M1, M2, and M3 for the soil blends B1, B2, B3, B4, and B5. The results for tests on unsoaked and soaked samples were compiled in Table 4.6 and represented graphically in Fig.4.2a and Fig.4.2j.

- Comparing the properties of *soaked and unsoaked* soils, based on Fig.6.5a and Fig.6.5b, it can be observed that the strength of unsoaked soils is generally higher, while the strength of soaked soils is much lower. Also, it can be stated in general, that the values of the *CBR*

for compacting moisture contents *M1, M2,* and *M3* decrease with increase in soil moisture content. Similar observations were also made by Hammond (1970).

Also, as the water content increases beyond the OMC, it acts as a lubricating agent reducing the friction between the soil particles resulting in lesser strength.

8.1.3 General Conclusions on Tests for UCS

The tests for *unconfined compressive strength* (UCS) were conducted for the soil blends B1, B2, B3, B4, and B5 at the three moisture contents M1, M2, and M3, using 38mm diameter and 100mm diameter molded specimens The results for tests were compiled in Table 4.7a and Table 4.7b. Details of the stress-stain curves are presented in Fig.4.3a to Fig.4.3e for 38mm diameter sample and Fig.4.4a to Fig.4.4e for 100mm diameter respectively. The following are the conclusions based on tests for *unconfined compressive strength* (UCS) performed on various blends of soil samples on unsoaked soil samples.

- It is also observed that in the case of unsoaked soil samples compacted to moisture contents of OMC-3% (or M1), the stresses taken by the soil specimens were higher when compared to stresses taken at OMC+3% (or M3). This is due to the reason that the presence of increased moisture content tends to reduce the internal friction developed. Similar observations were made by Zydron and Dabrowska (2012), and Lambe and Whitman (1979).

8.1.4 General Conclusions on Static Triaxial Test Observations

The tests for the determination of *shear strength* were performed based on *static triaxial tests* for the soil blends B1, B2, B3, B4, and B5 compacted to three different moisture contents M1, M2, and M3, using 38mm diameter and 100mm diameter molded specimens. The results were compiled in Table 4.8a and Table 4.8b. The following are the conclusions based on tests using the *static triaxial* test equipment performed on various blends of soil samples for un-consolidated un-drained test (or unsoaked) conditions.

- In the tests for triaxial strength for 38 mm diameter soil samples compacted at OMC, it is found that at high confining pressures of 200 kPa, the specimens are able to withstand

higher stresses compared to samples compacted at OMC-3% (or M1) and OMC+3% (or M3). A similar trend is observed in the case of tests for lower confining pressures of up to 100 kPa for various soil blends. These observations tally with the conclusions made by Kim and Kim (2006), and Cokca et al. (2004).

8.1.4 General Conclusions on Results of Tests Using the DCP

The tests using the *dynamic cone penetrometer* (DCP) were performed for unsoaked and soaked soil samples compacted at three different moisture contents M1, M2, and M3 for the soil blends B1, B2, B3, B4, and B5. The results for tests on unsoaked and soaked samples were compiled in Table 4.9.

- In the tests using the DCP, it is observed that the values of penetration indices (*DCPI*) ranged between 4.2 mm/blow and 12.64 mm/blow for unsoaked samples, while those for soaked specimens ranged between 21.8 mm/blow and 70.30 mm/blow various soil blends tested at compacted optimum moisture content. The results indicate that since *lateritic* soils possess lower fines content and higher sand content, the resistance to penetration is higher indicating a higher soil-stiffness. In comparison, in the case of *lithomargic* soils with high content of fines, the penetration resistance is lower indicating a lesser soil stiffness. These observations tally with the conclusions made by Hicks and Monismith (1971), and Omotosho (2004). The overall trend is similar to that observed in the case of the tests for CBR.

  Additionally, it may be noted that the resistance to penetration by the DCP for samples compacted at *M1* moisture contents are slightly higher than that at *M3*. In this case too, the overall trend is similar to that observed in the case of the tests for CBR for soaked soils.

8.1.5 General Conclusions on Results of Tests Using the PFWD

The tests using the *portable falling weight deflectometer* (PFWD) were performed for unsoaked and soaked soil samples compacted at three different moisture contents M1, M2, and M3 for the soil blends B1, B2, B3, B4, and B5. The results for tests on unsoaked and soaked samples were compiled in Table 4.13a and Table 4.13b.

- In the tests using the PFWD, it is observed that the values the *modulus of resilience* (E_{pfwd}) ranged between 154 MPa and 36 MPa for unsoaked samples while those for soaked specimens ranged between 50.7 MPa and 22.0 MPa for various soil blends tested at compacted optimum moisture content. The results indicate that since *lateritic* soils possess lower fines content and higher sand content, the *modulus of resilience* is higher indicating a higher soil-stiffness. In comparison, in the case of *lithomargic* soils with high content of fines, the *modulus of resilience* is lower indicating a lesser soil stiffness. These observations tally with the conclusions made by Hicks and Monismith (1971), Thompson and Robnett (1979) and Omotosho (2004). The overall trend is similar to that observed in the case of the tests for CBR.

  Also, it can be stated in general, that the values of the E_{pfwd} indicating the modulus of resilience for compacting moisture contents *M1, M2,* and *M3* decrease with increase in soil moisture content.

  It is also observed that although *lithomargic* soils possess moderately good *modulus of resilience* (E_{pfwd}) at unsoaked conditions, the strength reduces by about 95% in the case of soaked samples. The above observations tally with the conclusions made by Hammond (1970) as in the case of tests for CBR.

- In the case of *soaked* soils, it is observed based on Table 4.14b that the values of *modulus of resilience* (E_{pfwd}) of soils compacted to OMC (or M2) is higher than that for *M1* and *M3*. This is due to the reason that soaked soils tested at *M1* tend to have a *flocculent structure*, while the same tested at *M3* tend to have a *dispersive structure,* due to which the loads supported by these soaked samples tend to be lesser than that supported at OMC conditions (Lambe and Whitman, 1979). The overall trend is similar to that observed in the case of the tests for CBR.

8.2 CONCLUSIONS ON THE *SECOND PHASE* OF THE PRESENT WORK

The investigations using the cyclic triaxial test equipment were performed in the *second phase* of the study for various blends of *lateritic* and *lithomargic* soils as discussed in Chapter 5.

8.2.1 Conclusions on Tests Using the Cyclic Triaxial Equipment

Investigations using the cyclic triaxial test equipment were performed on various blends of lateritic and lithomargic soils to determine the *resilient modulus* or modulus of resilience according to the procedure described in AASHTO T 307-99 (AASHTO, 2003). The specimens were prepared as for unsoaked soil samples compacted at three different moisture contents M1, M2, and M3 for the soil blends B1, B2, B3, B4, and B5. speficied. The *resilient modulus* testing protocol includes the determination of the resilient modulus at various deviator stresses of 13.8 kPa, 27.6 kPa, 41.4 kPa, 55.2 kPa, and 68.9 kPa. Since it was observed that a deviator stress of 41kPa and a confining pressure of 14kPa could be used for estimating the modulus of resilience a measured using the PFWD (George , 2006), tests were performed at a deviator stress of 41 kPa ($0.41 kg/cm^2$) for a confining pressure of 14 kPa to determine the resilient modulus for the subgrade under investigation.

A graphical representation of the variation in modulus of resilience with respect to deviator stresses is shown in Fig. 8.1a for blend 100%L+0%S, B1 for purely lateritic soils. The variations between the modulus of resilience and the deviator loads indicate that lateritic soil blends develop high modulus of resilience when subjected to increasing deviator loads. The above observation tallies with conclusions made by Boateng-Poku and Drumm (1989) where it is seen that the modulus of resilience of coarse grained soils increased with increasing deviator stresses, which is considered to occur because of the strain hardening effect that takes place due to the reorientation of soil grains into a denser state. A similar trend is obtained in the case of lateritic blend of 75%L+25%S, B2 as shown in Fig. 8.1b.

Fig.8.1e provides a graphical representation of the variation in the *modulus of resilience* with respect to deviator stresses for blend *0%L+100%S,* B5 for *purely lithomargic* soils. The variations between the *modulus of resilience* and the deviator loads indicate that *lithomargic* soils are not capable of resisting increasing deviator loads. The above observation tallies with conclusions made by Boateng-Poku and Drumm (1989), Rahim (2005) where it is seen that the the *modulus of resilience* of fine-grained cohesive soils decreased with increasing *deviator stress*es, which is considered to occur because of the *stress softening behavior* or *strain softening*. A similar trend is obtained in the case of lithomargic blends of *50%L+50%S*, and *25%L+75%S* as in Fig. 8.1c and Fig. 8.1d.

8.3 CONCLUSIONS ON THE *THIRD PHASE* OF THE PRESENT WORK

In the *third phase* of study, it was proposed to analyze the effect of various parameters on the results obtained using various tests performed on soaked and unsoaked samples of blended *lateritic* and *lithomargic* soils for various moisture contents using regression equations developed using the Statistical Package for Social Sciences (SPSS) as discussed in Chapter 6. Most of the tests were performed on five blends of *lateritic* and *lithomargic* soils with tests performed for OMC-3% (or M1), OMC (or M2), and OMC+3% (or M3). Thus there were 15 data points in most tests performed. The correlations were developed using 10 randomly selected data points out of the total 15 data points.

8.3.1 Conclusions on Regressions for *Percentage of Fines* Vs *Specific Gravity*, *Maximum Dry Density* (*MDD*), *Permeability*, and *Atterbergs's Limit*

A number of regressions were developed correlating the values of *specific gravity*, *maximum dry density* (*MDD*), *permeability*, and *Atterbergs's limits* to the *percentage of fines*. Table 6.1 provides details on the summarized results obtained based on standard tests performed on various blends of lateritic soils.

Linear regression equations were developed for correlating the *percentage of fines* to the *specific gravity*, *MDD*, *permeability constant*, and the *Atterberg's limits* separately. The adjusted R-square values for the regressions were found to range between 0.90, and 0.98 within acceptable statistical significance limits of 0.01 or confidence interval of 99% for Fisher's test (or *F*-test) and Student's *t* test values. See Eq.6.1 to Eq.6.6.

8.3.2 Conclusions on Regressions Developed Based on the Results of Tests for *UCS*

A number of regressions were developed correlating the values of *unconfined compression test* (*UCS*) to the *percentage of fines, percentage of gravel, percentage of sand, maximum dry density* (*MDD*) and the *optimum moisture content* (*OMC*). Table 6.3 provides details on the summarized results obtained using *UCS* tests on various blends of lateritic soils.

The correlations between *percentage of fines* and the values *UCS* for various soil blends indicate that the two variables are correlated linearly with high adjusted R^2 values of 0.84 to 0.94 for various soil blends at different moisture content. See Table 6.4.

Similar correlations were developed between the values of *UCS* and the *percentage of gravel* for various soils blends. These indicate that the two variables are correlated using linear expressions with adjusted R^2 values of 0.73 to 0.90 for various moisture contents. See Table 6.5.

8.3.3 Conclusions on Regressions Developed Based on the Values for *Cohesion* Obtained Using Static Triaxial Tests

A number of regressions were developed correlating the values of *Cohesion* (***c***) to the *percentage of fines, percentage of gravel, percentage of sand, maximum dry density* (*MDD*) and the *optimum moisture content* (*OMC*). Table 6.9 provides details on the summarized results obtained using *triaxial* tests on various blends of lateritic soils.

The correlations between the *percentage of fines* and the values *Cohesion* (***c***) for various soil blends indicate that the two variables are correlated using exponential based expressions with a high adjusted R^2 value of 0.90 to 0.98 for various soil blends at different moisture contents. See Table 6.10.Similarly correlations were developed between the values of *Cohesion* (***c***) and the *percentage of gravel* for various soils blends. These indicate that the two variables are correlated exponential based expression with high adjusted R^2 values of 0.91 to 0.97 for various moisture contents. See Table 6.11.

8.3.4 Conclusions on Regressions Developed Based on the Values for *Angle of Internal Friction* Using Static Triaxial Tests

A number of regressions were developed correlating the values of *angle of internal friction* (Ø) to the *percentage of fines, percentage of gravel, percentage of sand, maximum dry density* (*MDD*) and the *optimum moisture content* (*OMC*). Table 6.9 provides details on the summarized results obtained using *triaxial* tests on various blends of lateritic soils.

The correlations between the *percentage of fines* and the values of *angle of internal friction* (Ø) for various soil blends indicate that the two variables are correlated linearly with high adjusted R^2 values of 0.91 to 0.97 for various soil blends at different moisture contents. See Table 6.15.

The correlations developed between the values of *angle of internal friction* (Ø) and the *percentage of sand* for various soils blends indicate that the two variables are correlated using

linearly with high adjusted R^2 values of 0.90 to 0.98 for various moisture contents. See Table 6.17.

8.3.5 Conclusions on Regressions Developed Based on Tests for *CBR*

A number of regressions were developed correlating the values of *CBR* to the *percentage of fines, percentage of gravel, percentage of sand, maximum dry density* (*MDD*) and *optimum moisture content* (*OMC*). Table 6.20 provides details on the summarized results obtained using *California Bearing Ratio* (*CBR*) tests on various blends of lateritic soils.

Consequently, it can also be said that an increase in the *percentage of gravel* for soil blends B1 to B5, resulted in an increase in the *CBR* values for unsoaked and soaked soils. The correlations between the *percentage of gravel* and the values of the *CBR* for various soil blends indicate that the two variables are correlated power based expression with high adjusted R^2 values of 0.88 to 0.93 and 0.90 to 0.95 for unsoaked and soaked soil conditions respectively for various soil blends at different moisture contents. Table 6.23 and Table 6.24 provide details on regression equations developed for the prediction of the *CBR* values based on variations in the *percentage of gravel* in blended *laterite* soils.

Similarly, the correlations between the values of the *CBR* and the MDD for various soil blends indicate that the two variables are correlated linearly with high adjusted R^2 values of 0.97 and 0.91 to 0.93 for unsoaked and soaked soil conditions respectively for various moisture contents. The regression equations are tabulated in Table 6.27 and Table 6.28 respectively.

The correlations developed between the values of the *CBR* and the OMC *for* various soils blends indicate that the two variables are correlated linearly with high adjusted R^2 values of 0.78 to 0.98 and 0.95 to 0.99 for unsoaked and soaked soil conditions respectively for various moisture contents. The regression equations are tabulated in Table 6.29 and Table 6.30.

8.3.6 Conclusions on Regressions Developed Based on Tests Using *DCP*

A number of regressions were developed correlating the values of *DCP* to the *percentage of fines, percentage of gravel, percentage of sand, maximum dry density* (*MDD*) and the *optimum moisture content* (*OMC*). Table 6.31 provides details on the summarized results obtained based

on tests conducted using the *Dynamic Cone Penetrometer* (*DCP*) on various blends of lateritic soils.

Consequently, it can also be said that an increase in the *percentage of gravel* for soil blends B1 to B5, resulted in an increase in the resistance to penetration, or in other words, a decrease in the *DCPI* values for unsoaked and soaked soils. The correlations between the *percentage of gravel* and the values of the *DCPI* for various soil blends indicate that the two variables are correlated based on exponential expression with adjusted R^2 values of 0.82 to 0.93 and 0.77 to 0.79 for unsoaked and soaked soil conditions respectively for various soil blends at different moisture contents. See Table 6.34 and Table 6.35.

The correlations developed between the values of the *DCPI* and the *OMC* for various soils blends indicate that the two variables are correlated linearly with high adjusted R^2 values of 0.97 to 0.99 and 0.88 to 0.90 unsoaked and soaked soil conditions for various moisture contents. The regression equations are tabulated in Table 6.40 and Table 6.41.

8.3.7 Conclusions on Regressions Developed Based on Tests Using *PFWD*

A number of regressions were developed correlating the values of *portable falling weight deflectometer* (E_{pfwd}) to the *percentage of fines, percentage of gravel, percentage of sand, maximum dry density* (*MDD*) and the *optimum moisture content* (*OMC*). Table 6.42 provides details on the summarized results obtained using E_{pfwd} tests on various blends of lateritic soils.

Based on the tests performed using the *portable falling weight deflectometer*, it may be observed that the increase in the resulting *percentage of fines* from 14 to 86 percent for various blends B1 to B5 has resulted in a corresponding decrease in the values of the modulus of resilience E_{pfwd} for unsoaked soil samples. A similar trend was observed in the case of tests on soaked soil samples.

The correlations between the *percentage of fines* and the values of the E_{pfwd} for various soil blends indicate that the two variables are correlated *linearly* with adjusted R^2 values of 0.90 to 0.96 and 0.81 to 0.90 for tests on unsoaked and soaked soils respectively for various soil blends at different moisture contents. See Table 6.43 and Table 6.44

Consequently, it can also be said that an increase in the *percentage of gravel* for soil blends B1 to B5, resulted in an increase in the E_{pfwd} values for unsoaked and soaked soils. The correlations between the *percentage of gravel* and the values of the E_{pfwd} for various soil blends indicate that the two variables are correlated *linearly* and power based expression with adjusted R^2 values of 0.81 to 0.93 and 0.70 to 0.85 for tests on unsoaked and soaked soils respectively for various soil blends at different moisture contents. See Table 6.45 and Table 6.46

The correlations developed between the values of the E_{pfwd} and the *OMC* for various soils blends indicate that the two variables are correlated linearly with adjusted R^2 values of 0.85 to 0.90 and 0.97 to 0.98 for unsoaked and soaked soil conditions for various moisture contents. See Table 6.51 and Table 6.52

8.3.8 Conclusions on Regressions Developed Based on Cyclic Triaxial Tests

A number of regressions were developed correlating the values of *resilient modulus* (M_r) obtained based on tests performed using the *cyclic triaxial* test equipment to the *percentage of fines, percentage of gravel, percentage of sand, maximum dry density* (*MDD*) and the *optimum moisture content* (*OMC*). Table 6.53 provides details on the summarized results obtained using *resilient modulus* (M_r) tests on various blends of lateritic soils.

The correlations developed between the values of the M_r and the *percentage of sand* for various soils blends indicate that the two variables are correlated *linearly* with high adjusted R^2 values of 0.92 to 0.97 for unsoaked soil conditions for various moisture contents. See Table 6.56.

Similarly, the correlations between the values of the M_r and the *MDD* for various soil blends indicate that the two variables are correlated *linearly* with high adjusted R^2 values of 0.86 to 0.98 for unsoaked soil conditions for various moisture contents. See Table 6.57.

The correlations developed between the values of the M_r and the *OMC* for various soils blends indicate that the two variables are correlated *linearly* with adjusted R^2 values of 0.95 to 0.90 for unsoaked soil conditions for various moisture contents. See Table 6.58.

8.3.9 Conclusions on the Results Obtained Using 38mm dia and 100mm dia Samples for Tests for *UCS* and Tests Using the Static Triaxial Equipment

The results obtained based on tests performed for the *UCS* (q_u), and the results of the tests for *cohesion* and *angle of internal friction* using the static triaxial equipment were compiled for

soil samples of 38 mm and 76 mm height, and samples of 100 mm diameter and 200 mm height as in Table 6.59. A number of correlations were developed relating the results obtained using the soil samples of the two sizes mentioned above. These correlations were also validated as explained in Chapter 6. The tests were performed on five blends of *lateritic* and *lithomargic* soils at OMC-3% (or M1), OMC (or M2), and OMC+3% (or M3) which generated 15 data points. The correlations were developed using 10 randomly selected data points out of the total 15 data points, while validations were performed using the remaining 5 data points.

8.3.9.1 Conclusion on correlation between UCS_{38} Vs UCS_{100}

In the analysis of results of the tests performed for determination of the *Unconfined Compressive Strength* (*UCS*) on 38 mm diameter samples (UCC_{38}) and 100 mm diameter samples (UCS_{100}), it may be observed that the *UCS* values are highly correlated with an R^2 value of 0.90, when fitted with a linear function. See Eq. 6.15 and Fig. 6.9a.

The regression equation developed was validated using the data for q_{u38} and q_{u100} set apart for the same which satisfied an R^2 value of 0.85. See Fig. 6.9b, this shows that the values of q_{u38} of soil blends can be effectively predicted using q_{u100} values for tests conducted on 100 mm diameter samples.

8.3.9.2 Conclusion on correlation between c_{38} Vs c_{100}

Tests were performed using Static triaxial test on samples of 38mm diameter and 100mm diameter to determine the values of *cohesion* (***c***). The analysis of results shows that the *Cohesion* measured using the 38 mm dia. soil samples can be correlated to the same obtained based on 100 mm dia. soil samples with a high R^2 value of 0.93 when fitted with a linear function. See Eq. 6.16 and Fig.6.10a.

The regression equation developed was validated using the data for $\boldsymbol{c_{38}}$ and c_{100} set apart for the same which satisfied an R^2 value of 0.98. This shows that the values of c_{38} of soil blends can be effectively predicted using c_{100} values for tests conducted on 100mm diameter samples. See Fig.6.10b.

8.3.9.3 Conclusions on correlation between $\Phi°_{38}$ and $\Phi°_{100}$

Tests were performed using static triaxial test equipment on soil samples of 38mm diameter and 100mm diameter to determine the values of *angle of internal friction* ($\phi°$). The analysis of results shows that the *angle of internal friction* obtained based on 38mm dia soil samples can be correlated to the same obtained based on 100 mm dia. soil samples with a high R^2 value of 0.92 when fitted with a linear function. See Eq. 6.17 and Fig. 6.11a.

The regression equation developed was validated using the data for $\phi°_{38}$ and $\phi°_{100}$ set apart which satisfied an R^2 value of 0.97. This shows that the values of $\phi°_{38}$ of soil blends can be effectively predicted using $\phi°_{100}$ values for tests conducted on 100 mm diameter samples. See Fig. 6.11b.

8.3.10 Conclusion on the Regressions Developed Based on *Static Triaxial Tests*, *CBR*, and *UCS*

The results of the tests performed on soil samples based on the *CBR*, *UCS* and *triaxial* tests are summarized in Table 6.60. The tests were performed on five blends of *lateritic* and *lithomargic* soils at OMC-3% (or M1), OMC (or M2), and OMC+3% (or M3) which generated 15 data points. The correlations were developed using 10 randomly selected data points out of the total 15 data points, while validations were performed using the remaining 5 data points.

8.3.10.1 Conclusions on correlations between *CBR* and *UCS* (q_u)

While analyzing the results of the tests performed on unsoaked CBR_u samples and the *UCS* (q_u) values measured using the tests for UCS on unsoaked samples, it can be seen that these two variables can be correlated linearly with an R^2 value of 0.67. See Eq. 6.18 and Fig. 6.12a. The regression equation developed was validated using the data set apart for the same which satisfied an R^2 value of 0.878. See Fig.6.12b. This shows that the values of CBR_u of soil blends can be effectively predicted using q_u values.

Similarly, it is seen that a regression between CBR_s for soaked samples, and *UCS* (q_u) measured using the tests for UCS on unsoaked samples can be developed. These two variables can be correlated linearly with an R^2 value of 0.802. See Eq. 6.19 and Fig. 6.12c. The regression equation developed was validated using the data set apart for the same which satisfied an R^2

value of 0.89. See Fig.6.12d. This shows that the values of CBR_u of unsoaked soil blends can be effectively predicted using q_u values for tests for *UCS* on unsoaked soils.

8.3.10.2 Conclusions on correlations between *CBR* and *Cohesion* (c)

On analyzing the results of the tests performed on unsoaked CBR_u samples and the *cohesion (c)* measured using the *triaxial* test on unsoaked samples, it can be seen that these two variables can be correlated linearly with an R^2 value of 0.66. See Eq. 6.20 and Fig. 6.13a. The regression equation developed was validated using the data set apart for the same which satisfied an R^2 value of 0.93. See Fig.6.13b. This shows that the values of CBR_u of soil blends can be effectively predicted using values of *cohesion (c)* measured using *triaxial* tests on unsoaked samples.

Similarly, it is seen that a regression between CBR_s for soaked samples, and *Cohesion (c)* measured using the triaxial test equipment on unsoaked samples can be developed. These two variables can be correlated linearly with an R^2 value of 0.73. See Eq. 6.21 and Fig. 6.13c. The regression equation developed was validated using the data set apart for the same which satisfied an R^2 value of 0.94. See Fig.6.13d. This shows that the values of of CBR_s of soaked soil blends can be effectively predicted using *cohesion (c)* values for triaxial tests on unsoaked soils.

8.3.10.3 Conclusions on correlations between *CBR* and *angle of internal friction* (ϕ)

While analyzing the results of the tests performed on unsoaked CBR_u samples and the *angle of internal friction* (ø) measured using the *triaxial* test on unsoaked samples, it can be seen that these two variables can be correlated linearly with an R^2 value of 0.87. See Eq. 6.22 and Fig. 6.14a. The regression equation developed was validated using the data set apart for the same which satisfied an R^2 value of 0.92. See Fig.6.14b. This shows that the values of CBR_u of soil blends can be effectively predicted using values of *angle of internal friction* (ø) measured using *triaxial* tests on unsoaked samples.

Similarly, it is seen that a regression between CBR_s for soaked samples, and *angle of internal friction* (ø) measured using the triaxial test equipment on unsoaked samples can be developed. These two variables can be correlated linearly with an R^2 value of 0.877. See Eq. 6.23 and Fig. 6.14c. The regression equation developed was validated using the data set apart for the same which satisfied an R^2 value of 0.94. See Fig.6.14d. This shows that the values of of CBR_s of

soaked soil blends can be effectively predicted using *angle of internal friction* (ø) measured using triaxial tests on unsoaked soils.

8.3.11 Conclusions on Regressions Developed for Results Based on *CBR*, *PFWD*, *DCP* and Cyclic Triaxial tests: Unsoaked Soil Samples

The results of the tests performed on unsoaked soil samples based on the *CBR*, *PFWD, DCP,* and the values of the *modulus of resilience* (M_r) obtained based on the *cyclic triaxial* test equipment are summarized in Table 6.61a for unsoaked samples. The tests were performed on five blends of *lateritic* and *lithomargic* soils at OMC-3% (or M1), OMC (or M2), and OMC+3% (or M3) which generated 15 data points. The correlations were developed using 10 randomly selected data points out of the total 15 data points, while validations were performed using the remaining 5 data points.

8.3.11.1 Conclusions on Correlations between *CBR* and E_{pfwd}

While analyzing the results of the tests performed on unsoaked CBR samples (CBR_u) and the values of the *modulus of resilience* obtained using the PFWD (E_{pfwd}) on unsoaked soil samples, it can be seen that these two variables can be correlated linearly with an R^2 value of 0.86. See Eq. 6.24 and Fig. 6.15a. The regression equation developed was validated using the data set apart for the same which satisfied an R^2 value of 0.86. See Fig.6.15b. This shows that the values of CBR_u of soil blends can be effectively predicted using E_{pfwd} values. Similar

8.3.11.4 Conclusions on Correlations between *CBR* and *Modulus of Resilience* (M_r)

On analyzing the results of the values of CBR_u for tests on unsoaked soils, and the *modulus of resilience* (M_r) measured using the *cyclic triaxial* test equipment on unsoaked samples, it can be seen that these two variables can be correlated linearly with an R^2 value of 0.95. See Eq. 6.27 and Fig. 6.18a. The regression equation developed was validated using the data set apart for the same which satisfied an R^2 value of 0.87. See Fig.6.18b. This shows that the values of CBR_u for tests on unsoaked soils can be effectively predicted using values of the *modulus of resilience* (M_r) measured using *cyclic triaxial* test equipment on unsoaked samples.

8.3.11.6 Conclusions on correlations between M_r and *DCPI*

On analyzing the results of the *modulus of resilience* (M_r) measured using the *cyclic triaxial* test equipment on unsoaked samples, and the $DCPI_u$, measured using the *dynamic cone penetrometer* on unsoaked samples, it can be seen that these two variables can be correlated linearly with an R^2 value of 0.90. See Eq. 6.29 and Fig. 6.20a. The regression equation developed was validated using the data set apart for the same which satisfied an R^2 value of 0.82. See Fig.6.20b. This shows that the values of the *modulus of resilience* (M_r) measured using the *cyclic triaxial* test equipment on unsoaked samples, can be effectively predicted using values of the $DCPI_u$, measured using *dynamic cone penetrometer* on unsoaked samples.

8.4.2 Conclusions on the Set of Multiple Regression Equations Developed for Results Based on *CBR*, *PFWD*, *DCP*, Cyclic Triaxial Tests, Static Triaxial Tests, and Tests for UCS for Soaked and Unsoaked Samples

The results of the tests performed on soaked and unsoaked soil samples based on the *CBR*, *PFWD, DCP*, tests using the *cyclic triaxial* test equipment, tests using the *static triaxial* test equipment, and the tests for UCS are summarized in Table 6.60, Table 6.61a, and Table 6.61b for unsoaked and soaked samples. The tests were performed on five blends of *lateritic* and *lithomargic* soils at OMC-3% (or M1), OMC (or M2), and OMC+3% (or M3) which generated 15 data points. The correlations were developed using all the 15 data points. Tests for validation could not be performed since more than one independent variable is used for prediction of the dependent variable. Table 6.63 provides details on the correlations developed for unsoaked and soaked soil specimens.

8.5 CONCLUSIONS ON THE *FOURTH PHASE* OF THE PRESENT WORK

The *fourth phase* of study provides details on *FEM* based analyses using *Plaxis-2D* for various configurations of embankment models for tests performed on various lateritic soil blends as discussed in Chapter 7. The conclusions on the same are provided in the sub-sections below.

8.5.1 Conclusions on *FEM*-based Analyses on Embankment Models

Based on the results summarized in Table 7.2a, Table 7.2b and Appendix 6 for tests performed using the FEM-based approach; the following conclusions can be made:

- In the analyses for stresses and strains for the top surface of the embankments, it was observed from Table 7.2a and Table A.6.1a that the maximum stresses and strains, occurred close to the mid part of the loading section of the embankment in the case of various blends of lateritic soils.

It can be seen from the above discussions based on Table A6.1a, Table A6.1b and Table A6.1c that, as the toe angle is increased from 30^o to 60^o, the vertical stresses increase from -39.7 kPa to -51.1 kPa, and the vertical strains increase from -184.13 $x10^{-3}$% to -240.63 $x10^{-3}$%. This indicates that embankments with steeper side slopes experience higher stresses and strains when analyzed for the same height.

Based on the Table A6.2a, for the embankment model of 3m height with a toe angle of 30^o and for a lateritic composition of 0%L+100%S, the maximum vertical stress is found to be -17.31 kPa close to the middle of the top surface of the embankment. Similarly, the maximum vertical strain is found to be approximately -472.122 $x10^{-3}$%.

For the same embankment mentioned above, if the toe angle is set to 45^o to the horizontal, it is observed according to Table A6.2b that, a maximum vertical stress of -19.44 kPa occurs close to the middle of the top surface of the embankment. Similarly, the maximum vertical strain is found to be approximately -536.115 $x10^{-3}$%. For the embankment mentioned above, if the toe angle is set to 60^o to the horizontal, it is observed according to Table A6.2c that, a maximum vertical stress of -21.93kPa occurs close to the middle of the top surface of the embankment. Similarly, the maximum vertical strain is found to be approximately -608.177 $x10^{-3}$%.

Based on the Table A6.5a, for the embankment model of 3m height with a toe angle 30^o and for a lateritic composition of 75%L+25%S, the maximum vertical stress is found to be -36.77 kPa close to the middle of the top surface of the embankment. Similarly, the maximum vertical strain is found to be approximately -213.09 $x10^{-3}$%.

For the same embankment mentioned above, if the toe angle is set to 45^o to the horizontal, it is observed according to Table A6.5b that, a maximum vertical stress of -42.5 kPa occurs close to the middle of the top surface of the embankment. Similarly, the maximum vertical strain is found to be approximately -245.77 $x10^{-3}$%.

Based on the Table A6.6a, for the embankment model of 3m height with a toe angle of 30^{o} and for a lateritic composition of 25%L+75%S, the maximum vertical stress is found to be -20.71 kPa close to the middle of the top surface of the embankment. Similarly, the maximum vertical strain is found to be approximately -367.352 $x10^{-3}$%. For the same embankment mentioned above, if the toe angle is set to 45^{o} to the horizontal, it is observed according to Table A6.6b that, a maximum vertical stress of -23.12 kPa occurs close to the middle of the top surface of the embankment. Similarly, the maximum vertical strain is found to be approximately -414.534 $x10^{-3}$%.

From Table 7.4c, it can be seen that the total displacement for an embankment of 3m height made of lateritic constitution of (75%L+25%S), with a toe angle of 45 degrees is 7.31 $x10^{-3}$ m. But for an embankment of the same dimension made of *lithomargic* soil (25%L+75%S), the total displacement is 12.33 $x10^{-3}$ m. This indicates that *lithomargic* soils suffer larger deformations when compared to lateritic soils.

CHAPTER IX

MAJOR CONTRIBUTIONS, LIMITATIONS OF THE STUDY, AND FUTURE SCOPE OF WORK

9.1 INTRODUCTION

The strength and stiffness of soil subgrade depend upon the load carrying capacity of the underlying soil layers. Soil subgrades must be capable of resisting traffic loads superimposed by the pavement layers above. The subgrades further transmit the traffic loads imposed to the underlying layers keeping the deformations within the elastic limit under adverse climatic conditions. The strength and stability of subgrades play a major role in resisting structural failure of pavements.

Poor subgrade strength, overloading due to traffic loads, and seismic vibrations can cause distress to pavement subgrades and embankments. Additionally, inadequate compaction, poor sub soil drainage, and low bearing strength of soils cause failure of embankments, especially in submersible regions. Studies on unsoaked and soaked soils will enable pavement engineers to address these issues effectively.

AASHTO formulated the guidelines for the analysis of pavement structures based on the *resilient modulus* for the *Mechanistic-Empirical* approach for design of pavement structures (AASHTO 1986; Monismith1989). Investigations on determination of the *modulus of resilience* using the cyclic triaxial test equipment is one of the *direct laboratory-based* approaches recommended by AASHTO (1993) for characterizing base and subgrade soils.

In view of the importance given to the assessment of the *modulus of resilience* of the subgrade in pavement design, it was proposed to correlate the observations made using traditional subgrade evaluation approaches to the *modulus of resilience* measured using the PFWD and the *cyclic triaxial* test equipment.

9.2 MAJOR CONTRIBUTIONS OF THE STUDY

The *first phase* of the work dealt with the characterization of soil-properties and the strength and stiffness of *lateritic* and *lithomargic* soils for the District of Dakshina Kannada, Karnataka State, India. The study encompassed experimental investigations on static properties of soil such as, the *Atterberg's limits*, *grain-size distribution*, *specific gravity*, *bulk-density*,

maximum dry density (*MDD*), *optimum moisture content* (*OMC*), and the permeability, along with investigations using the tests for *California Bearing Ratio* (*CBR*), unconfined compressive strength (UCS), the tests for cohesion and angle of friction using the triaxial test equipment. The *first phase* of investigations also included studies on the strength and stiffness characteristics of laterite soil-samples blended with varying percentages of fines for moisture contents at *dry-of-optimum*, *optimum*, and *wet-of-optimum* using the *dynamic cone penetrometer* (*DCP*) and the *portable falling weight deflectometer* (*PFWD*). These studies were performed for various blends of *lateritic* and *lithomargic* soils for the region of Dakshina Kannada in Southern India

The *third phase* of the study was related to the development of correlations based on the test results of investigations performed in the *first phase* and the *second phase*. Correlations were developed considering the *percentage of fines* as an important dependent variable. Regression equation were also developed considering the values of *UCS*, *cohesion* and *angle of internal friction* determined using *static triaxial test*, the values of the *CBR*, *DCPI*, and the values of the *modulus of resilience* determined using the *PFWD* and the *Cyclic triaxial* tests. The regressions developed were also validated using a different set of data. The relationships developed in *phase three* are expected to provide a further insight into the influence of *fines*, *gravel*, *sand*, *MDD*, *OMC*, and moisture content on the strength and stiffness characteristics of blended lateritic soils. The major contributions of the study on regressions developed can be listed as follows:

- The study on the influence of *fines*, *gravel*, *sand*, *MDD*, and *OMC* on the values of the *UCS, CBR, cohesion, angle of internal friction, DCPI,* E_{pfwd}, and M_r also revealed that as the fines content increased, the strength and stiffness of soils reduced. The correlations developed were of high R-square value, and were considered to be of immense use to field engineers in understanding the underlying relationship between various parameters, and in estimating the strength and stiffness of lateritic subgrades of the region.
- Further, it could also be demonstrated that in the case of tests for unsoaked soils, the values of strength and stiffness were higher for soil samples compacted to *OMC-3%* due to the effect of *capillary suction*, while in the case of soaked soil samples, it was seen that the strength and stiffness were higher for soil samples compacted to *OMC* due to the reason that soaked soils possessed *flocculent structure* at *OMC-3%* and *dispersive structure* at OMC+3%. Similar observations were made by a number of researchers.

- At the final stages, a number of multiple linear regressions were also developed, which gave further insight into the interdependence between various tests results and the variables involved in each study.

The *fourth phase* of the study was related to performing *FEM-based* analyses using *Plaxis-2D* for various configurations of embankments constructed using various blends of lateritic soils compacted to *OMC*. From the *FEM* analysis, it was found that the lateritic soil undergoes lesser deformation when compared to lithomargic soils. This indicates that *lithomargic* soils suffer larger deformations when compared to lateritic soils.

9.3 LIMITATIONS OF THE STUDY AND SCOPE FOR FUTURE WORK

The following are the limitations of the study, and scope for future work.

1. It is felt that further studies on strength and stiffness can be performed on stabilized *lateritic* and *lithomargic* soil blends using cyclic triaxial equipment, PFWD, and DCP. Soils blended with cement, lime, fly ash, terrazyme, and various other new products can be investigated.
2. Similar studies can be performed for black-cotton soils, and other expansive soils.

REFERENCES

1. AASHTO (1986), "Standard Method for Testing Resilient Modulus," AASHTO 274-82, Washington, D.C.
2. AASHTO (1993), "AASHTO Guide for the Design of Pavement Structures," AASHTO, Washington, D.C.
3. AASHTO (1994), "Standard Test Method for Determining the Resilient Modulus of Soils and Aggregate Materials," AASHTO TP 46-94, American Association of State Highway and Transportation Officials (AASHTO) Provisional Standard.
4. AASHTO (1999), "Determining the Resilient Modulus of Soils and Aggregate Materials," AASHTO T 307-99, AASHTO, Washington, D.C.
5. AASHTO (2000), "Florida Method of Test for Non Repetitive Static Plate Load Test of Soils and Flexible Pavement Components Designation," FM 5-527 Modified AASHTO T 222-78,
6. Acum, W. E. A. and L. Fox (1951), "Computation of Load Stresses in a Three Layer Elastic System," *Geotechnique*, Vol. 2, pp. 293-300.
7. Adunoye G.O (2014). "Fines Content and Angle of Internal Friction of a Lateritic Soil: An Experimental Study", *American Journal of Engineering Research* (AJER) , e-ISSN : 2320-0847 p-ISSN : 2320-0936,Vol.03, Issue-03, pp.16-21.
8. Al-Amoudi, O. S. B., Asi, I. M., Al-Abdul Wahab, H. I., and Khan, Z. A. (2002), "Clegg hammer-California bearing ratio correlations", *J. Materials in Civil Engineering ASCE*, 14(6), pp. 512-523.
9. Ansal, A.M., Erken, A. (1989), "Undrained behavior of clay under cyclic shear stresses," *ASCE Journal of Geotechnical Engineering*, 115 (7): pp.968-983.
10. Asphalt-Institute. (1991), "Thickness Design - Asphalt Pavements for Highways and Streets", Manual Series No.1 (MS-1), *Asphalt Institute*, Lexington, KY.
11. ASTM (2003), "Resilient Modulus Testing for Pavement Components," Gary N. Durham, W. Allen Marr, Willard L. Degroff, (2003) Eds., ASTM-STP 1437, ASTM International, West Conshohocken, Site accessed on 24th May 2014.
12. Ayers, M. E. (1990), "Rapid Shear Strength Evaluation of In Situ Granular Materials Utilizing the Dynamic Cone Penetrometer", *Ph.D. Dissertation*, University of Illinois.
13. Bayoglu, Esra (1995), "Shear Strength and Compressibility Behavior of Sand-Clay Mixtures," *M.S. Thesis*, Middle East Technical University, Turkey.
14. Bergen, A.T. and Monismith, C.L. (1973), "Characteristics of Subgrade Soils in Cold Regions for Pavement Design Purposes," *Highway Research Record* 431, Highway Research Board, National Research Council, Washington D.C., pp. 25-37.
15. Brinkgreve, R.B.J., Vermeer, P.A. (2001), "Plaxis 3-D Tunnel", Balkema Publishers, Tokyo.
16. Brown, S.F., O'Reilly, M.P. & Loach, S.C. 1990, "The Relationship Between California Bearing Ratio and Elastic Stiffness for Compacted Clays," *Ground Engineering* 23 (8) pp. 27-31.
17. Cai, Y., Gu, C., Wang, J., Juang, C.H., Xu, C and Hu, X (2012). "One-way Cyclic Tri-axial Behavior of Saturated Clay: Comparison between constant and variable confining pressure", *J. Geotech. Geoenviron. Eng*. 139, pp. 797–809.
18. Chai, G., and Roslie, N. (1998), "The Structural Response and Behavior Prediction of Subgrade Soils Using Falling Weight Defelectometer in Pavement Construction," *Proc. 3rd*

Int. Conf. On Road & Airfield Pavement Technology, Beijing, China (www.dot.state.mn.us/app/mnpave/docs/dcp_mississippi.pdf Accessed on Jan. 12, 2014).
19. Chai, J., Horpibulsuk., S., Shen., S., Carter, J.P., (2014), "Consolidation Analysis of Clayey Deposits Under Vacuum Pressure with Horizontal Drains," *Geotext. Geomembr*. 42 (5), 437–444
20. Chen, D. H., Lin, D. F., Liau, P. H, and Bilyeu, J. (2005), "A Correlation Between Dynamic Cone Penetrometer Values and Pavement Layer Moduli*," Geotechnical Testing J*., 38(1), pp. 42-49.
21. Chou, Y. T. (1976), "Evaluation of Nonlinear Resilient Modulus of Unbound Granular Materials from Accelerated Traffic Test Data," U.S. Army Engineer Waterways Experiment Station, Vicksburg, *MS, Final Technical Report*.
22. Choudhury, Deepankar, Shukla, Jaykumar, Katdare, Amey, Patankart, Vilas and Tiruvengala, Padma (2013) "Slope Stability and Settlement Analysis for Dry Bulk Terminal at Mozambique: A Case Study", *Electronic Journal of Geotechnical Engineering*, (ISSN: 1089-3032), USA, Vol. 18, Bundle E, pp. 859-874.
23. Cokca, E. Erol. O. and Armangil, F. (2004), "Effects of compaction moisture content on the shear strength of an unsaturated clay," *Geotechnical and Geological Engineering* 22, 2004, © 2004, Kluwer Academic Publishers, Printed in the Netherlands, pp. 285–297.
24. Darter, M.I., Elliott, R.P., and Hall, K.T. (1992) "Revision of AASHTO Pavement Overlay Design Procedure, Appendix: Documentation of Design Procedures, Final report" Project 20-7/39, *National Cooperative Highway Research Program, Transportation Research Board*, Washington, D.C. (www.wsdot.wa.gov/ biz/mats/pavement/EVERSERS/ Everseries User Guide.pdf, Accessed on June 22, 2014)
25. Das, B. (1983), "Advanced Soil Mechanics", McGraw-Hill Book Company, Washington, New York, London
26. Dash, H.K., Sitharam, T.G., Baudet,B.A.(2010). "Influence of Non-Plastic Fines on the Response of a Silty Sand to Cyclic Loading", *Soils Foundation*. Vol.50 (5), pp.695–704.
27. Dehlen, G. L. (1969), "The Effect of Non-Linear Material in the Behavior of Pavements Subjected to Traffic Loads," *Ph.D. Thesis*, University of California, Berkley.
28. Diaz-Rodríguez, J.A. (1989), "Behavior of Mexico City Clay Subjected to Un-drained Repeated Loading," *Canadian Geotechnical Journal*. 26 (1), pp. 159-162.
29. Dodds, A., Logan, T., Mclachlan, M., and Patrick, J. (1999), "Dynamic Load Properties of New Zealand Base course," *Transfund New Zealand Research Report* 151.
30. Dyskin AV, Estrin Y, Kanel-Belov AJ, Pasternak E (2001), "Toughening by Fragmentation—how topology helps," *Advanced Engineering Materials*, 2001, 3(1):885–888.
31. Fleming, P. R., Lambert, J. P., Frost, M. W., and Rogers, C. D. F. (2000), "In-Situ Assessment of Stiffness Modulus for Highway Foundations During Construction", *Proc. 9th Int. Conf. Asphalt Pavements*, Copenhagen, Denmark, 15, pp.12, [CD-ROM].
32. Florin, V. A. And Ivanov, P. L. (1961), "Liquefaction of Saturated Sandy Soils," *Proc. 5th International Conference on Soil Mechanics and Foundation Engineering*, Paris Dunod, 1, pp.107-111.
33. Fortunato, E., Pinelo, A., and Fernandes, M.M (2010). "Characterization of the Fouled Ballast Layer in the Sub-structure of a19th century railway track under renewal", *Soils Found*, Vol.50 (1), pp.55–62.

34. Fredlund, D. G. And Rahardjo, H. (1993), "Soil Mechanics for Unsaturated soils," Wiley, New York, pp. 517.
35. George Varghese, Rao, Nageshwar,C H, Shivashankar, R. (2009a), "PFWD, DCP and CBR Correlations for Evaluation of Lateritic Subgrades," *International Journal of Pavement Engineering*, Taylor and Francis Publications, Vol. 10, Issue 3 (June), pp. 189-199.
36. George, K. P. (2006), "Portable FWD (PRIMA 100) for In-situ Subgrade Evaluation," conducted by the Department of Civil Engineering, in cooperation with Mississippi Department of Transportation (MDOT), and the U.S. Department of Transportation, Federal Highway Administration (FHWA), Mississippi.
37. George, K. P., and Uddin, W. (2000), "Subgrade Characterization for Highway Pavement Design", *Final Report, Mississippi Department of Transportation*, Jackson, MS, pp.245.
38. George, Varghese, Ch., Nageshwar Rao, Shivashankar, R. (2009b), "Investigations on Unsoaked Blended Laterite using PFWD, PBT, DCP, and CBR Tests," *Journal of Indian Roads Congress*, Vol. 70, No.3, pp. 223-233.
39. George, Varghese, Hegde, Ramakrishna, Vishnuvardhana, M., Santosh G., Gotamey, Dwarika (2012), "Accelerated Consolidation of Coir Reinforced Lithomargic Laterite Soil Blends with Vertical Sand Drains for Pavements," *Electronic Journal of Geotechnical Engineering (EJGE)*, Vol. 17, July, pp. 2115-2133.
40. Green, J. L. And J. W. Hall (1975), "Nondestructive Vibratory Testing of Airport Pavements Volume I: Experimental Test Results and Development of Evaluation Methodology and Procedure," *Federal Aviation Administration Report No. FAA-RD-73-205-1*, pp.214.
41. Gregory, G.H., (2007). "Correlation of California bearing ratio with shear strength parameters", *Transportation Research Record: Journal of the Transportation Research Board*, 1989, pp.148–153.
42. Gudishala, R. (2004), "Development of Resilient Modulus Prediction Models for Base and Subgrade Pavement Layers From In-Situ Devices Test Results", *MS Thesis*, Louisiana State University and Agricultural and Mechanical College, Louisiana, USA, pp. 133.
43. Gupta M. K. (1977), "Liquefaction of Sands during Earthquakes," *Ph.D Thesis*, University of Roorkee, Roorkee, India.
44. Hakan Guneyli and Tolga Rusen (2015), "Effect of Length-to-Diameter Ratio on the Unconfined Compressive Strength of Cohesive Soil Specimens" *Bulletin of Engineering Geology and the Environment*, Volume 75, Issue 2, pp. 793–806.
45. Hammond, A.A., (1970), "A Study of Some Lateritic Gravels From Kumasi District," *Build. Road Res. Inst*., Kumasi, Ghana, Project Rept. SM5, pp.17.
46. Han, Z. and Vanapalli, S.K (2016). "State-of-the-Art: Prediction of Resilient Modulus of Unsaturated Subgrade Soils", *Int. J. Geomech*, 16, 04015104.
47. Hegde, Ramakrishna (2013), " Investigations on Accelerated Consolidation of Coir Reinforced Lateritic, Lithomargic Clay and Bended Soils With Vertical Sand Drains For Pavement Foundation," *Ph.D thesis* submitted to the Dept of Civil Engineering National Institute of Technology, Karnataka, India.
48. Hegde, Ramakrishna, George, Varghese, Kumar, Nirmal A.G., Prashanth, Durga, L.A., and Santosh G. (2012), "Model Study on Accelerated Consolidation of Coir Reinforced Lateritic Lithomarge Soil Blends with Vertical Sand Drains for Pavement Foundations," *Open Journal of Soil Science (OJSS)*, Vol. 2, pp. 320-332.
49. Hoffmann, O. J. M., Guzina, B. B., & Drescher, A. (2004), "Stiffness Estimates Using Portable Deflectometers," *Transportation Research Record*, (1869), 59-66.

50. Huang, Y. H. (2004), "Pavement Analysis and Design," Prentice-Hall, Englewood Cliffs, NJ.
51. Inam, A., Ishikawa,T., Miura,S (2012). "Effect of Principal Stress Axis Rotation on Cyclic Plastic Deformation Characteristics of Unsaturated Base Course Material", *Soils Foundations*, Vol. 52(3), pp. 465–480.
52. IS: 2720 Part V (1985) , "Indian Standard Methods of Test for Soils: Determination of Liquid and Plastic Limit, Compendium of Indian Standards on Soil Engineering," Part 1: Laboratory Testing of Soils for Civil Engineering Purposes, Bureau of Indian Standards, New Delhi, pp. 109-114.
53. IS: 1498 (1970), "Indian Standard Classification and Identification of Soils for General Engineering Purposes, Compendium of Indian Standards on Soil Engineering ," Part 1: Laboratory Testing of Soils for Civil Engineering Purposes, Bureau of Indian Standards, New Delhi, pp. 23-40.
54. IS: 2720 Part III (1964),"Indian Standard Methods of Test for Soils: Determination of Specific Gravity," SP 36 (Part 1) : 1987, Compendium of Indian Standards on Soil Engineering: Part 1: Laboratory Testing of soils for Civil Engineering Purposes, Bureau of Indian Standards, New Delhi, pp. 65-67.
55. IS: 2720 Part VIII (1983), " Indian Standard Methods of Test for Soils: Part 8: Determination of Water Content - Dry Density Relation Using Heavy Compaction," Compendium of Indian Standard on Soil Engineering: Part 1: Laboratory Testing of Soils for Civil Engineering Purposes, Bureau of Indian Standards, New Delhi
56. Jafarpisheh SH and Vafaeian M (2003), "The Investigation of Time Settlements of Soil as a Result of Drilling Shallow Tunnels," *6th Iranian Tunnel Conference*, Tehran, pp.769-783.
57. Jones, A. (1962), "Tables of Stresses in Three-Layer Elastic Systems," *Highway Research Board Bulletin No. 342*, Stress Distribution in Earth Masses, pp. 176-214.
58. Jurgenson, L., (1934), "The Application of Theories of Elasticity and Plasticity to Foundation Problems", *In: Contributions to Soil Mechanics 1925–1940*. Boston: Boston Society of Civil Engineers, 148–183.
59. Kato, S., Yoshimura, Y., Kawai, K., and Sunden, W (2001). "Effects of Suction on Strength Characteristics of Un-Confined Compression Test for a Compacted Silty Clay"*J.Geotech.Eng*.,687,pp.201–218 (in Japanese)
60. Kato, Y., Nakata, Y., Hyodo, M., and murata, H (2001). "One-Dimensional Compression Properties of Crushable Soils Related to Particle Characteristics." *Proc., 14th Southeast Asian Geotechnical Conf*., Geotechnical Engineering Meeting Society's Meet, K. K. S. Ho and K. S. Li, eds., Southeast Asian Geotechnical Society (SEAGS), Pathumthani, Thailand, pp. 527–532.
61. Kirkpatrick, W. M. (1965). "Effects of Grain Size and Grading on the Shearing Behaviour of Granular Materials." *Proc., Sixth Int. Conf. On Soil Mech. And Found. Engg*., Montreal, Quebec, Canada, Vol. 1, pp. 273-276.
62. Kitamura, Ryosuke and Sako, Kazunari (2010). "Contribution of "Soils and Foundations" to Studies on Rainfall-Induced Slope Failure", *Soil and Foundations*, vol. 50, no. 6 pp. 955-964. DOI: 10.3208/sandf.50.955
63. Koga, Y., and Matsuo, (1990), "Shaking Table Tests of Embankments Resting on Liquefiable Sandy Ground," *Soils Foundation*, pp. 162–174.
64. Kokusho, T., Yoshida, Y. And Esashi, Y. (1982), "Dynamic Properties of Soft Clay For Wide Strain Range," *Soils and Foundations*, 22, pp. 1-18.

65. Kumar, R. Srinivasa, Ajmi, Alhammadi Shabbab, and Valkati, Bhasker (2015), "Comparative Study of Subgrade, Soil Strength Estimation Models Developed Based on CBR, DCP and FWD Test Results," *International Advanced Research Journal in Science, Engineering and Technology*, ISSN 2394-1588, Vol. 2, Issue 8, pp. 92-102.
66. Lambe, W. T. (1951), "Soil Testing for Engineers". *John Wiley and Sons, Inc*., New York.
67. Latha Madhavi G and Sitharam T. G. (2008), "Effect of Particle Size and Gradation on The Behaviour of Granular Materials Simulated Using DEM," *Indian Geotechnical Journal*, 38(1), pp.68-88.
68. Lee, K.L. and A. Albaisa (1974), "Earthquake-Induced Settlement in Saturated Sand," *J. Soil Mech. and Found*. Div., 100 (4), pp.387-400.
69. Lefebvre, G.S., Leboeuf, D., and Demers, B. (1989), "Stability Threshold for Cyclic Loading of Saturated Clay," *Canadian Geotechnical Journal* 26 (1): pp. 122-131.
70. Lekarp, F., Isacsson, U. And Dawson, A. (2000), "State of the Art. I: Resilient Response of Unbound Aggregates," *Journal of Transportation Engineering,* Vol. 126, No. 1.
71. Li D, Selig ET. (1994), "Resilient modulus for Fine-grained Subgrade soils," *Journal of Geotechnical Engineering, ASCE* 120(6), pp. 939-957.
72. Livneh, M., Ishai, I., and Livneh, N. A. (1992), "Automated DCP Device versus manual DCP device," *Rd. And Transport Res.*, 1(4). P. 42.
73. Loh, E., Usamath, T., and Deepak, T., "Shoreline Instability Study on Fun Island Resorts, Maldives," *Journal of Environmental Protection*, Vol. 3 No. 10, 2012, pp. 1302-1309. doi: 10.4236/jep.2012.310148.
74. Maher, M.H., Papp Jr., W. J., Gucunski, N. (1996), "Measurement of Soil Resilient Properties Using Non-contacting Proximity Sensors," *Transportation Research Record 1548*, TRB, National Research Council, Washington D.C., pp. 16-23.
75. Michelow, J. (1963), "Analysis of Stresses and Displacements in an N-layered Elastic System under a Load Uniformly Distributed on a Circular Area", *Chevron Research Corporation*, Richmond, California.
76. Monismith, C.L. (1989), "MR Testing-Interpretation of Laboratory Results for Design Purposes". *Workshop on Resilient Modulus Testing*, Oregon State University, Corvallis, http://books.google.co.in/books.
77. Nakao, T. and Fityus, S, (2008) "Direct Shear Testing of a Marginal Material Using a Large Shear Box," *Geotechnical Testing Journal*, Vol.31,No-5, pp.1 11,https://doi.org/10.1520/GTJ101237. ISSN 0149-6115.
78. Nazarian, S., and Feliberti, M. (1993), "Methodology for Resilient Modulus Testing of Cohesionless Subgrades," *Transportation Research Record 1406*, TRB, National Research Council, Washington D.C., pp. 108-115.
79. Nazarian, S., Yuan, D., and Arellano, M., (2002), "Quality Management of Base and Subgrade Materials with Seismic Methods," *Proc. 81st Annual Meeting Transportation Board*, Washington, DC, pp. 50-60.
80. Nguyen, Bao Thach and Mohajerani, Abbas. (2014). "Resilient Modulus of some Victorian fine-grained soils at OMC, wet-of-OMC and Soaked conditions", *Australian Geomechanics,* Vol. 49 No 2.
81. Norusis, M.J., SPSS for Windows, Professional Statistics, release 6.0, 1993 (SPSS Inc.) (Chicago, IL).
82. *Proc., 4th Intern. Conf. on Soil Mech. and Found. Engr*., Vol. 1, pp. 393-394.

83. Peattie, K. R. (1962), "Stress and Strain Factors for Three-Layer Elastic Systems," *Highway Research Board Bulletin No. 342*, Stress Distribution in Earth Masses, pp. 215-253
84. Porter, O. J. (1950). "Development of the Original Method for Highway Design, Development of CBR Flexible Pavement Design Method for Airfields", *Symposium, Trans. ASCE*, 115, pp. 461-467.
85. Pyke, R., H.B. Seed and C.K. Chan (1975), "Settlement of Sand Under Multidirectional Shaking," *J. Of the Geotechnical Engineering Division, Proc. Of ASCE,* 191(4), pp. 379-398.
86. R. Mokwa and m. Akin (2009) "Measurement and Evaluation of Subgrade Soil Parameters: Phase 1-Synthesis of Literature," Tech. Rep. FHWA/MT-09-006/8199, Western Transportation Institute, Montana State University, Bozeman, Mont, USA.
87. Rao, Ch. Nageshwar (2008), "Studies on Strength and Stiffness Characteristics for Lateritic Soil for Pavement Subgrades," *Ph.D thesis* submitted to the Dept of Civil Engineering National Institute of Technology, Karnataka, India.
88. Rao, Nageshwar Ch., George, Varghese, and Shivashankar, R. (2010), "Effect of Fines and Moisture Content on PFWD Resilient Modulus of Un-soaked Blended Laterite Sub-grades," *Highway Research Journal of Indian Roads Congress*, Vol. 3, No. 2, pp. 111-116, July-Dec.
89. Sawangsuriya, A., Edil, T., and Bosscher, P. (2002), "Laboratory Evaluation of the Soil Stiffness Gauge (SSG)," *81st Annual Meeting of the Transportation Research Board*, January, Washington, D.C., Paper No. 02-3608, pp.1-23.
90. Scott, R. And H. K. Ko. 1970, "Stress Deformation and Strength Characteristics," *Int. State of the arts volume*, *The Seventh Intl. Conf. On Soil Mech. And Found. Engg.*
91. Seed, H. B., Chan, C. K. And Lee, C. E. (1967), "Resilience Characteristics of Subgrade Soils and their Relation to Fatigue Failures in Asphalt Pavements," *Proceedings of First International Conference on the Structural Design of Asphalt Pavements*, University of Michigan, Ann Arbor, Michigan, pp. 611-636.
92. Siekmeier, J. A., Young, D., and Beberg, D. (1999), "Comparison of The Dynamic Cone Penetrometer with Other Tests During Subgrade and Granular Base Characterization In Minnesota," *Nondestructive Testing of Pavements And Back Calculation Of Moduli, ASTM STP 1375*, West Conshohocken, PA, pp. 175-188.
93. Sitaram, T.G, Govindaraju, L. And Sridharan, A. (2004), "Dynamic Properties and Liquefaction Potential of Soils," *Geotechnics and Earthquake Hazards*, Vol. 87.
94. Sowers, G.F. and C. S. Hedges, (1966), "Dynamic Cone for Shallow In-Situ Penetration Testing, Vane Shear and Cone Penetration Resistance Testing of In-Situ Soils," *ASTM STP 399, American Society of Testing and Materials,* 1966, pp. 29.
95. Tagore, M R, World Bank Guidelines on Techno-Economic Feasibility of Highway Projects – DPR Case Studies, Invited Paper for Workshop on World Bank Guidelines on Techno-Economic Feasibility of Highway Projects, Organised by Engineering Staff College of India, Hyderabad, 3-7 November 2003.
96. Tarek Omar and Abouzar Sadrekarimi (2015) "Effect of Tri-Axial Specimen Size On Engineering Design and Analysis" *International Journal of Geo Engineering*. Vol. 6(5), https://www.researchgate.net/publication/279270091.
97. Thagesen, B. (1996), "Tropical Rocks and Soils, in: Highway and Traffic Engineering in Developing Countries" London.
98. Theyse, H. (2002), "Stiffness, Strength, and Performance of Unbound Aggregate Material", *Application of South African HVS and laboratory results to California flexible pavements Davis*, California: University of California Pavement Research Center.

99. Thom, N. H., and Brown, S. F. (1988), "The Effect of Grading and Density on the Mechanical Properties of a Crushed Dolomitic Limestone," *In Proceedings of the 14th ARRB Conference*, Part 7: pp. 94–100.
100. Toll, D. G. (2000), "The Influence of Fabric on the Shear Behavior of Unsaturated Compacted Soils," *Geotechnical Special Publication*, No. 99, ASCE, pp. 222–234.
101. Tripathy, S., Hesham, E and Thomas, H.R., (2014), "Soil-water Characteristic Curves From Various Laboratory Techniques," *In Unsaturated Soils: Research & Applications*, edited by N. Khalili et al. (CRC Press, London, 2014), pp. 1701–1707.
102. Uddin, W., Garza, S. (2002), "In Situ Material Characterization of Pavement-Subgrade Systems Using FWD Data and Validation by 3D-FE Simulations," *2002 federal aviation administration airport technology transfers Conf. University of Mississippi University*, MS 38677-1848, USA, pp. 13.
103. Venkatramaiah, C., (2006) "Geotechnical Engineering", Revised Third Edition, New Age International, New Delhi, 419-435.
104. Vinson, T.S. (1978), "Parameters Effects on Dynamic Properties of Frozen Soil*," Journal of the Geotechnical Engineering Division*, ASCE, Vol. 104, No. GT10, Oct., pp. 1289-1306.
105. Waterways Experiment Station. (WES) (2001), ''Pavement Design for Airfields,'' *U.S. Army Corps of Engineers, Waterways Experiment Station,* Rep. No. UFC 3-260-03. WES, Miss.
106. Wong, Steven T. Y., Dominic, E.L., and Robinson, R.G. (2017) "Behaviour of MH Silts with varying Plasticity Indices, *Geotechnical Research*", E-ISSN 2052-6156, Vol. 4 Issue 2, June, pp. 118-135. Themed issue on 19th Southeast Asian Geotechnical Conference.
107. Wu, W., Arellano, M., Chen, D-H., Bilyeu, J., and He, R. (1998), "Using a Stiffness Guage as an Alternative Quality Control Device in Pavement Construction, Texas Department of Transportation, Austin, TX, 17" in Comparison of Moduli obtained from the Soil Stiffness Gauge with Moduli from other tests, Auckpath Sawangsuriya,Tuncer B. Edil, and Peter J. Bosscher, Paper submitted for presentation and publication at the Transportation Research Board 81st Annual Meeting January 13-17, 2002 Washington, D.C., pp.1-25.
108. Yoder, E. J., and Witczak M. W. (1975), "Principles of Pavement Design," *2nd ed., John Wiley & Sons*, New York, pp. 711.
109. Zydron, Tymoteusz Zydro, and Dabrowska, Joanna (2012), "The Influence of Moisture Content on Shear Strength of Cohesive Soils from the Landslide Area Around Gorlice," *AGH Journal of Mining and Geo Engineering*, Vol. 36, No. 2, pp. 309-317.

WEBSITES

1. Website: Cornell (2014) Typical Values of Young's Elastic Modulus and Poisson's Ratio for Pavement Materials. Online at http://www.clrp.cornell.edu/CDOT/Handouts/4c%20%20 Materials%20Table.pdf. Site accessed on 6th June 2014.

.

Details of Papers Published and Under Review

Papers Published in International Journals

1. Kumar, Anil. & George, Varghese (2018), **"Effect of Soil Parameters on Resilient Modulus using Cyclic Tri-axial tests on Lateritic Sub-grade Soils from Dakshina Kannada, India"**, *Geotechnical and Geological Engineering* (*Springer*), Published online 27April 2018. https://DOI.org/10.1007/s10706-018-0550-7.

2. George, Varghese and Kumar, Anil (2016) "**Studies on Modulus of Resilience using Cyclic Tri-axial Test and Correlations to PFWD, DCP, and CBR**" *International Journal of Pavement Engineering* (*Taylor and Francis*) published online: 06 Oct 2016. DOI: 10.1080/10298436.2016.1230428.

3. George, Varghese and Kumar, Anil (2017)"**Effect of Soil Parameters on Modulus of Resilience Based on Portable Falling Weight Deflectometer Tests on Lateritic Sub-grade Soils**", *International Journal of Geotechnical Engineering (Taylor and Francis)*, published online : 22 Nov 2017. DOI: 10.1080/19386362.2017.1403075.

4. Kumar, Anil; George, Varghese; Marathe, Shriram (2016) "**Stability Analysis of lateritic soil Embankment sub-grade Using plaxis-2**D", *International Journal for Research in Civil Engineering*", Vol.2, Issue 1, January 2016.

Papers Published in Indian Origin Journals

1. Kumar, Anil, George, Varghese, and Marathe, Sriram (2016) *"***Establishing Relationships for Strength Characteristics of Lateritic Soils with Varying Silt Fractions***" International Journal of Earth Sciences and Engineering* (SCI-Journal), ISSN 0974-5904, Volume 09, No. 04 August 2016, P.P.885-887.

2. Kumar Anil, George Varghese, and Verma Rakesh (2013). "**Shake-Table and Its Applications in Fields of Research in Civil Engineering**", NITK Research Bulletin, Vol. 22, No. 1, Jul., pp. 27-29.

Conference Papers Published:

1. Anil Kumar, Varghese George, Shriram Marathe and Naveen (2015) "**Strength characteristic of Lateritic soil with varying Silt fractions**", ***International Conference on Emerging Trends in Engineering (ICETE- 2015)***, International Conference held in NMAMIT-Nitte, Karnataka, India. May 2015.

Journal Papers - under Review

1. George, Varghese and Kumar, Anil. "**Investigation on influence depth using the PFWD, tests for strength and stiffness of lateritic soils of Dakshina Kannada district, and development of regressions equations**" *International Journal of Pavement Engineering (Taylor and Francis)*, originally submitted on 28-08-2017, Manuscript No.GPAV-2017-0272. (Paper to be revised).

2. George, Varghese and Kumar, Anil. "**Investigation and analysis of Influence depth based on PFWD- tests and *PLAXIS*-2d for lateritic and lithomargic soils**", *Journal of the Institution of Engineers* (India): Series A (*Springer*), originally submitted on 23-06-2017, Manuscript No. - IEIA-D-17-00098 (Paper to be revised).

SUMMARY OF PUBLICATIONS

	Published/accepted	**Under Review**	Total
Journals	4 International	2 International	6
	2 Indian	-	2
Conferences	1 International	-	1
		Total	**9**